Constrained Internal Model Control

A thesis submitted to the University of Manchester for the degree of Doctor of Philosophy in the Faculty of Engineering and Physical Sciences

2011

Ambrose Adebayo Adegbege

School of Electrical and Electronic Engineering

Contents

Word Count=109,226

List of Tables

List of Figures

Abstract

Most practical control problems must deal with constraints imposed by equipment limitations, safety considerations or environmental regulations. While it is often beneficial to maintain operation close to the limits in order to maximize profit or meet stringent product specifications, the violation of actuator constraints during normal operation can result in serious performance degradation (sometimes instability) and economic losses. This thesis is concerned with the development of control strategies for multivariable systems which systematically account for actuator constraints while guaranteeing closed-loop stability as well as graceful degradation of non-linear performance.

A novel anti-windup structure is proposed which combines the efficiency of conventional anti-windup schemes with the optimality of model predictive control (MPC) algorithms. In particular, the classical internal model control (IMC) law is enhanced for optimal performance by incorporating an on-line optimization. The resulting control scheme offers both stability and performance guarantees with moderate computational expense. The proposed optimizing scheme has prospects for industrial applications as it can be implemented easily and efficiently on programmable logic controllers (PLC).

Declaration

No portion of the work referred to in this thesis has been submitted in support of an application for another degree or qualification of this or any other university or other institution of learning.

Copyright Statement

i. The author of this thesis (including any appendices and/or schedules to this thesis) owns certain copyright or related rights in it (the "Copyright") and s/he has given The University of Manchester certain rights to use such Copyright, including for administrative purposes.

ii. Copies of this thesis, either in full or in extracts and whether in hard or electronic copy, may be made **only** in accordance with the Copyright, Designs and Patents Act 1988 (as amended) and regulations issued under it or, where appropriate, in accordance with licensing agreements which the University has from time to time. This page must form part of any such copies made.

iii. The ownership of certain Copyright, patents, designs, trade marks and other intellectual property (the "Intellectual Property") and any reproductions of copyright works in the thesis, for example graphs and tables ("Reproductions"), which may be described in this thesis, may not be owned by the author and may be owned by third parties. Such Intellectual Property and Reproductions cannot and must not be made available for use without the prior written permission of the owner(s) of the relevant Intellectual Property and/or Reproductions.

iv. Further information on the conditions under which disclosure, publication and commercialisation of this thesis, the Copyright and any Intellectual Property and/or Reproductions described in it may take place is available in the University IP Policy (see `http://www.campus.`

manchester.ac.uk/medialibrary/policies/intellectual-property.pdf), in any relevant Thesis restriction declarations deposited in the University Library, The University Library's regulations (see http://www.manchester.ac.uk/library/aboutus/regulations) and in The University's policy on presentation of Theses.

Dedication

This page is dedicated to my son

Anthony Adesanmi Adegbege.

Acknowledgment

I am grateful to the almighty God, the author of life and wisdom, for giving me the grace to embark on this journey of known to the unknown. I am indeed grateful for His inspirations and strength that sustained me through the many inevitable crossroads of life and of this thesis.

I would like to thank my supervisor Dr. William P. Heath for his availability, readiness to help and for his many suggestions during the course of this thesis. I am intrigued by his patience and willingness to help on any issues even outside the four corners of research. In the period of three years, he has nurtured me from being a student to an independent researcher. I am grateful to have a man like William as my PhD supervisor.

I must also thank my fellow colleagues at the control systems centre for creating such a conducive learning and working environment. In particular, thanks to Dr. Oskar Vivero and Dr. Yiqun Zou from whom I took on the mantle of responsibilities. I will like to mention Syazreen Ahmad, Maria del Carmen Rodriguez Lin, Mobolaji Osinuga, Olufemi Osinnuyi, Mohamed Kara Mohamed, Yang Xuejiao for sharing ideas and for their great company. I will like to specially thank Sonke Engelken and Razak Alli-Oke for proofreading portion of this thesis. Many thanks to Dr. Joaquin Carrasco for all his supports and for sharing many jokes about research and the antipathies among researchers. You have all impacted my life.

I must also express my gratitude to the Victoria Park Fellowship, Daisy Bank

road, Manchester, for supporting me spiritually and my family through out the course of this thesis. I will like to say special thanks to Elder Malcolm and Siobhan Brook, Elder Brian and Tegwen Rainford, Elder Peter and kathy March, Senior citizens Alan and Marion Turnbull, the Ekaka's family, the Otokiti's family, the Shehu's family to mention a few.

I am also indebted to the Federal Government of Nigeria for providing the financial sponsorship for this research work through the Petroleum Technology Development Fund (PTDF). I am indeed grateful for counting on me to do the nation proud among the committee of nations represented within the United Kingdom's educational sector.

Special thanks to the members of my family for their prayers and moral supports. I thank my parents Patrick and Folasele Adegbege who brought me into this world and prepared the foundation for my current achievements. Many thanks to Francis for proofreading portion of this thesis and for his many visits during the course of the work.

I cannot but appreciate the immense support from my wife Olamiposi Adegbege. She is my angel and God sent. I thank her for doing virtually everything and leaving me only to read the books. My final thanks to Anthony, my son, who delayed his coming until the final moments of submission of this thesis.

The Author

Ambrose Adebayo Adegbege received the B.Sc. degree (with first class honours) in electronic and electrical engineering from the Obafemi Awolowo University, Ile-Ife, Nigeria, in 2004, and the M.Sc. degree (with distinction) in advanced control and systems engineering from the University of Manchester, Manchester, U.K., in 2006. He was also awarded the prestigious Professor Neil Munro's prize for the best dissertation in his class.

Ambrose joined the National Center for Technological Management (NACETEM), Ile-Ife, Nigeria shortly after his B.Sc in 2004 and worked as a member of a research team on 'Polymer Electronics'. He was with Mobil Producing Nigeria (MPN) as a machinery instrument and electrical engineer from 2006 until 2008 before taking up a PhD position at the University of Manchester. His doctoral work was supported by the federal government of Nigeria through the Petroleum Technology Development Fund (PTDF) scholarship. His current research interest is in the field of constrained control. Ambrose is happily married and a father of one.

Chapter 1

Introduction

1.1 Background

Most practical control problems must deal with constraints imposed by equipment limitations, safety considerations or environmental regulations. While it is often beneficial to maintain operation close to the limits in order to maximize profit or meet stringent product specifications, the violation of actuator constraints during normal operation can result in serious performance degradation (sometimes instability) and economic losses. This thesis is concerned with the development of control strategies for multivariable systems which systematically account for actuator constraints while guaranteeing closed-loop stability as well as graceful degradation of nonlinear performance.

The thesis derives motivation from the oil and gas upstream industry where the surface facilities include processes such as crude oil separation, gas compression, natural gas liquids (NGL) extraction, storage and power generation systems. Due to economic reasons, safety concerns or environmental regulations, most of these processes are fitted with control systems with objectives such as maintaining levels in a separator to avoid spillage, preventing liquid

carry-over into gas compressors, maintaining the hot-oil system temperature and maintaining quality products from extraction units to meet sale specifications. These control systems must deal with constraints imposed by equipment and actuator limits (such as control valves, motors and pumps), stringent product specifications, safety limits or environmental regulations from relevant government environmental protection agencies.

These requirements often mean the deployment of advanced control methodologies other than the conventional Proportional-Integral-Derivative (PID) control loops. One key feature of advanced control methodologies, such as model predictive control (MPC) and the novel optimizing internal model control (IMC) structure proposed in this thesis, is that constraints are systematically accounted for during the controller design and implementation. This allows operation closer to the constraints and hence increased profit. Under the same operating conditions, classical PID controls would require frequent operator interventions such as re-adjustment of set-points, repositioning of valves and dampers etc. This inefficient operation would often result in poor performance and economic losses.

Within the upstream sector, the few advanced control packages in use are generally considered as "black boxes" . They usually require vendors specialists for installation, troubleshooting and tuning. This thesis provides some insights into the development of such advanced control packages and proposes more efficient implementation strategies.

Over the last two decades, control design for processes under actuator constraints such as saturation nonlinearities has received significant attention leading to advances in optimizing control methodologies such as model predictive control (MPC) [10; 11; 12; 13] and anti-windup schemes [6; 2; 14; 8; 5; 15; 16; 17; 18]. On the other hand, internal model control (IMC) is an attractive control design strategy for inherently stable plants [19; 2]. It provides an open-loop framework for checking closed-loop stability and also highlights the inherent performance limitations due to model uncertainties,

non-minimum phase plant characteristics and actuator constraints. Internal model control has also been shown to be optimally robust to additive type uncertainties for input constrained systems [20; 21].

This thesis seeks to harness these attractive features of the internal model control structure for an effective anti-windup design with guaranteed closed-loop stability as well as an acceptable level of performance, but with online optimization included in the control structure. The proposed optimizing anti-windup combines the efficiency of conventional anti-windup with the optimality properties of MPC while requiring considerably less computational effort.

1.2 Research Approaches to Constrained Internal Model Control

Constrained control generally refers to control systems with input, output or state constraints. The research within this field primarily focuses on otherwise linear systems. Meanwhile, internal model control refers to a family of controllers that involve the explicit use of the plant model within the control formulation. The strength of such a control structure has long been identified and was consolidated in the series of papers by Morari and co-workers [22; 23; 24]. The concept is based on finding an inverse of the plant which is then augmented with a linear filter that can be tuned for trade-off between robustness and performance. For constrained systems, the controller must be designed to account for the effects of such constraints. Two approaches to constrained internal model control that have received considerable research attention are:

- Predictive Internal Model Based Control and
- Internal Model Control anti-windup Schemes

It well known that predictive internal model based control algorithms explicitly account for the effects of constraints *a priori* during control formulation [24]. The control inputs are computed in an open-loop fashion such that the output response predicted using the model of the plant has some desirable characteristics. In general, the control algorithm attempts to compute an approximate inverse of the plant via the solution of an online constrained optimization problem [25; 26]. Out of the many computed future control moves, only the first is applied to the plant. The whole computation is repeated again during the next sampling time. The computational and storage requirements of the receding horizon control can be extensive, restricting the application of such predictive algorithms to slow processes with many applications in the chemical and petrochemical industries. Robust MPC design techniques also increase the controller computational burden enormously and often result in very conservative solutions or in an infeasible control problem [27]. Recent advances in computing power and efficient solution algorithms have brought predictive control within the reach of electro-mechanical systems [28]. However, tuning for robustness and performance are still obtained in an obscure fashion with limited physical interpretations. The link between predictive internal model control and other forms of predictive algorithms is well discussed in the survey paper [29]. Model-state formulation of internal model predictive control was considered in [30]. A state-space interpretation of the predictive internal model control with stability considerations was developed in [31].

IMC anti-windup approaches follow the two-step control design methodology [6]. The linear controller is first designed, neglecting the effects of actuator nonlinearities, such that the control loop has desirable characteristics. The linear controller is then compensated or conditioned to account for the effects of control input constraints. The standard IMC structure introduced in [22] has been shown to possess some inherent anti-windup characteristics when the plant and the model are driven by the same saturated control signal. In this case, the control loop is effectively open loop; stability may not be an issue but the performance may be seriously degraded. Other IMC anti-

windup schemes have been developed to deal with the performance degradations. Popular IMC-based anti-windup designs are discussed in [1; 2]. The IMC anti-windup structure has also appeared in different guises such as in the model-based anti-windup schemes [32; 14], the two-degrees of freedom IMC anti-windup [33] and the mismatch anti-windup scheme of [34]. Many popular anti-windup schemes [35; 36; 37; 38; 21] also have the IMC as special cases.

An additional category is the family of controllers based on gain scheduling and control rescaling (static or dynamic). The concept of rescaling was first introduced into internal model control as a directionality preservation heuristic in [6]. A similar idea was used in [39; 40] and in the context of nonlinear systems in [41].

This thesis explores the two main streams of research to constrained control highlighted above and proposes a new convex synthesis procedure with both closed-loop stability and performance guarantees. In particular, the proposed optimizing anti-windup synthesis procedure provides a framework for combining the optimality of an online optimization with the efficiency of conventional anti-windup offline convex synthesis at moderate computational expense. When directionality is an issue, especially for highly ill-conditioned plants, the optimizing anti-windup framework offers a systematic way of incorporating such directional characteristics into the control synthesis. The effectiveness of the proposed anti-windup synthesis procedure as compared to several existing schemes is demonstrated using simulated examples.

1.3 Outline of the Thesis

The thesis is arranged into nine chapters. Chapter 2 covers the preliminaries and analysis tools necessary for the discussion of the main contributions contained in chapter 3 through to chapter 8. The conclusion and recommendations for future research are presented in chapter 9. The outline of the thesis is as follows:

Chapter 3: A comprehensive review of the internal model control structure and its relation to the general anti-windup design framework is carried out. In particular, all existing linear anti-windup schemes are parameterized in terms of the internal model controller and the right coprime factorization of the plant. This parameterization allows the extension of existing anti-windup techniques to the synthesis of IMC anti-windup with both stability and performance guarantees while retaining its intuitive appeal.

Chapter 4: A systematic approach to anti-windup synthesis based on the internal model control structure is proposed for open loop stable input constrained multivariable plants. The anti-windup design is defined solely in terms of the plant's inner and outer factors without introducing independent dynamics into the closed-loop. The anti-windup synthesis is directly linked to some closed-loop sensitivities which provide insights into the effectiveness of many LMI-based anti-windup techniques. The trade-off between stability robustness and performance is captured through a simple weight structure that determines the closed-loop bandwidth of interest.

Chapter 5: A unified theory of all existing optimal directionality compensation schemes is developed in terms of a standard quadratic program (QP). It is shown that the QP is equivalent to a modified QP in parallel with a feedthrough link. The equivalent representation can be used to obtain a decoupled control structure suitable for both analysis and

synthesis. It is further noted that both QPs are sector-bounded, monotone non-decreasing, slope restricted and odd. Hence, a general class of multipliers such that the Zames-Falb multipliers can be employed to establish the stability of existing directionality compensation schemes.

Chapter 6: An optimizing anti-windup incorporating directionality compensated is synthesized with stability and performance guarantees. The proposed synthesis approach incorporates *a priori* information about the input saturations and the directional nature of the plant into the control computation to guarantee closed-loop stability and a given level of performance. As compared to existing saturating anti-windup synthesis methods, the introduction of the directional characteristics of the plant into the synthesizing framework offers an additional degree of freedom in the anti-windup optimization.

Chapter 7: A robust synthesis of optimizing anti-windup subject to infinity-norm bounded uncertainties is presented using the integral quadratic constraints (IQC) approach. The IQC theorem allows the combination of static nonlinearities such as the QP-based directionality compensation with infinity-norm bounded uncertainties in one framework. Aside from allowing the incorporation of robustness in a less conservative manner, the design approach offers a systematic way of dealing with implementation issues arising from the presence of an algebraic loop in the resulting interconnection.

Chapter 8: A novel two-stage anti-windup structure is proposed for input constrained multivariable control problems. The two-stage scheme uses a relatively simple quadratic program strategy within the internal model framework to optimize both the transient and the steady state behaviours of the closed-loop systems during input saturations. A robust stability test is described for the two-stage anti-windup scheme using the passivity theorem and interpretations in the integral quadratic constraint (IQC) framework.

1.4 Contributions of the Thesis

The main contributions of this thesis are summarized as follows:

Chapter 6: The synthesis approach of chapter 6 is novel. As compared to existing optimizing anti-windup schemes [42; 43; 44; 7; 8], the design approach is particularly attractive in that it allows the incorporation of the plant's directional characteristics into the anti-windup synthesis to guarantee closed-loop stability as well as improved nonlinear performance. The anti-windup design is cast as a convex optimization problem over linear matrix inequality constraints using a decoupled structure similar to that proposed in the literature for anti-windup schemes with simple saturation.

Chapter 7: A robust synthesis of optimizing anti-windup subject to infinity-norm bounded uncertainties such as those arising from unmodeled or neglected dynamics is developed. In particular, the synthesis approach of [21; 45] is applied to the optimizing anti-windup design problem. Apart from allowing the incorporation of robustness in a less conservative manner, an additional advantage is that the resulting scheme offers a systematic way of dealing with algebraic loops and well-posedness of the arising interconnection as compared to [46].

Chapter 8: A novel two-stage internal model control (IMC) anti-windup structure is proposed for open loop stable multivariable plants. The design is based on the online solution of two low-order quadratic programs (QP) at each time step which addresses both transient and steady state behaviours of the system. The proposed two-stage structure allows for optimal closed-loop performance over a much wider operating range as compared to existing optimizing anti-windup schemes. Since it does not require the receding horizon computation of MPC, the two-stage IMC offers a computationally less intensive and more transparent (in terms of tuning for robustness) alternative to MPC algorithms.

Almost all the material discussed in chapters 3, 4 and 5 is established in the literature. Nevertheless, the interpretation and insights offered in chapter 4 using the two-degree of freedom internal model control appear to be novel."

1.5 Publications

Conference papers

1. Adegbege A.A. and Heath W.P., Two-Stage Multivariable Anti-Windup Design for Internal Model Control. In Proceedings of the 9th International Symposium on Dynamics and Control of Process Systems. Leuven, Belgium, July 5-7, 2010.

2. Adegbege A.A. and Heath W.P., Stability Conditions for Constrained Two-Stage Internal Model Control. In proceedings of the 49th IEEE Conference on Decision and Control, Atlanta, December 15-17, 2010.

3. Adegbege A.A. and Heath W.P., Anti-Windup Synthesis for Optimizing Internal Model Control. To be presented at the 50th IEEE Conference on Decision and Control and European Control Conference, Orlando, Florida, December 12-15, 2011.

Journal papers

1. Adegbege A.A. and Heath W.P., Internal Model Control Design for Input Constrained Multivariable Processes, AIChE Journal, vol. 57, no.12, pp. 3459-3472, 2011.

The discussions in chapter 8 are based on journal paper 1. The contribution in chapter 6 is under review for a journal while that of chapter 7 is in preparation for publication. Parts of chapters 5 and 8 were presented at

conferences 1 and 2 respectively. The conference paper 3 to be presented at the CDC/ECC conference in December, 2011 is partly based on chapter 6.

Chapter 2

Preliminaries

This chapter introduces basic mathematical tools and selected background materials relevant for use in subsequent chapters. General references are cited in each section which contain more comprehensive treatment of the topics.

2.1 Function Spaces and Operators

The mathematical concepts of systems and operator theory are important for performance specifications and stability analysis in control engineering. Generally, systems are represented as operators and their input and output signals as functions from appropriate vector spaces. The operator norms provide a natural way of quantifying sizes of system which is fundamental to systems theory.

2.1.1 Normed and Inner Product Spaces

Our primary interest is norms defined on spaces of functions which map from $\mathbb{R}^n$ to $\mathbb{C}^m$ or $\mathbb{R}^m$ where $\mathbb{R}$ denotes the set of real numbers and $\mathbb{C}$ complex numbers. The most frequently appearing function spaces in control engineering are the l_p^m and L_p^m $(p \geq 1)$ which are used to describe discrete-time and continuous-time function spaces respectively. The subscript p in $L_p^m(l_p^m)$ refers to the type of p-norm used to define the space, while the superscript m is the dimension of the signal. The infinite time axis is denoted as $\mathcal{T} \subset \mathbb{R}$ with $\mathcal{T}$ typically being $\mathbb{R}$, $\mathbb{Z}$, $\mathbb{R}_+$ or $\mathbb{Z}_+$ where $\mathbb{R}_+$ denotes the set of nonnegative real numbers and $\mathbb{Z}_+$ denotes the set of nonnegative integers. The notations as $L_p(-\infty, 0]$, $L_p[0, -\infty)$ and $L_p(-\infty, \infty)$ will be used to explicitly define what time axis is used for continuous time spaces while $l_p(\mathbb{Z}_+)$ and $l_p(\mathbb{Z})$ will be used for discrete time spaces. We first define some vector norms.

Definition 1. For a vector $x \in \mathbb{C}^m$ or $\mathbb{R}^m$, the $p-$norm is defined as follows;

$$|x|_p = \left(\sum_{i=1}^{m} |x_i|^p \right)^{1/p} \qquad \text{for} \quad 1 \leq p < \infty \text{ and} \tag{2.1}$$

$$|x|_\infty = \max_{1 \leq i \leq m} |x_i| \qquad \text{for} \quad p = \infty. \tag{2.2}$$

The spatial norm defined in (2.1) is the Euclidean norm when the subscript $p = 2$. Whenever the subscript p in the left hand side of (2.1) is suppressed, we will assume by default the Euclidean norm $|x| = |x|_2$. We also define the following generalization of the Euclidean norm.

Definition 2. Let $W = W^T \in \mathbb{R}^{m \times m}$ be positive definite. The W-norm is defined as

$$|x|_W = \left(x^T W x \right)^{1/2} \quad x \in \mathbb{R}^m. \tag{2.3}$$

When W is restricted to be diagonal i.e. $W = \text{diag}(w_i)$, $w_i \in \mathbb{R} \mid w_i > 0, i = 1 \cdots m$, the W-norm reduces to the weighted Euclidean norm defined as

$$|x|_W = \left(\sum_{i=1}^{m} w_i x_i^2 \right)^{1/2}. \tag{2.4}$$

Definition 3. The $L_p^m(-\infty, \infty)$ is the vector space of piecewise continuous functions $f : \mathbb{R} \to \mathbb{R}^m$ such that

$$||f||_p = \left(\int_{-\infty}^{\infty} |f(t)|_p^p dt \right)^{1/p} \qquad \text{for} \quad 1 \leq p < \infty \text{ and} \tag{2.5}$$

$$||f||_\infty = \operatorname*{ess\,sup}_{t \in \mathbb{R}} |f(t)|_\infty \qquad \text{for} \quad p = \infty. \tag{2.6}$$

Definition 4. The $l_p^m(\mathbb{Z})$ is the vector space of discrete time functions $f : \mathbb{Z} \to \mathbb{R}^m$ such that

$$||f||_p = \left(\sum_{t=-\infty}^{\infty} |f(t)|_p^p \right)^{1/p} \qquad \text{for} \quad 1 \leq p < \infty \text{ and} \tag{2.7}$$

$$||f||_\infty = \sup_{t \in \mathbb{Z}} |f(t)|_\infty \qquad \text{for} \quad p = \infty. \tag{2.8}$$

In most cases, any normed vector space, such as L_p^m or l_p^m, will be generally denoted by $\mathcal{L}_p^m$. The vector space $\mathcal{L}_p^m$ can be given additional structure, although more restrictive, by equipping it with an inner product. A vector space with an inner product is called inner product space. The norm on inner product spaces can be defined in terms of the inner product

$$\|f\| = \sqrt{\langle f, f \rangle}.$$

A complete inner product space is called a Hilbert space. Examples of Hilbert spaces are $L_2^m[0, \infty)$ and $l_2^m(\mathbb{Z}_+)$, which consist of all square integrable and Lebesgue measurable functions defined on the intervals $\mathbb{R}_+$ and $\mathbb{Z}_+$ with the inner products defined as

$$\langle f, g \rangle = \int_0^\infty f(t)^* g(t) dt \qquad \text{for } f, g \in L_2^m[0, \infty) \text{ and}$$

$$\langle f, g \rangle = \sum_{t=0}^{\infty} f(t)^* g(t) \qquad \text{for } f, g \in l_2^m(\mathbb{Z}_+)$$

for the discrete and continuous time respectively. We denote Hilbert spaces by $\mathcal{H}$ in order to distinguish their special structure from the normed vector space $\mathcal{L}$. The following definition provides the link between time domain

inner product space and the frequency domain inner product space.

Definition 5. The Hilbert spaces $l_2^m(\mathbb{Z}_+)$ and $L_2^m[0,\infty)$ have inner product defined respectively as

$$\langle f, g\rangle = \sum_{t=0}^{\infty} f(t)^* g(t) = \frac{1}{2\pi}\int_{-\pi}^{\pi} \hat{f}^*(j\omega)\hat{g}(j\omega)d\omega = \left\langle \hat{f}, \hat{g}\right\rangle \qquad \text{and}$$
$$\langle f, g\rangle = \int_0^{\infty} f(t)^* g(t)dt = \frac{1}{2\pi}\int_{-\infty}^{\infty} \hat{f}^*(j\omega)\hat{g}(j\omega)d\omega = \left\langle \hat{f}, \hat{g}\right\rangle.$$

Here, $\hat{f}$ and $\hat{g}$ denote the Fourier transforms of f and g, defined as

$$\tilde{f}(j\omega) = \lim_{N\to\infty}\sum_{t=0}^{N} f(t)e^{-j\omega t} \qquad \text{for all } \omega \in [-\pi, \pi] \text{ and}$$
$$\tilde{f}(j\omega) = \lim_{T\to\infty}\int_0^{T} f(t)e^{-j\omega t}dt \qquad \text{for all } \omega \in \mathbb{R}$$

for the discrete and continuous time respectively.

This bilateral transform that relates $\mathcal{L}_2$ spaces in the frequency domain to the $\mathcal{L}_2$ spaces in the time domain is what is called Parseval's relation or Plancherel theorem.

2.1.2 Operators

An operator G is a mapping from one normed space into another. We only consider the case where the input and the output spaces are the same i.e. $G : \mathcal{L}_2^m \to \mathcal{L}_2^n$. The operator is said to be biased if $G(0) \neq 0$ and unbiased if $G(0) = 0$. We will always assume the latter for our future developments. We will also adopt the shorthand notation $G(f)$=Gf for mapping of a linear operator.

Definition 6. Let α, $\beta \in \mathbb{R}$ and $f, g \in \mathcal{L}_2^m$. An operator $G : \mathcal{L}_2^m \to \mathcal{L}_2^n$

1. is linear if
$$G(\alpha f + \beta g) = \alpha G(f) + \beta G(g). \tag{2.9}$$

2. is bounded if the induced norm

$$||G||_{i,2} = \sup_{f \neq 0} \frac{||G(f)||_2}{||f||_2} \tag{2.10}$$

is finite. Furthermore, for linear and bounded operators, the induced norms satisfy the important submultiplicative rule

$$\|G_1 G_2\|_{i,2} \leq \|G_1\|_{i,2} \|G_2\|_{i,2} .$$

3. is Lipschitz if there exists a $k \in \mathbb{R}_+$ such that

$$\|G(f) - G(g)\|_2 \leq k \|f - g\|_2 . \tag{2.11}$$

4. has a Hilbert adjoint denoted by $G^* : \mathcal{L}_2^n \to \mathcal{L}_2^m$ if it is linear, bounded and such that

$$\langle Gf, g \rangle = \langle f, G^* g \rangle . \tag{2.12}$$

The adjoint exists uniquely and satisfies $||G^*||_{i,2} = ||G||_{i,2}$. The operator is self-adjoint if $G^* = G$.

Definition 7 (Extended Spaces)**.** Let $f : \mathcal{T} \to \mathbb{C}^m$, the extended space $\mathcal{L}_e^m$ is defined as

$$\mathcal{L}_e^m = \{ f : \mathcal{T} \to \mathbb{C}^n \mid \|f_T\| < \infty \ \forall T \geq 0 \} .$$

Here, f_T is a truncation defined by

$$f_T(t) = \begin{cases} f(t) & \text{when } t \leq T \quad (t, T \in \mathcal{T}), \\ 0 & \text{when } t > T. \end{cases}$$

Definition 8. An operator $G : \mathcal{L}_e^m \to \mathcal{L}_e^m$ is said to be causal (non-anticipative) if

$$f_T G(f_T)(t) = f_T G(f)(t) \quad \forall T \in \mathcal{T}.$$

We can think of the operators as mathematical objects that represent our system. Let $\mathcal{R}_p^{n \times m}$ denote the space of rational proper transfer functions,

then the operator $G \in \mathcal{R}_p^{n\times m} : \mathcal{L}_e^m \to \mathcal{L}_e^n$ has a state space realization which is often denoted by $\left[\begin{array}{c|c} A & B \\ \hline C & D \end{array}\right]$. G is said to be stable if all the eigenvalues of A are in the open left half-plane or equivalently for discrete systems, if they are strictly inside the unit disk.

We use the standard notation $\mathcal{RH}_\infty^{n\times m} \subset \mathcal{R}_p^{n\times m}$ for the space of stable real-rational transfer functions of size n by m, and $\mathcal{RH}_2^{n\times m} \subset \mathcal{RH}_\infty^{n\times m}$ for the space of stable, strictly proper, real-rational transfer functions of size n by m.

A comprehensive treatment on functional analysis may be found in [47; 48]. Other literature that could be consulted are [49; 50; 51].

2.2 Static and Sector-bounded Nonlinearities

We consider a class of nonlinearities which are static or memoryless and satisfy some sector or conic conditions. This class of nonlinearities has received much attention in stability analysis and control synthesis for linear systems subject actuator constraints such as the anti-windup compensation problem. A nonlinear function $\phi(u,t) : \mathbb{R}^m \times \mathcal{T} \to \mathbb{R}^m$ is said to be memoryless or static if the output at any instant of time t is uniquely determined by its input at that instant.

Definition 9. A nonlinear function $\phi : \mathbb{R}^m \to \mathbb{R}^m$ with $\phi(0) = 0$ is said to be monotone nondecreasing, slope-restricted to the interval $[a, b]$ and bounded by $c > 0$ if the following inequalities are respectively satisfied

C1: $\quad [\phi(x) - \phi(y)]^T (x - y) \geq 0 \ \forall x, y \in \mathbb{R}^m$

C2: $\quad [\phi(x) - \phi(y) - a\,(x - y)]^T [\phi(x) - \phi(y) - b\,(x - y)] \leq 0 \ \forall x, y \in \mathbb{R}^m$

C3: $\quad |\phi(x)|_2 \leq c|x|_2 \ \forall x \in \mathbb{R}^m.$

The nonlinearity ϕ is odd if $\quad \phi(-x) = -\phi(x)\ \forall\ x \in \mathbb{R}^m$.

Definition 10 (Sector-Bounded Nonlinearity (e.g.[52; 53]))**.** Let $\phi(u,t) : \mathbb{R}^m \times \mathcal{T} \to \mathbb{R}^m$ be a memoryless (possibly time varying) nonlinearity and $K = K_1 - K_2 = K^T$ for some $K_1, K_2 \in \mathbb{R}^{m\times m}$. We say $\phi\,(u,t)$ belongs to the sector $[K_1, K_2]$, or simply $\phi\,(u,t) \in [K_1, K_2]$ if

$$[\phi(u,t) - K_1 u]^T[\phi(u,t) - K_2 u] \leq 0\ \forall u \in \mathbb{R}^m \text{and } t \in \mathcal{T}. \tag{2.13}$$

In this thesis, we consider a class of static nonlinearities belonging to the sector $[0, I]$. For this case, the nonlinearities satisfy the stronger sector condition

$$\phi(u)^T W[\phi(u) - u] \leq 0\ \forall u \in \mathbb{R}^m, \tag{2.14}$$

where $W = W^T > 0$. This generalized sector condition allows the treatment of coupled nonlinearities common in optimizing control such as the in optimal directionality compensation schemes [7; 8] and the MPC [54]. Details of such nonlinearities will be discussed subsequently. A special case is when the nonlinearity is decoupled (i.e. $\psi_i(u) = \psi_i(u_i)$) with each component $\psi_i(u_i)$ inscribed in the sector $[0, 1]$. In this case, W is also restricted to be diagonal. This is the most widely used sector condition in anti-windup literature (e.g.[15; 21]). In this thesis, we explore the extra freedom in allowing W to be non-diagonal and its impact on the anti-windup synthesis and performance.

In what follows, we consider some popular examples of static nonlinear operators.

2.2.1 Saturation and Deadzone

Definition 11. A saturation function sat(.) is defined as

$$\text{sat}(u) = \begin{cases} u^{max} & \text{when } u > u^{max}, \\ u & \text{when } u^{min} \leq u \leq u^{max}, \\ u^{min} & \text{when } u < u^{min}. \end{cases} \tag{2.15}$$

We only consider the case when the saturation is symmetrical i.e. $u^{max} > 0$ and $u^{min} = -u^{max}$. The usefulness of this function is that it represents one of the simplest definitions of saturation that exist in the literature. In addition, any arbitrary saturation function can be put into the standard normalised form ($u^{min} = -1, u^{max} = 1$) by appropriate scalings on the input and output signals. The ideal deadzone function is defined as

$$\text{dz}(u) = \begin{cases} u - u^{max} & \text{when } u > u^{max}, \\ 0 & \text{when } u^{min} \leq u \leq u^{max}, \\ u - u^{min} & \text{when } u < u^{min}. \end{cases} \tag{2.16}$$

The ideal deadzone is a natural complement of the ideal saturation in the sense that

$$\text{sat}(u) + \text{dz}(u) = u. \tag{2.17}$$

The definitions in (2.15) and (2.16) imply that both functions sat(.) and dz(.) define bounded operators on $\mathcal{L}_2$ and satisfy

$$\frac{\|\text{sat}(u)\|_2}{\|u\|_2} \leq 1, \qquad \frac{\|\text{dz}(u)\|_2}{\|u\|_2} \leq 1 \qquad \forall u \in \mathcal{L}_2. \tag{2.18}$$

We now extend the definition to the multivariable case where $u = [u_1, \cdots, u_m]^T \in \mathcal{L}_2^m$.

Definition 12 (Multivariable Saturation Function)**.** A memoryless nonlinear operator $\text{Sat}(.) : \mathbb{R}^m \to \mathbb{R}^m$ is said to be a saturation function if

1. it is decentralised i.e. $\text{Sat}(u) = [\text{sat}_1(u_1), \cdots, \text{sat}_m(u_m(t))]^T$ and

2. each component $\text{sat}_i(u_i)$ satisfy the definition in (2.15).

Definition 13 (Multivariable Deadzone Function)**.** The deadzone function $\text{Dz} : \mathbb{R}^m \to \mathbb{R}^m$ is defined as

$$\text{Dz}(u) = u - \text{Sat}(u) \qquad \forall u \in \mathbb{R}^m, \tag{2.19}$$

where Dz(.) and Sat(.) are the component-wise multivariable saturation and deadzone functions defined respectively as

$$\text{Sat}(u) = \begin{bmatrix} \text{sat}_1(u_1) \\ \text{sat}_2(u_2) \\ \vdots \\ \text{sat}_m(u_1) \end{bmatrix} \text{ and } \text{Dz}(u) = \begin{bmatrix} \text{dz}_1(u_1) \\ \text{dz}_2(u_1) \\ \vdots \\ \text{dz}_m(u_1) \end{bmatrix}. \tag{2.20}$$

The notations Sat(.) and Dz(.) are used to denote the multivariable saturation and deadzone functions respectively to distinguish them from the scalar-valued functions sat(.) and dz(.). Note that the operators Sat(.) and Dz(.) both belong to the sector [0, I] and satisfy the stronger sector condition (2.14) with diagonal and positive definite W.

2.2.2 Quadratic Program

Definition 14. A Quadratic Program QP is a minimization problem of the form

$$\begin{aligned} v^* = &\arg\min_v \frac{1}{2} v^T H v + v^T x \\ &\text{subject to } Lv \leq b \\ &\text{and } Mv = d \end{aligned} \tag{2.21}$$

where $H = H^T \in \mathbb{R}^{m\times m}$, $L \in \mathbb{R}^{n\times m}$ and $M \in \mathbb{R}^{p\times m}$. The problem is convex if $H \geq 0$. A vector $v^* = (v_1^*, \cdots v_m^*)$ is called optimal, or a solution of the problem, if it has the smallest objective value among all vectors that satisfy the constraints. If such a vector exists, the problem is said to be feasible and v^* is a feasible solution, otherwise the problem is infeasible. Solving the QP (2.21) means either finding an optimal v^* solution if one exists, else proving that no feasible solution exists or that there is no bounded optimum.

The QP formulations that naturally arise in optimizing anti-windup and model predictive control takes the form of (2.21). Such QPs have been shown to satisfy some sector bound conditions [54]. This property is stated in the following lemma.

Lemma 1 (QP as a Sector Bounded Nonlinearity [54])**.** Let $\psi(x) : \mathbb{R}^m \to \mathbb{R}^m$ be given by the quadratic program problem (2.21). If H has full rank and 0 is always feasible, then ψ satisfies

$$\psi(x)^T H\psi(x) - \psi(x)^T x \leq 0 \ \forall x. \tag{2.22}$$

□

This is a generalized sector-bound condition and the QP can be represented as belonging to the sector [0 I] after two linear transformations. Detailed proof can be found in [54].

Remark 1. The saturation and deadzone functions can be given quadratic program interpretations. This relationship was explored to generalize stability results for Lur'e-type systems to MPC in [55; 56]. Similar observation has also been made that algebraic loops normally encountered in static anti-windup synthesis correspond to the solution of a particular class of quadratic program [57]. These observations as well as the generalized sector-bound results [54] will be explored further later in this thesis.

Further details on general memoryless nonlinearities may be found in [52; 58] and [59] for quadratic programs.

2.3 Linear Matrix Inequalities

Definition 15 (Linear Matrix Inequalities)**.** A linear matrix inequality (LMI) is an inequality, in the free variables $x = (x_1, \cdots x_m) \in \mathbb{R}^m$, that for fixed symmetric matrices $F = (F_0, \cdots F_m)$ with $F_i = F_i^T \in \mathbb{R}^{n \times n}$ has the form

$$F(x) = F_0 + \sum_{i=1}^{m} x_i F_i > 0. \tag{2.23}$$

$F(x)$ is said to be affine in the decision variables $x = (x_1, \cdots x_m)$. The LMI (2.23) is a convex constraint on x. Although the definition (2.23) may seem restrictive, it can represent a wide variety of convex constraints. In particular, the matrix constraints or matrix decision variables that arise in many control applications such as the Lyapunov inequality, can be expressed in the form (2.23) in terms of its components.

Nonlinear inequalities can be converted to LMI form by using the Shur complements.

Definition 16 (Schur Complements)**.** Let $Q(x) = Q(x)^T, \quad R(x) = R(x)^T$ and $S(x)$ depend affinely on x, then LMI

$$\begin{bmatrix} Q(x) & S(x) \\ S(x)^T & R(x) \end{bmatrix} > 0 \tag{2.24}$$

is equivalent to the matrix inequality

$$R(x) > 0, \qquad Q(x) - S(x)R(x)^{-1}S(x)^T > 0 \tag{2.25}$$

or equivalently,

$$Q(x) > 0, \qquad R(x) - S(x)^T Q(x)^{-1} S(x) > 0. \tag{2.26}$$

Another property which has found application in the conversion of nonlinear

inequalities, such as Bilinear Matrix Inequalities (BMIs), to LMIs is congruence transformation.

Definition 17 (Congruence Transformation)**.** Let $S \in \mathbb{R}^{n\times n}$ and $R \in \mathbb{R}^{n\times n}$ be given. Then S and R are said to be congruent, if there exists a non singular matrix P such that the following relation holds

$$R = P^T S P. \tag{2.27}$$

Lemma 2 (Congruence Transformation)**.** Given that $R \in \mathbb{R}^{n\times n}$ and $S \in \mathbb{R}^{n\times n}$ are congruent and P is non-singular, then

$$R > 0 \text{ if and only if } P^T R P > 0. \tag{2.28}$$

Proof. if $R > 0$, then $x^T R x > 0 \ \forall x \in \mathbb{R}^n \ x \neq 0$. Since R and S are congruent, there exists a non-singular P such that $S = P^T R P$. Because P is non singular, we can write $y = Px \ \neq 0 \ \forall y \neq 0$ such that $x^T R x = y^T P^T R P y$. Hence $R > 0$ if and only if $P^T R P > 0$. □

In other words, definiteness of a matrix is preserved under congruence transformation. This implies for example, that some rearrangements of matrix elements do not change the feasible set of an LMI. This property is very useful for eliminating bilinear terms in matrix inequalities that arise sometimes in control synthesis problems. A useful reference covering the theory of LMI and its application to control is [60].

2.4 Fractional Representation of Transfer Functions

In this section, we develop some basic tools based on factorization theory on rational transfer function which will play an important role in the control synthesis of this report. A detailed treatment of the topic can be found in [61; 62; 49; 50]

2.4.1 Coprime Factorization

Definition 18. Two transfer function matrices $M \in \mathcal{RH}_\infty^{m\times p}$ and $N \in \mathcal{RH}_\infty^{n\times p}$ are said to be right coprime if there exist $X_r \in \mathcal{RH}_\infty^{p\times m}$ and $Y_r \in \mathcal{RH}_\infty^{p\times n}$ such that

$$X_r M + Y_r N = I. \tag{2.29}$$

If in addition, M is both square and invertible in $\mathcal{RH}_\infty$, and

$$P = NM^{-1} \tag{2.30}$$

for some $P \in \mathcal{R}_p^{n\times m}$, then NM^{-1} is said to be a right coprime factorization of P.

Similarly, two transfer function matrices $\tilde{M} \in \mathcal{RH}_\infty^{q\times n}$ and $\tilde{N} \in \mathcal{RH}_\infty^{q\times m}$ are said to be left coprime if there exist $X_l \in \mathcal{RH}_\infty^{n\times q}$ and $Y_l \in \mathcal{RH}_\infty^{m\times q}$ such that

$$\tilde{M} X_l + \tilde{N} Y_l = I. \tag{2.31}$$

If in addition, $\tilde{M}$ is both square and invertible in $\mathcal{RH}_\infty$, and

$$P = \tilde{M}^{-1}\tilde{N} \tag{2.32}$$

for some $P \in \mathcal{R}_p^{n\times m}$, then $\tilde{M}^{-1}\tilde{N}$ is said to be a left coprime factorization

of P.

Remark 2. Right-coprime factorizations are unique up to right-multiplication by a unit in $\mathcal{RH}_\infty$ (A transfer function matrix Q is a unit in $\mathcal{RH}_\infty^{p\times p}$ if $Q, Q^{-1} \in \mathcal{RH}_\infty^{p\times p}$). If $P = NM^{-1}$ is a right-coprime factorization , then

$$P = \left\{NQ^{-1}\right\}\left\{MQ^{-1}\right\}^{-1} \tag{2.33}$$

is also a right-coprime factorization. Furthermore, all real rational right-coprime factorizations of P can be generated from any given right coprime factorization in this way. Similarly, left-coprime factorizations are unique up to left-multiplication by a unit in $\mathcal{RH}_\infty^{q\times q}$.

2.4.2 Inner-Outer Factorization

Definition 19. A transfer function G_i is called inner if $G_i \in \mathcal{RH}_\infty^{n\times p}$ and $G_i(jw)^* G_i(jw) = I$, for all w. If in addition G_i is square, then G_i is said to be all-pass. Similarly, $G_o \in \mathcal{RH}_\infty^{p\times m}$ is outer if, G_o has a full row rank $\forall$ Re $s > 0$ (or if its transmission zero is inside the unit disk for discrete equivalent). If for some $G \in \mathcal{RH}_\infty^{n\times m}$, $G = G_i G_o$ is said to be inner-outer factorization of G if G_i is inner and G_o is outer.

The adjective "inner G_i" indicates that all the zeros of G_i lie inside the right half-plane while "outer G_o" indicates that G_o has all its zeros outside the right half-plane. Note that G_i inner implies that G_i is a tall matrix (has at least as many rows as columns) and G_o outer implies that G_o is a wide matrix (has at least as many columns as rows). A useful property of an inner matrix is that it preserves inner product

$$\langle G_i f, G_i g\rangle = \langle f, g\rangle \quad \forall\ f, g\ \in \mathcal{L}_2^p. \tag{2.34}$$

It follows that G_i preserves norm

$$\|G_i v\|_2 = \|v\|_2 \ \forall v \in \mathcal{L}_2^p. \tag{2.35}$$

Remark 3. It is well known that every transfer function matrix in $\mathcal{RH}_\infty$ has an inner-outer factorization [61]. An inner matrix is unique up to pre-multiplication by a unit in $\mathcal{RH}_\infty$.

2.5 Uncertainty Descriptions

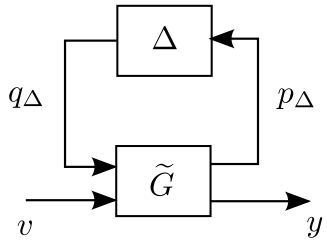

Figure 2.1: General plant uncertainty description

We consider the general framework of Fig. 2.1 where $\widetilde{G}$ is the generalized plant which includes both the nominal plant G_{22} and the interconnection structure specifying how uncertainty enters the plant. $\widetilde{G}$ and Δ are considered as bounded operators on $\mathcal{L}_2[0,\infty)$. $\tilde{G}$ maps $[q_\Delta^T, u^T]^T$ to $[p_\Delta^T, y^T]^T$ according to

$$\begin{bmatrix} p_\Delta \\ y \end{bmatrix} = \overbrace{\begin{bmatrix} G_{11} & G_{12} \\ G_{21} & G_{22} \end{bmatrix}}^{\widetilde{G}} \begin{bmatrix} q_\Delta \\ u \end{bmatrix} \tag{2.36}$$
$$q_\Delta = \Delta p_\Delta.$$

Assuming that $(I - G_{11}\Delta)^{-1}$ is non-singular, the map from v to y is given by

$$y = [G_{22} + G_{21}\Delta(I - G_{11}\Delta)^{-1}G_{12}]v. \tag{2.37}$$

In general, Δ is not known exactly. We however restrict discussion to $\Delta \subset \mathbf{\Delta}$ where $\mathbf{\Delta}$ is a set of bounded linear operators on $\mathcal{L}_2$. A number of uncertainty descriptions can be put into the general form of Fig. 2.1 by simply choosing the form of the operator G and the uncertainty set $\mathbf{\Delta}$. These are usually classified as unstructured and structured uncertainty descriptions.

2.5.1 Unstructured Uncertainties

We consider first, the unstructured uncertainty class where the set $\mathbf{\Delta}$ is the unit ball in operator space i.e.

$$\mathbf{\Delta} = \{\Delta \in \mathcal{RH}_\infty : \|\Delta\|_\infty \leq 1\}. \tag{2.38}$$

The most common unstructured uncertainty descriptions are the additive and the multiplicative uncertainties. These uncertainty descriptions are suited for representing high-frequency errors arising from unmodeled dynamics, resonance, parasitic coupling or a host of other unspecified effects. Others are the inverse multiplicative and matrix fractional uncertainties. Inverse multiplicative uncertainty is used to characterize errors arising from low-frequency parametric uncertainty while the coprime-factor uncertainty description provides for the combination of multiplicative and inverse multiplicative uncertainties in one framework and for dealing with the cross-over from low-frequency to high-frequency errors.

The additive uncertainty description $[G = G_{22} + W_1 \Delta W_2]$ or the input multiplicative uncertainty $[G = G_{22}(I + W_1 \Delta W_2)]$ description can be put into the general form of Fig. 2.1 by setting

$$\widetilde{G} = \begin{bmatrix} 0 & W_2 \\ W_1 & G_{22} \end{bmatrix} \text{ or } \widetilde{G} = \begin{bmatrix} 0 & W_2 \\ G_{22}W_1 & G_{22} \end{bmatrix} \tag{2.39}$$

respectively. Here W_1 and W_2 are frequency dependent stable transfer functions or weightings.

Similarly, right coprime-factor uncertainty $[G = (N + \Delta_N)(M + \Delta_M)^{-1}]$ can be obtained by setting

$$\tilde{G} = \begin{bmatrix} 0 & -M^{-1} & M^{-1} \\ I & -NM^{-1} & NM^{-1} \end{bmatrix} \tag{2.40}$$

where the nominal plant is expressed as the right coprime-factor $G_{22} = NM^{-1}$ and $\Delta = \begin{bmatrix} \Delta_N \\ \Delta_M \end{bmatrix}$. Similar expressions can be obtained for the left coprime-factor uncertainty.

2.5.2 Structured Uncertainties

Sometimes, it is beneficial to impose additional structure on the perturbation set $\mathbf{\Delta}$, in addition to a norm bound. The interconnection in Fig. 2.1 can be chosen so that Δ is block diagonal and such that it takes the form

$$\mathbf{\Delta} = \{\text{diag}(\Delta_1, \cdots, \Delta_k) \text{ with } \Delta_i \in \mathcal{RH}_\infty : \|\Delta_i\|_\infty \leq 1\}. \tag{2.41}$$

For example, suppose we choose

$$\tilde{G} = \begin{bmatrix} 0 & -M^{-1} & M^{-1} \\ 0 & -M^{-1} & M^{-1} \\ I & -NM^{-1} & NM^{-1} \end{bmatrix} \tag{2.42}$$

in the general form of Fig. 2.1. Then we have again the right coprime factor description. Note that we have imposed additional structure on Δ than in the unstructured representation in section 2.5.1 above. Here, Δ takes the form

$$\begin{bmatrix} \Delta_N & 0 \\ 0 & \Delta_M \end{bmatrix}$$

with p_Δ and q_Δ appropriately partitioned. This is an example of structured uncertainty description.

The discussion here is by no means exhaustive, extensive treatment can be found be in [49; 50; 63].

2.6 Integral Quadratic Constraints

Definition 20 (Integral Quadratic Constraints [64; 65])**.** A bounded operator $\Delta : \mathcal{L}_2^m \to \mathcal{L}_2^m$ is said to satisfy the Integral Quadratic Constraints (IQC) defined a bounded and self-adjoint operator Π or simply $\Delta \in \text{IQC}(\Pi)$ if the following inequalities holds

$$\left\langle \begin{bmatrix} u \\ v \end{bmatrix}, \Pi \begin{bmatrix} u \\ v \end{bmatrix} \right\rangle \geq 0 \ \forall \ v = \Delta(u), \ u \in \mathcal{L}_2^m. \tag{2.43}$$

In principle, the operator Π can be any measurable hermitian valued function $\Pi(jw) : j\mathbb{R} \to \mathbb{C}^{2m \times 2m}$ satisfying $\Pi(jw) = \Pi^*(jw) \ \forall w$.

If Δ has the block-diagonal structure $\Delta = \text{diag}[\Delta_1, \Delta_2]$ and Δ_i satisfies the IQC defined by

$$\Pi_i = \begin{bmatrix} \Pi_{i(11)} & \Pi_{i(12)} \\ \Pi^*_{i(12)} & \Pi_{i(22)} \end{bmatrix} \text{ for } i = 1, 2$$

then, the diagonal operator Δ satisfies the IQC defined by

$$\Pi = \left[\begin{array}{cc|cc} \Pi_{1(11)} & & \Pi_{1(12)} & \\ & \Pi_{2(11)} & & \Pi_{2(12)} \\ \hline \Pi^*_{1(12)} & & \Pi_{2(22)} & \\ & \Pi^*_{2(12)} & & \Pi_{2(22)} \end{array}\right] \tag{2.44}$$

where (2.44) represents the diagonal augmentation of the operators $\Pi_i, i = 1, 2$.

The theory of IQCs has recently received prominent attention in robust control. Many classical robust control tools and concepts such as small gain,

passivity, circle criterion, Popov's criterion and Zames-Falb multiplier can be conveniently expressed by IQCs. The IQC theory also provides a framework for combining plant uncertainties and nonlinearities for both robust analysis and synthesis. Detailed discussions on the theory of IQCs can be found in [64; 65; 50].

Chapter 3

Internal Model Control and Anti-windup

3.1 Introduction

Internal Model Control (IMC) is an attractive control design strategy for inherently stable plants [19; 2]. It provides an open-loop framework for checking closed-loop stability and also highlights the inherent performance limitations due to model uncertainties, non-minimum phase plant characteristics and actuator constraints. It offers intuitive tuning for robustness via a simple filter structure which can be given physical interpretations. However for saturating systems, the internal model control structure has received much criticism for its poor performance [39; 2; 34; 4]. Although closed-loop nominal stability can be guaranteed in certain situations, the nonlinear performance may be excessively sluggish especially when the plant has lightly damped modes, slow dynamics or non-minimum phase zeros [6]. This closed-loop performance degradation is not surprising as the original internal model control structure was never intended as an anti-windup scheme. However, several authors have considered various enhancements of the standard IMC, includ-

ing predictive elements [66; 67], anti-windup capability [6; 2; 33] and online optimization for coordinating actuators subject to constraints [9; 68]. In this chapter, we provide a brief review of the IMC structure evolution. We also introduce the concept of modern anti-windup architectures where the IMC structure arises as a special case.

For subsequent discussions, we consider a class of stable and linear systems described by

$$y = Gu + d \tag{3.1}$$

where G is a rational transfer function matrix and $y, d \in \mathcal{L}^p$, $u \in \mathcal{L}^m$ are the Laplace transform (or discrete equivalent, Z-transform) of the output signal $y(t)$, the manipulated input signal $u(t)$ and the output disturbance $d(t)$ signal respectively. In this chapter we assume G is known. The nominal unconstrained linear controller denoted as K (for error feedback controller) or Q (for internal model controller) is assumed to have been designed to meet some acceptable nominal stability and performance criteria. The plant is subject to control input saturations described in Def. 12. In general, the treatment is developed such that it can be applied for both continuous and discrete time cases. Thus the equations will not specify the domain unless it is necessary. For compactness of expressions, we will also not differentiate between a signal and its Laplace (or Z-) transform counterparts except when it becomes necessary to make such a distinction.

3.2 The Internal Model Control Structure Evolution

The standard internal model control (IMC) structure introduced in [22] is illustrated in Fig. 3.1 where G, G_{22} and Q denote the plant, the model of the plant and the IMC controller respectively. The design of Q for optimal performance and robustness is well discussed in the literature [19; 2]. With

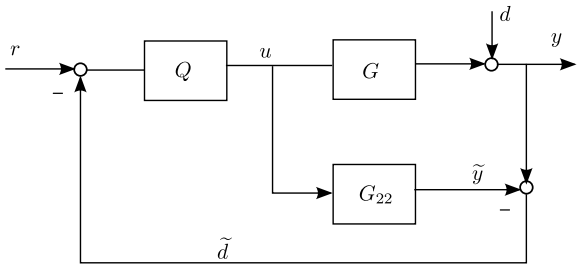

Figure 3.1: The standard IMC structure

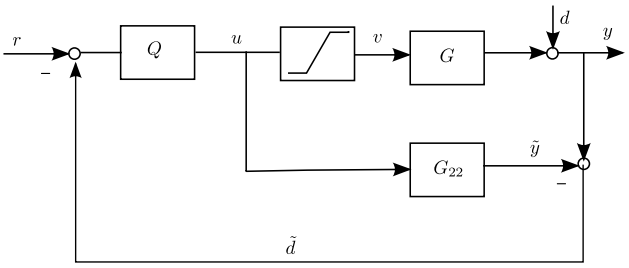

Figure 3.2: The IMC structure with saturating actuator without anti-windup

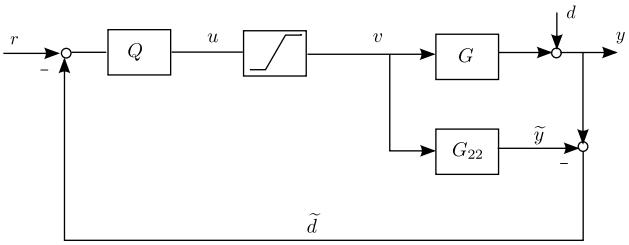

Figure 3.3: The conventional IMC anti-windup structure

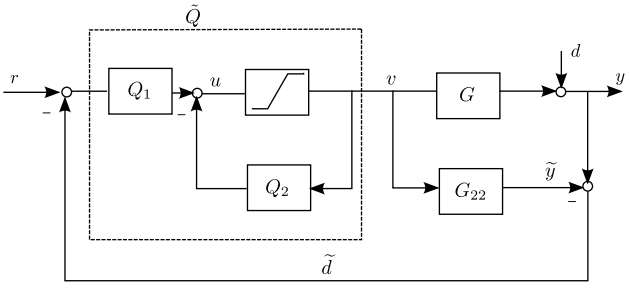

Figure 3.4: The modified IMC anti-windup structure

the assumption of perfect model i.e. $G = G_{22}$, the closed loop equations are given by

$$\begin{aligned} u &= Q\,(r - d) \\ y &= GQr + (I - GQ)\,d. \end{aligned} \tag{3.2}$$

The stability of G and Q guarantees nominal stability of the unsaturated closed loop system [19]. However, for saturating system where the actual plant input is $v(t) = \text{sat}(u(t))$, the standard IMC implementation of Fig 3.2 can lead to significant performance degradation and nominal stability is no longer guaranteed [19]. In this case, the plant and the model are driven by different inputs. The resultant model-plant mismatch is shown in the closed loop equation (3.3).

$$u = Q\,(r - d) + QG(u - v). \tag{3.3}$$

A first step towards avoiding the state mismatch between the plant and the model is the conventional IMC anti-windup structure of Fig. 3.3 [19; 2]. Although closed loop nominal stability is guaranteed when there is no model mismatch, the nonlinear performance may be excessively sluggish especially when the plant has lightly damped modes, slow dynamics or non-minimum phase zeros [6]. This closed-loop performance degradation is not surprising as the saturation effect on the plant output is not fed back directly to the controller. The closed loop equation (3.4) shows that the controller only acts on the error between the reference signal r and the output disturbance estimate $\tilde{d}$.

$$\begin{aligned} u &= Q\left(r - \tilde{d}\right) \\ y &= Gv + d. \end{aligned} \tag{3.4}$$

One way of achieving a graceful performance degradation for saturating systems is by using the modified IMC anti-windup structure of Fig. 3.4 [2]. The

unsaturated controller Q is factorized as

$$Q = (I + Q_2)^{-1} Q_1 \tag{3.5}$$

such that Q_2 is strictly proper and in feedback interconnection with the nonlinearity. It is also important that there are no unstable pole-zero cancellations between the factors Q_1 and $(I+Q_2)^{-1}$. This is necessary for the internal stability of the closed-loop system. Assuming no plant-model mismatch, the closed loop equations are given by

$$\begin{aligned} u &= Q_1 (r - d) - Q_2 v \\ y &= Gv + d. \end{aligned} \tag{3.6}$$

Here, the controller not only acts on the error between the reference signal and the output disturbance but it is also fed directly with information on the saturating control actions. When the system is away from saturation (i.e. $v = u$), equation (3.6) reduces to the closed loop equations for the implementation in Fig. 3.1. For a given Q, there are different ways of assigning Q_1 and Q_2. It is imperative that appropriate choices are made to achieve a good nonlinear performance while ensuring stability. The following cases of controller factorizations of Q are discussed in the literature [2; 7; 9; 1].

Option 1. $Q_1 = Q(\infty)$, where $Q(\infty) = \lim_{s\to\infty} Q(s)$ or $\lim_{z\to\infty} Q(z)$.

This factorization was proposed in [1]. The performance in this case can be greatly improved, but stability of the closed-loop system is not guaranteed. This choice cannot be used directly if Q is non-minimum phase. If Q is non-minimum phase and Q_1 is chosen as $Q(\infty)$, then Q_2 must be unstable. A naive application may result in closed-loop instability. For strictly proper plants, this choice corresponds to the Hanus conditioning techniques [69; 2; 7]. Consider the classical unity feedback system of Fig. 3.5 where K_1 and K_2 are

assigned based on the Hanus conditioning as

$$K_1 = K(\infty) \tag{3.7}$$

$$K_2 = K_1 K^{-1} - I \tag{3.8}$$

and K is the classical feedback controller. The equivalence of the factorization in the modified IMC structure of Fig. 3.4 and the classical feedback system of Fig. 3.5 can be established by assigning $K_1 = Q_1$ and $K_2 = Q_2 - Q_1 G_{22}$ where K and Q are related by $K = Q(I - G_{22}Q)^{-1}$. It also follows that if G_{22} is strictly proper, then $K(\infty) = Q(\infty)$. The performance for this choice may suffer when $K(\infty)$ or $Q(\infty)$ is not diagonal.

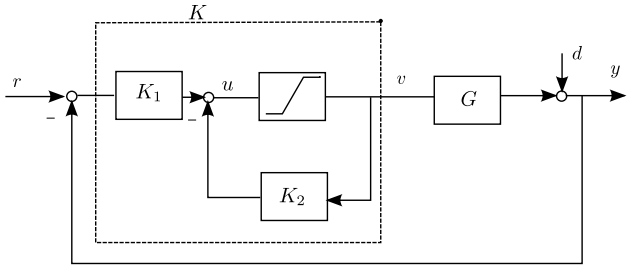

Figure 3.5: The classic feedback control structure with anti-windup

Option 2. $Q_1 = \Lambda Q + (I - \Lambda)Q\,(\infty)$.

Here, $\Lambda = \lambda I$ is a diagonal weighting matrix and $\lambda \in [0, 1]$. The choice of $\lambda = 1$ results in the conventional IMC structure($Q_2 = 0, Q_1 = Q$) which chops off the control input resulting in performance deterioration (sluggish response) but nominal stability is guaranteed [19; 6]. On the other hand, the choice of $\lambda = 0$ corresponds to the factorization proposed in [1] where $Q_1 = Q(\infty)$ and $Q_2 = Q_1 Q^{-1} - I$. The performance in this case is often improved, but nominal stability of the closed-loop system is not necessarily guaranteed. A trade-off between performance and stability can therefore be achieved by appropriate choice of λ, provided Q is minimum phase [2].

Option 3. $Q_1 = f_A G Q$.

Here, f_A is a non-causal filter that must be chosen such that $f_A GQ$ is minimum phase and $f_A G|_{s=\infty}$ or $f_A G|_{z=\infty}$ is I. This is the factorization proposed in [2]

where f_A is such that Q_1 solves implicitly an optimization problem. Similar factorization was suggested in [43] as an extension of the Hanus conditioning technique in the context of discrete-time systems. It should be noted that the choice $f_A = G^{-1}$ is equivalent to choosing $\lambda = 1$ in option 2 above.

Although the factorization options 2 and 3 provide useful ways of parameterizing the IMC anti-windup, they could be quite restrictive. The design of f_A is based on intuition and may require a modification to the plant model to achieve a decoupled response for directional plants [2; 43]. On the other hand, parametrization in terms λ reduces the anti-windup design to a line search over the interval $[0, 1]$ while imposing the stability and the performance constraints. This search space is very limited. Moreover, the choice $\lambda = 0$ does not represent an extreme choice for the maximum achievable nonlinear performance. A more systematic way of parameterizing the IMC anti-windup can be achieved via the coprime factorization of the nominal plant or the nominal controller. In this case, the IMC anti-windup design can be reduced to a convex search over the space of all the right coprime factors of the linear plant [34; 21] or its dual space of all the left coprime factors of nominal feedback controller [35; 36; 5]. This option is pursued further throughout this thesis.

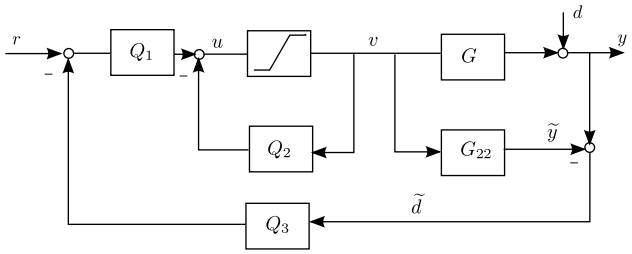

Figure 3.6: The complete IMC anti-windup structure

For the sake of generality, we consider the complete IMC anti-windup structure Fig. 3.6. This structure extends the two-degree of freedom internal model control [19; 35] to the anti-windup design problem. The extra degree of freedom is introduced through the inclusion of the disturbance rejection filter Q_3. This configuration has the advantage that the anti-windup com-

pensation, disturbance rejection and servo-tracking can be designed quasi-independently [70; 33]. The structure is particularly superior to the modified IMC structure when the reference signal r and the disturbance signal d have different dynamic characteristics or when the plant has significant time delays. For the latter case, the disturbance filter Q_3 often takes the form of a predictor [66; 31; 67] that projects the disturbance estimate $\tilde{d}$ forward in time to compensate for any dead-time characteristics at the plant output. Detailed treatment of the different design choices for Q_3 is discussed in [67]. The anti-windup plus delay compensation scheme of [71] may also be interpreted in the complete IMC framework of Fig. 3.6. For the linear case and assuming no modeling errors, the closed-loop equation of the complete IMC structure reduces to

$$\begin{aligned} u &= Q(r - Q_3 d) \\ y &= GQr + (I - GQQ_3)d. \end{aligned} \tag{3.9}$$

The extra design choice may be used to design Q_3 such that the adverse effect of unmeasured disturbance on closed-loop performance is attenuated. It also follows from (3.9) that the stability of the closed-loop is guaranteed if the nominal plant G, the nominal IMC controller Q and the disturbance filter Q_3 are all stable.

For the constrained case, the closed-loop equations reduce to

$$\begin{aligned} u &= Q_1(r - Q_3 d) - Q_2 v \\ y &= Gv + d \\ v &= \mathrm{Sat}(u). \end{aligned} \tag{3.10}$$

The closed-loop is stable provided all the elements G, Q_1, Q_2, Q_3 as well as the nonlinear loop (the feedback interconnection of the saturation nonlinearity and Q_2) are stable. Note that setting the disturbance filter $Q_3 = I$ recovers the modified IMC structure of Fig. 3.4. If in addition, we have $Q_1 = Q$ and $Q_2 = 0$, then the conventional IMC structure of Fig. 3.3 is recovered.

In this thesis, we will not explore the design parameter Q_3 as the inclusion of such an independent dynamic will lead to an overall controller of higher order than the plant. This may also results in control implementation issues. Since the linear or nominal system is already assumed to be well-designed in the sense that the closed loop has acceptance performance for unsaturated control inputs, we will only focus on anti-windup compensation design for saturating systems. Hence, we will only consider the design parameters Q_1 and Q_2 and assume that $Q_3 = I$.

We now consider an example to illustrate the effects of the different IMC controller factorizations on the nonlinear performance of an input-constrained multivariable system.

Example 1. Consider the following example taken from [2] where

$$G(s) = \frac{10}{100s+1}\begin{bmatrix} 4 & -5 \\ -3 & 4 \end{bmatrix} \tag{3.11}$$

with $|u_i| \leq 1$, $i = 1, 2$ and a step reference input of $[0.63 \quad 0.79]^T$.
The classical IMC controller design for a step input is

$$Q(s) = \frac{100s+1}{10(20s+1)}\begin{bmatrix} 4 & 5 \\ 3 & 4 \end{bmatrix} \tag{3.12}$$

and the corresponding unity feedback controller is

$$K(s) = \frac{100s+1}{200s}\begin{bmatrix} 4 & 5 \\ 3 & 4 \end{bmatrix} \tag{3.13}$$

Following the development in [2], the plant model is slightly modified as

$$\widetilde{G}(s) = \frac{10}{100s+1}\begin{bmatrix} 4 & \frac{-5}{0.1s+1} \\ \frac{-3}{0.1s+1} & 4 \end{bmatrix} \tag{3.14}$$

in order to satisfy the requirement of $f_A G(s)|_{s=\infty} = I$. The non-causal filter f_A is then designed for $\widetilde{G}(s)$ such that $f_A \widetilde{G}(s)|_{s=\infty} = I$ where $f_A = 2.5(s+1)I$.

The factorization of $Q(s)$ is obtained as $Q_1 = f_A \widetilde{G} Q$.

Fig. 3.7 shows the plant output responses for the unsaturated standard IMC, the saturated standard IMC without anti-windup and the conventional IMC anti-windup structures. This illustrate the performance degradation due to problems of control windup associated with input constrained MIMO plants. Fig. 3.8 shows the plant responses when the modified IMC structure is used with the different factorizations for Q in options 1 through 3. In this example, it happens that $Q(\infty) = K(\infty)$ and thus the resulting plant responses using the factorization schemes of [69] and [1] are the same. The factorization option 3 [2] gives the best performance. This scheme will be used as benchmark for comparing other anti-windup methodologies to be discussed subsequently in this thesis.

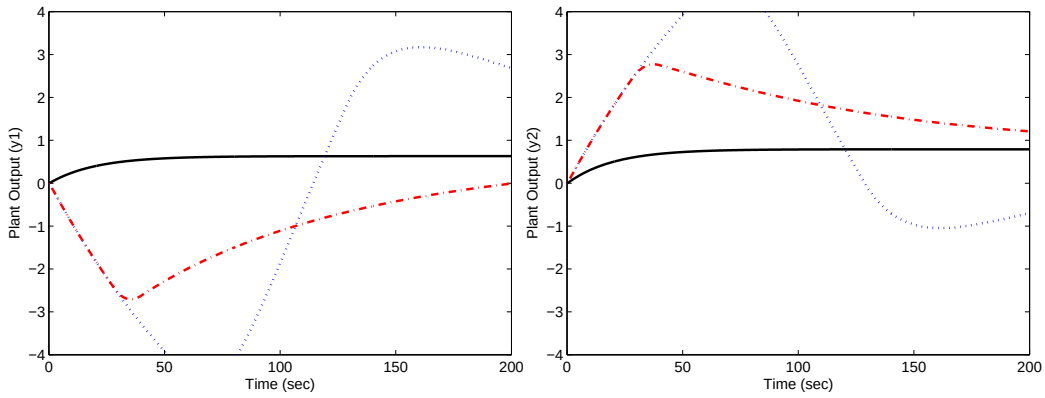

(a) Plant output response y(1) (b) Plant output response y(2)

Figure 3.7: Example 1-Plant output responses: solid- unsaturated IMC, dashed- saturated IMC and dashdot-conventional IMC anti-windup scheme

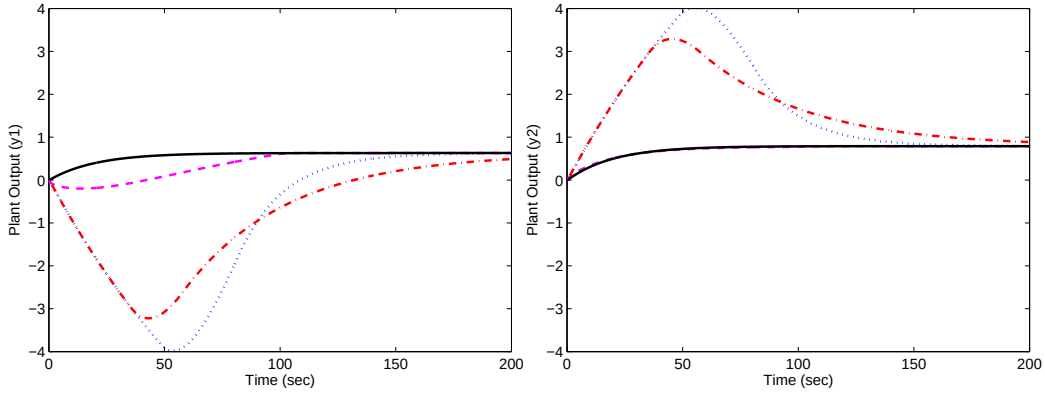

(a) Plant output response y(1) (b) Plant output response y(2)

Figure 3.8: Example 1-Plant output responses for different Q factorizations: solid- unsaturated IMC, dotted- Option 1, dashdot-Option 2 with $\lambda = 0.7$ and dashed-Option 3

3.3 Internal Model Control Design for Non-minimum Phase Systems

The anti-windup IMC structure in figure 3.4 is problematic when the IMC controller is non-minimum phase. Consider the factorization of Q into Q_1 and Q_2 where we require

$$Q = (I + Q_2)^{-1} Q_1. \tag{3.15}$$

If we choose Q_1 based on option 2 above i.e. $Q_1 = \lambda Q + (I - \lambda I) Q(\infty)$, then $Q_2 = \lambda (Q(\infty) Q^{-1} - I)$. It follows that if Q is non-minimum phase, Q_2 is unstable for $\lambda \neq 0$.

Therefore, for a non-minimum phase multivariable plant G, it is desirable to an IMC controller such that Q is both biproper and minimum phase. The recommended IMC design technique is to factorize the plant into an all-pass part G_+ and a minimum phase part G_- as

$$G = G_+ G_- \tag{3.16}$$

where G_+ contains all the non-minimum characteristics of G. The IMC controller is then obtained as

$$Q = G_-^{-1} f \tag{3.17}$$

where f is a low pass diagonal filter. There are generally different methods for achieving the factorization in (3.16). We present a brief overview of different factorization algorithms in the literature [72; 23; 19; 73].

Method 1. Dynamic decoupling [72]. The discrete-time equivalent is presented in [23; 19]. In this method, the system is factorized into all-pass and minimum phase part as

$$G_+(s) = \text{diag}\left\{ \prod_{i=1}^{k} \frac{-\frac{1}{\rho_i}s + 1}{\frac{1}{\rho_i}s + 1}, \cdots, \prod_{i=1}^{k} \frac{-\frac{1}{\rho_i}s + 1}{\frac{1}{\rho_i}s + 1} \right\} \tag{3.18}$$

where ρ_i $(i = 1, \ldots, k)$ are the non-minimum zeros of $G(s)$. The IMC controller is then obtained as $Q = G^{-1}G_+f$. This method generally leads to the introduction of RHP zeros not originally present in the system $G(s)$ [19] and hence the resulting Q may be non-minimum phase.

Method 2. Interactive IMC Control [72; 23]. Suppose the square system $G(s)$ has only one RHP zero ρ, the effect of the RHP zero can be shifted to one output considered to be of least importance. This is usually achieved by choosing a triangular structure for G_+. Consider a two-input two-output system, shifting the effect of the RHP zero to the first output results in the following lower triangular factorization

$$G_+^{L.T}(s) = \begin{bmatrix} 1 & 0 \\ \frac{\alpha s}{\frac{1}{\rho_i}s+1} & \frac{-\frac{1}{\rho_i}s+1}{\frac{1}{\rho_i}s+1} \end{bmatrix}. \tag{3.19}$$

An upper triangular factorization results when the effect of the RHP zero is

shifted to the second output as

$$G_+^{U.T}(s) = \begin{bmatrix} \frac{-\frac{1}{\rho_i}s+1}{\frac{1}{\rho_i}s+1} & \frac{\beta s}{\frac{1}{\rho_i}s+1} \\ 0 & 1 \end{bmatrix}. \tag{3.20}$$

The off-diagonal factors α and β are computed as follows (see [72] for detailed discussions)

$$\begin{aligned} \alpha =& \frac{-2\hat{g}_{j1}(\rho)}{\rho\hat{g}_{j2}(\rho)} \quad \text{for arbitrary } j \\ \beta =& \frac{-2\hat{g}_{j2}(\rho)}{\rho\hat{g}_{j1}(\rho)} \end{aligned}$$

where $\hat{g}_{ji}$ represents the (j,i) elements of the inverse of $G(s)$.

A similar triangular structure for G_+ can be obtained by using the concept of the generalized interactor matrices [74]. The idea of controller interactor matrices has also been used in the conditioning anti-windup design for feedback controllers with non-minimum characteristics [75; 7].

Method 3. IMC design based on reduced order of the model after Wang *et al* [76]. Here, a model reduction algorithm is used to find a second-order rational transfer function plus dead-time model. The aim is that this model should be a good approximation to the controller. For example, the reduced order for $\det(G)$, the determinant of G, is represented as

$$\det(\tilde{G}) = \frac{b_2 s^2 + b_1 s + G(0)}{a_2 s^2 + a_1 s + 1} e^{-Ls} \tag{3.21}$$

where L is an unknown time delay and its obtained by minimizing the error between $\det(G)$ and $\det(\tilde{G})$ over all possible range of L. The original literature contains algorithm for obtaining L.

The desired decoupled closed loop response is obtained as $H(s) = \text{diag}\{h_{ii}(s)\}$

with

$$h_{ii}(s) = e^{-\left(\tau(\det(\tilde{G}))-\tau_i\right)s} \prod_{\rho \epsilon Z^+_{\det(\tilde{G})}} \left(\frac{\rho - s}{\rho + s}\right)^{\eta_z(\det(\tilde{G}(s)))-\eta_i(z)} f_i(s)$$

$$\tau_i = \min_{j|G^{ij}\neq 0} \tau(G^{ij})$$

$$\eta_i(z) = \min_{j|G^{ij}\neq 0} \eta_z(G^{ij})$$

where $f_i(s)$ is the ith loop IMC filter, adj $(G) = [G^{ji}]$, $\tau(.)$ is the time delay of $(.)$, $\eta_z(.)$ is the number of non-minimum zeros of $(.)$ and $Z^+_{\det(\tilde{G})}$ is the set of unstable zeros of $(.)$.

The IMC controller can be obtained as

$$Q_{ii} = \frac{G^{ii}}{\det\tilde{G}} h_{ii} \tag{3.22}$$

$$Q_{ji} = \frac{G^{ij}}{\det\tilde{G}} h_{ii} \quad \forall i, j \quad (j \neq i). \tag{3.23}$$

As illustrated in [73], this method is most useful for plants with multiple time delays but at the expense of introducing time delays and non-minimum phase zeros in the IMC controller. Hence, it is problematic for anti-windup design.

Method 4. All-Pass factorization in terms of Blaschke products [77; 49]. Consider the square system $G(s)$ with ρ_i $(i = 1, \ldots, k)$ RHP zeros and associated input and output zero directions η_i and ξ_i, respectively. Then $G(s)$ can be factored as

$$G(s) = G_-(s)\mathcal{B}_k(s) \cdots \mathcal{B}_1(s) \tag{3.24}$$

where $G_-(s)$ is the minimum phase factor and $\mathcal{B}_i(s)$ corresponds to the all-pass factor associated with ρ_i. $\mathcal{B}_k(s) \cdots \mathcal{B}_1(s)$, known as the Blaschke products [77] and $G_-(s)$ are given as

$$\mathcal{B}_i(s) = I - \frac{2Re(\rho_i)}{s + \bar{\rho}_i} \eta_i \eta_i^* \tag{3.25}$$

$$G_- = C(sI - A)^{-1}\mathcal{B}^{(k)} + D. \tag{3.26}$$

The $\mathcal{B}^k(s)$ is computed from the following iterative procedure starting with $\mathcal{B}^{(0)} = B$

$$\mathcal{B}^{(i)} = \mathcal{B}^{(i-1)} - 2Re(\rho_i)\xi_i\eta_i^* \quad \text{for } i = 1, \cdots, k.$$

This factorization scheme is applicable to strictly proper systems (i.e. plants having the feedthrough term $D = 0$) and does not introduce non-minimum phase zeros into the IMC controller (3.17).

Method 5. Inner-Outer Factorization.
Any rational proper system $G(s)$ can be factorized as

$$G(s) = G_i G_o \tag{3.27}$$

where G_i is inner i.e. $G_i(jw)^* G_i(jw) = I$, for all w and G_o is outer i.e. G_o is stable and minimum phase. Numerical procedures exist in the literature (e.g. [19; 49; 78]) for obtaining the state space realizations for the factorization in (3.27). A particular inner-outer factorization algorithm is given as follows.

Inner-Outer Factorization Algorithm [19]

Let $G \in \mathcal{RH}_\infty$ be bi-proper with no zeros on the imaginary axis and with a minimal state-space realization

$$G = \left[\begin{array}{c|c} A & B \\ \hline C & D \end{array}\right]. \tag{3.28}$$

Then, a particular inner-outer factorization of G is given by

$$G_i = \left[\begin{array}{c|c} A + B\mathcal{R}^{-1}F_o & B\mathcal{R}^{-1} \\ \hline C + \mathcal{Q}F_o & \mathcal{Q} \end{array}\right], \quad G_o = \left[\begin{array}{c|c} A & B \\ \hline -F_o & \mathcal{R} \end{array}\right] \tag{3.29}$$

where F_o is chosen according to $F_o = -(\mathcal{Q}^T C + (B\mathcal{R}^{-1})^T X)$ with X as the stabilizing solution of the algebraic Riccati equation

$$(A - B\mathcal{R}^{-1}\mathcal{Q}^T C)^T X + X(A - B\mathcal{R}^{-1}\mathcal{Q}^T C) - X(B\mathcal{R}^{-1})(B\mathcal{R}^{-1})^T X = 0,$$

$D = \mathcal{QR}$ is the QR factorization of D into an orthogonal matrix $\mathcal{Q}$

$(\mathcal{Q}^T\mathcal{Q} = I)$ and an upper triangular matrix $\mathcal{R}$.

Compared with (3.16), $G_+ = G_i$ and $G_-(s) = G_o$. This implies that the IMC controller (3.17) obtained through this scheme is minimum phase. The inner-outer factorization algorithm above requires G to be bi-proper. If G is strictly proper (i.e. $D = 0$), a common practice is to set $D = \epsilon I$ where ϵ is chosen small to obtain a satisfactory result. IMC control design based on this scheme has successfully been applied to the quadruple coupled-tank system (e.g. [79]).

In summary, it is desirable in standard anti-windup designs for internal model control that the nominal IMC controller be minimum phase. However, designing a minimum-phase IMC controller for plants with non-minimum phase zeros may demand that certain level of interactions be tolerated in the closed loop response. The all-pass based factorization methods 4 and 5 discussed above provide means for achieving this compromise. In particular, the inner-outer factorization scheme will be further exploited for the design of multivariable IMC anti-windup control for non-minimum phase systems.

3.4 Anti-windup Design Methods: A Study of Structure and Configurations

The underlying principle of anti-windup schemes for linear systems with saturating actuators is to provide a mechanism for modifying the control during saturation so as to account for the detrimental effects of input nonlinearities. The aim of such modifications is mainly to recover as much as possible the linear performance or to provide graceful performance degradation when there are actuator saturations. In the early anti-windup compensation schemes, modifications of the control were usually carried out in an ad-hoc fashion and based on intuition. These early schemes (see [35; 32] for a survey) pro-

vide problem-specific solutions to the anti-windup design challenge and often lack a rigorous theoretical basis as well as stability and performance guarantees. There have been attempts to unify these primitive schemes into a general framework suitable for stability analysis [35; 32; 14]. Recently, new anti-windup designs results have appeared in the literature which provide rigorous stability analysis and performance guarantees [80; 34; 5; 15; 16; 21]. These generally fall into the class of anti-windup [18] where the anti-windup design problem is reduced to linear matrix inequalities (LMI) formulation of convex optimization problem. Some of these modern anti-windup schemes are discussed within the general anti-windup framework of Fig. 3.9.

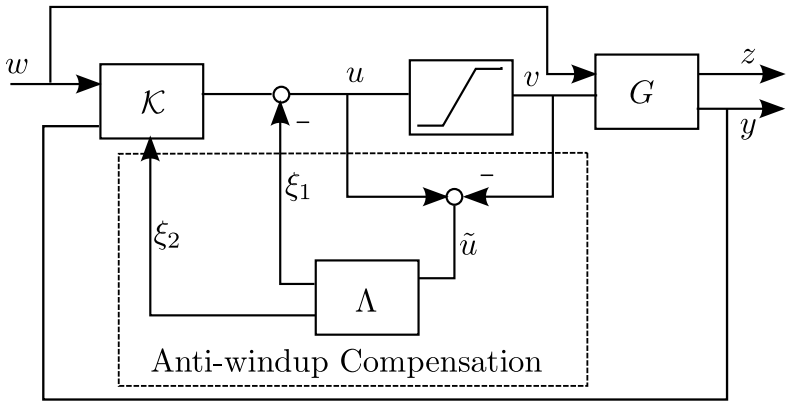

Figure 3.9: The general anti-windup framework

Let the nominal or unconstrained control have the following state-space realization

$$K \sim \begin{aligned} \dot{x}_k &= A_k x_k + B_w w + B_y y \\ u &= C_k x_k + D_w w + D_y y, \end{aligned}$$

then the compensated or augmented controller $\mathcal{K}$ in Fig. 3.9 can be expressed as

$$\mathcal{K} \sim \begin{aligned} \dot{x}_k &= A_k x_k + B_w w + B_y y + B_{\xi_2}\xi_2 \\ u &= C_k x_k + D_w w + D_y y + D_{\xi_2}\xi_2 - \xi_1. \end{aligned} \tag{3.30}$$

In this general framework, the difference between the unsaturated control u

and the saturated control v is fed through a compensating filter Λ to generate the two conditioning signals ξ_1 and ξ_2. The input w denotes the exogenous signals which may include the reference signal, the disturbance signal and the effects of measurement noise while z is the performance signal to which a performance criterion is usually associated. Typically, the performance is specified in terms of the minimization of some $\mathcal{L}_2$ gain from the exogenous input w to the performance output z [5; 15]. Other performance specifications have been adopted depending on the goal of the anti-windup design [36; 16; 81; 46].

The anti-windup design problem then reduces to the problem of finding appropriate control modifications such that *a*) the nominal closed-loop remains unmodified if there are no input saturations *b*) the closed-loop stability is ensured during control input saturations; *c*) the nonlinear performance during saturations is optimized by minimizing appropriate performance criterion; and *d*) the linear performance (which is assumed desirable) is recovered swiftly after a period of saturation. These anti-windup design objectives were first formalized in [37].

Many of the existing anti-windup appear as special cases of the general anti-windup framework of Fig. 3.9 depending on the choice of the filter Λ and on how the conditioning signals ξ_1, ξ_2 are injected into the linear control. There are following cases;

Full Authority Anti-windup In this case, the anti-windup compensator can inject signals directly to the states and to the output of the pre-designed linear controller. This corresponds to setting $B_{\xi_2} = I$ and $D_{\xi_2} = 0$ in (3.30). This configuration characterizes most of the early classical anti-windup schemes which were unified into the coprime-factorization framework [35]. The full authority configuration was also employed in [5; 15] and incorporating robustness in [82] to develop LMI-based synthesis procedure with global stability and performance guarantees.

External Anti-windup Here, the anti-windup compensator can only affect both or either of the input or the output of the linear controller. This corresponds to setting $B_{\xi_2} = B_y$ and $D_{\xi_2} = D_y$ in (3.30). This is a stricter condition as the anti-windup compensation can no longer directly modify the states of the unconstrained controller. This situation naturally arise when anti-windup compensator is to be retrofitted into an existing embedded control application or where the controller in implemented using analogue hardware (e.g. [83]).

Static Anti-windup For static anti-windup schemes, Λ is taken to be constant gain which must be synthesized such that the linear controller is conditioned during saturations while guaranteeing closed loop stability. The compensating filter Λ in Fig. 3.9 assumes the following form

$$\xi = \begin{bmatrix} \xi_1 \\ \xi_2 \end{bmatrix} = \begin{bmatrix} \Lambda_1 \\ \Lambda_2 \end{bmatrix} \tilde{u}. \tag{3.31}$$

The first attempt at synthesizing a globally stabilizing anti-windup compensation with guaranteed performance level employed the static anti-windup configuration [80; 5].

Dynamic Anti-windup Here, Λ is taken to be a linear and time-invariant filter which modifies the system behavior during saturations and it is such that the linear performance is recovered as fast as possible. Including the dynamics, the compensating filter assumes the following form

$$\Lambda \sim \begin{aligned} \dot{x}_{aw} &= \Lambda_a x_{aw} + \Lambda_b \tilde{u} \\ \xi &= \Lambda_c x_{aw} + \Lambda_d \tilde{u}. \end{aligned} \tag{3.32}$$

Popular dynamic anti-windup schemes [6; 2; 3; 38; 33] may also interpreted using the generic anti-windup configuration [14]. When the order of the filter (3.32) is equal to the order of the plant, the anti-windup compensation is referred to as full-order dynamic anti-windup compensation. Anti-windup compensations with order less than the

order of the plant have also appeared in the literature [16; 84]. These are generally referred to as low-order anti-windup

We now consider the coprime-factorization parametrization of anti-windup schemes and how it relates to the internal model control-based anti-windup structures [6; 2].

3.4.1 Coprime-Factor based Anti-windup Schemes

For the subsequent discussion, we consider the one-degree of freedom nominal controller represented as

$$K \sim \left[\begin{array}{c|c} A_k & B_k \\ \hline C_k & D_k \end{array}\right].$$

We assume that the nominal controller K stabilizes the plant G. Since the plant G is also assumed stable, we can write [77]

$$Q = K(I + GK)^{-1} = (I + KG)^{-1}K \tag{3.33}$$

where Q is the stable internal model controller. This assumption follows the design approach of modern anti-windup schemes where the nominal controller is assumed to have been designed to induce desirable properties including nominal stability and performance (see e.g. [16; 21]). In what follows, we establish the link between the coprime-factor based anti-windup parameterizations and the modified internal model control anti-windup structure.

3.4.1.1 Left-Coprime factor based Anti-windup parametrization

Using the static configuration corresponding to (3.31), Kothare *et al* [35] parametrize almost all existing linear anti-windup controllers in terms of the

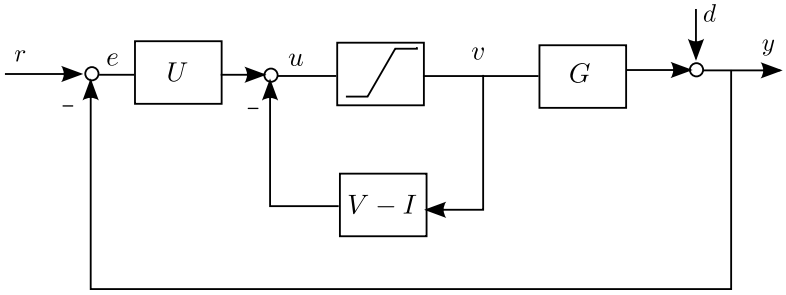

Figure 3.10: Anti-windup framework based on left-coprime factorization

left-coprime factorization of the nominal controller $K = V^{-1}U$ where U and V have the following state-space representations

$$\begin{bmatrix} V & U \end{bmatrix} = \left[\begin{array}{c|cc} A_k + J_1 C_k & J_1 & B_k + J_1 D_k \\ \hline J_2 C_k & J_2 & J_2 D_k \end{array}\right] \tag{3.34}$$

$$J_1 = -\Lambda_1 (I + \Lambda_2)^{-1} \tag{3.35}$$

$$J_2 = (I + \Lambda_2)^{-1}. \tag{3.36}$$

Here, J_1 is to be designed such that $A_k + J_1 C_k$ is stable and J_2 is non-singular. The design parameter J_1 can be assigned almost arbitrarily provided the pair (C_k, A_k) is observable. The resultant anti-windup system is represented in Fig. 3.10 where the compensated controller is given by $\mathcal{K} = [I - V \quad U]$ and the closed-loop equation is

$$u = Ue - (V - I)v. \tag{3.37}$$

Comparing this with the closed-loop equation for the modified IMC anti-windup where

$$u = Q_1 e - (Q_2 - Q_1 G)v, \tag{3.38}$$

we have that $Q_1 = U$ and $Q_2 = V^{-1}(I + KG) - I$. Substituting for $(I + KG)$ in the second term using the relation in (3.33), we have following equivalence

$$\begin{aligned} Q_1 &= U \\ Q_2 &= UQ^{-1} - I. \end{aligned} \tag{3.39}$$

A generalization of the static anti-windup configuration [35] was proposed in [36] which permits a dynamic anti-windup compensation. Given an initial arbitrary left-coprime factorization of the nominal controller $K = V^{-1}U$, the anti-windup design problem is reduced to finding a free parameter R such that the compensated controller is given by $\mathcal{K} = [I - \tilde{V} \quad \tilde{U}]$ with

$$\begin{aligned} \tilde{U} &= RU \\ \tilde{V} &= RV \end{aligned} \tag{3.40}$$

where R is a unimodular transfer function matrix (i.e R is a stable unit and has a stable inverse R^{-1}). This parameterization extends the fixed-order left-coprime factorization of [35] to all possible coprime factorizations of the controller. This extra degree of freedom allowed the anti-windup design problem to be formulated in the H_∞ design framework [36]. The downside however, is that the order of the extra parameter R is appended to the order of the linear controller to give the order of the augmented controller. This could lead to a significant increase in the overall controller order with its associated implementation issues. This parameterization was extended to incorporate uncertain plants in [85].

3.4.1.2 Right-Coprime factor based Anti-windup parametrization

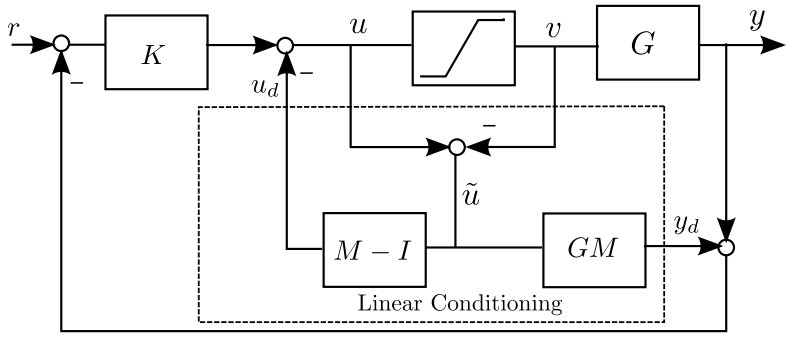

Figure 3.11: Anti-windup framework based on right coprime factorization

An anti-windup structure introduced in [34] is shown in Fig. 3.11. This structure corresponds to the external anti-windup configuration where most

of the existing linear anti-windup schemes are interpreted in terms of a linear dynamic filter M. The filter M is designed independently of the nominal controller such that desired closed-loop nonlinear characteristics are induced. Among the different design choices available for M, it has been shown that a suitable choice is based on the coprime-factor of the nominal plant G [81]. Writing the closed-loop equation for Fig. 3.11 gives

$$u = (M + KGM)^{-1}Ke - [(M + KGM)^{-1} - I]v \tag{3.41}$$

where e is the error between the reference signal r and the plant output y. Comparing with the modified IMC structure of Fig. 3.3 with closed-loop equation (3.38), we have the following equivalence

$$\begin{aligned} Q_1 &= M^{-1}Q \\ Q_2 &= M^{-1} - I. \end{aligned} \tag{3.42}$$

It follows trivially that when $M = I$, the anti-windup structure of Fig. 3.11 recovers the conventional IMC structure of Fig. 3.3 where $Q_1 = Q$ and $Q_2 = 0$ [6]. Typically, M is chosen as part of the right coprime factorization of the plant $G = NM^{-1}$ (e.g. [16]) with

$$\begin{bmatrix} M \\ N \end{bmatrix} = \left[\begin{array}{c|c} A + BF & B \\ \hline F & I \\ C + DF & D \end{array}\right] E \tag{3.43}$$

where F is such that $A + BF$ is Hurwitz and E is a non-singular constant matrix.

If we choose the left-coprime factorization of the nominal controller $K = V^{-1}U$ and the right-coprime factorization of the nominal plant $G = NM^{-1}$ such that the following Bezout identity is satisfied

$$VM + UN = I, \tag{3.44}$$

then the two coprime-factorization based anti-windup parameterizations of

[35] and [34] are equivalent. It is desirable, but not necessary, to have the design parameters J_2 and E to be identity so as to eliminate algebraic-loops in the controller implementation. The design freedom of choosing $E \neq I$ has recently been investigated in [86] and exploited in [81; 45]. Special properties such as inner N (i.e. $N(jw)^*N(jw) = I$, $\forall w$) can also be obtained by choosing F and E appropriately. Such properties may prove very useful when designing IMC-based anti-windup compensator for systems with non-minimum phase characteristics as will be discussed in the chapter 4. A similar anti-windup parameterization to that of the modified IMC in (3.42) is the Youla parameterization based anti-windup configuration [87; 88]. The IMC anti-windup design of [2] may also be interpreted in terms of the parametrization of (3.42) where the non-causal filter f_A is now chosen as $f_A = N^{-1}$. This interpretation provides insights into the design of the filter f_A which was not clear in [2] except that it satisfies some technical conditions.

From (3.39) and (3.42), we can see that the modified IMC anti-windup design can be interpreted as choosing a particular left-coprime factorization of the nominal controller K or a particular right-coprime factorization of the nominal plant G.

3.5 Summary

We have shown the inherent anti-windup characteristics of the internal model control structures. The link between the IMC anti-windup design and the coprime-factor based anti-windup schemes allows the parameterization of all existing linear anti-windup schemes for stable plants in terms of the internal model controller. This parametrization provides a way for extending the existing modern anti-windup synthesis techniques to the design of IMC anti-windup while retaining the its transparent tuning for robustness as well as its simple characterization of the trade-off between stability and performance.

Chapter 4

Anti-windup Design for Multivariable Internal Model Control: LMI Approach

4.1 Introduction

Internal model control (IMC) is a preferred control design choice for inherently stable plants due to its transparent tuning for robustness [19]. The IMC structure has been shown to possess some intrinsic anti-windup characteristics for saturating systems [6; 89] while also preserving the robustness of the unsaturated control loop to additive type norm-bounded uncertainties [16; 20]. However, nonlinear performance may be excessively sluggish especially when the plant has lightly damped modes, slow dynamics or non-minimum phase zeros. This performance degradation has led to a number of enhancements to the internal model control to improve the nonlinear performance [1; 2; 90; 33]. The IMC anti-windup designs in [1] and [2] are particularly useful when the IMC controller Q is minimum-phase. Internal stability problems may arise if the IMC controller Q has non-minimum phase zeros.

Although not always desired, there are various reasons why the nominal IMC controller may include non-minimum phase zeros. For instance, the classical decoupling IMC design procedures for square multivariable plants with non-minimum zeros often introduces extra non-minimum zeros in the closed-loop dynamics such that the resulting IMC controller Q is non-minimum phase [72; 74].

It is standard in the anti-windup literature to express the saturated loop in terms of a feedback interconnection involving a deadzone nonlinearity and a feedthrough term (e.g. [34; 5; 36]). With this equivalent representation, the effects of the input saturations can be considered as a fictitious disturbance signal at the input [36] or the output [34] of the linear plant. The anti-windup design may therefore be considered as design strategy for rejecting this fictitious disturbance. This interpretation allows the extension of existing classical linear control design methods for disturbance rejection (e.g [91]) to the anti-windup design problem.

The main contribution of this chapter is the synthesis of dynamic anti-windup for open-loop stable plants using the internal model control structure and its interpretations in terms of the existing schemes. The anti-windup compensation is defined solely in terms of the plant and its inner-outer factors as opposed to similar schemes (e.g. [36; 33]) where independent dynamic elements are introduced leading to increased controller order. The synthesizing LMI has a similar structure to that in [21], but the treatment here provides insights into the effectiveness of such LMI-based anti-windup scheme. As compared to other dynamic compensation techniques (e.g. [3; 37; 34; 38]), the approach considered here offers a systematic way of anti-windup design while taking advantage of the attractive features of internal model control structure.

The rest of the chapter is structured as follows. In section 4.2, the anti-windup design is posed as a disturbance rejection control problem. Using the modified internal model control structure, loop sensitivities are derived that

capture the effects of the input saturations on closed loop stability and performance. In section 4.3, the stability of the proposed IMC anti-windup design is established through the multivariable circle criterion. Closed-loop stability check is reduced to the feasibility of a linear matrix inequality (LMI). An optimal solution of the anti-windup problem which guarantees both closed-loop stability and a given level of performance is discussed in section 4.4. The performance objective is specified in terms of an induced $\mathcal{L}_2$ gain which is directly linked with the behaviour of the closed-loop system under saturation. Finally in section 4.5, a simulated case-study example is used to demonstrate the effectiveness of the proposed method and to compare its performance with several existing anti-windup schemes in the literature.

4.2 IMC Anti-windup Based on Inner-Outer Factorization

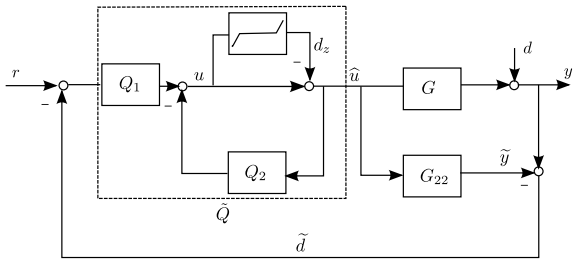

Figure 4.1: IMC anti-windup with deadzone nonlinearities.

We consider the modified internal model control structure of Fig. 3.4 where the anti-windup design reduces to that of finding appropriate factorization of the nominal internal model controller Q into Q_1 and Q_2 such that nonlinear performance is enhanced while guaranteeing closed-loop internal stability. At the same time, the desired linear performance is to be recovered when there are no input saturations i.e. Q_1 and Q_2 are constrained to satisfy $Q = (I + Q_2)^{-1}Q_1$ during linear operation. Using the fact that saturation

and deadzone nonlinearities are related through the identity(e.g. [34; 5; 36])

$$\mathrm{Dz}(u) = u - \mathrm{Sat}(u) \tag{4.1}$$

where Dz(.) and Sat(.) represent the deadzone and saturation functions respectively, the modified IMC anti-windup structure of Fig. 3.4 can be equivalently represented as Fig. 4.1. Assuming no plant-model mismatch, the closed-loop equations are given by

$$\begin{aligned} \begin{bmatrix} y \\ u \\ \hat{u} \end{bmatrix} &= \begin{bmatrix} GQ & I - GQ & -G(I+Q_2)^{-1} \\ Q & -Q & (I+Q_2)^{-1}Q_2 \\ Q & -Q & -(I+Q_2)^{-1} \end{bmatrix} \begin{bmatrix} r \\ d \\ d_z \end{bmatrix} \\ d_z &= \mathrm{Dz}(u). \end{aligned} \tag{4.2}$$

The effect of the input nonlinearities on both closed-loop performance and stability can be judged from the contributions of the sensitivities functions T_{yd_z}, T_{ud_z} and $T_{\hat{u}d_z}$ from d_z (assumed to be a fictitious disturbance signal without the non linearities) to y, u and $\hat{u}$ respectively. These sensitivities are obtained from (4.2) as

$$T_{yd_z} = -G(I+Q_2)^{-1} \tag{4.3}$$

$$T_{ud_z} = (I+Q_2)^{-1}Q_2 \tag{4.4}$$

$$T_{\hat{u}d_z} = -(I+Q_2)^{-1}. \tag{4.5}$$

T_{ud_z} plays an important role in determining the closed-loop stability as it represents the loop transfer function matrix around the static nonlinearity. $T_{\hat{u}d_z}$ and T_{yd_z} on the other hand represent the difference between the desired linear performance and the degraded nonlinear performance as they capture respectively the effects of the nonlinearity on the input and output of the plant G. The three sensitivities T_{yd_z}, T_{ud_z} and $T_{\hat{u}d_z}$ all contain the term $(I+Q_2)^{-1}$ which also appears in the factorization of the IMC controller Q [cf. [36; 33] where the sensitivities are expressed in terms of an additional independent design parameter]. The sensitivity function $T_{\hat{u}d_z}$ is of primary importance in judging the performance of the anti-windup design

as it governs the disturbance rejection properties of the equivalent structure Fig. 4.1 to the fictitious disturbance signal d_z due to the effect of the input nonlinearity.

To achieve a good nonlinear performance and closed-loop stability, the anti-windup design needs to realize the following aims.

1. The sensitivities $T_{yd_z} = -G(I + Q_2)^{-1}$ and $T_{\hat{u}d_z} = -(I + Q_2)^{-1}$ must be small in some sense. This is to ensure that the effect of the fictitious disturbance due to input nonlinearities on the plant's input and output is lessened.

2. The factor Q_2 is chosen such that any non-minimum phase zeros of Q appears only in Q_1. This is necessary to ensure internal stability of the closed-loop system. This requirement also implies that there are no unstable pole-zero cancellations between Q_1 and $(I + Q_2)^{-1}$. A further implication is that any non-minimum phase zeros of G or Q appears in the sensitivity T_{yd_z} which places a fundamental limitation on the achievable performance of the anti-windup design depending on the location of such non-minimum phase zeros.

3. The slow poles of G are canceled from the sensitivity $T_{yd_z} = -G(I + Q_2)^{-1}$. The slow poles of G will induce sluggish response of T_{yd_z} to the fictitious disturbance signal. This requirement is desirable for good performance since it will ensure swift recovery of linear performance after a period of control input saturations.

Suppose the plant admits an inner-outer factorization $G = G_i G_o$ where G_i is inner (i.e. $G_i(jw)^* G_i(jw) = I, \forall w$) and G_o is outer(i.e. G_o is minimum phase and invertible). Suppose further that G_o has a right coprime factorization $G_o = N_o M_o^{-1}$. Then a natural way of achieving the above objectives is by choosing $(I + Q_2)^{-1}$ as M_o. With this choice, we have that $T_{yd_z} = -G_i N_o$ and $T_{\hat{u}d_z} = -M_o$. It follows that the poles of G do not appear in T_{yd_z} as the poles of G_i are the stable mirror image of the non-minimum phase zeros

of G. It is easy to show that this choice is equivalent to the right coprime factor paramterization of (3.42) as follows.

Lemma 3. Let $G \in \mathcal{RH}_\infty$ be bi-proper with no zeros on the imaginary axis and with a minimal state-space realization $G = \left[\begin{array}{c|c} A & B \\ \hline C & D \end{array}\right]$. Suppose $G = G_i G_o$ where G_i is inner and G_o is outer with $G_o = N_o M_o^{-1}$ a right coprime factorization where $N_o, M_o \in \mathcal{RH}_\infty$, then G has the fractional representation $G = NM^{-1}$ where $N = G_i N_o$ and $M = M_o$. Furthermore, M and N are coprime and admit the following state space realizations

$$\begin{bmatrix} M \\ N \end{bmatrix} = \begin{bmatrix} M_o \\ G_i N_o \end{bmatrix} = \left[\begin{array}{c|c} A + BF & B \\ \hline F & I \\ C + DF & D \end{array}\right] \tag{4.6}$$

where F is the state feedback gain associated with the coprime factorization of G_o such that $A + BF$ is Hurwitz.

Proof. Let the factors G_i and G_o be computed from (3.29) as

$$G_i = \left[\begin{array}{c|c} A + BR^{-1}F_o & BR^{-1} \\ \hline C + \mathcal{Q}F_o & \mathcal{Q} \end{array}\right], G_o = \left[\begin{array}{c|c} A & B \\ \hline -F_o & \mathcal{R} \end{array}\right] \tag{4.7}$$

where $D = \mathcal{QR}$ is a QR factorization of D and F_o is such that $F_o = -(\mathcal{Q}^T C + (B\mathcal{R}^{-1})^T X)$ with X a stabilizing solution of the algebraic Riccati equation

$$(A - B\mathcal{R}^{-1}\mathcal{Q}^T C)^T X + X(A - B\mathcal{R}^{-1}\mathcal{Q}^T C) - X(B\mathcal{R}^{-1})(B\mathcal{R}^{-1})^T X = 0.$$

Let the factors N_o and M_o be computed from G_o as

$$\begin{bmatrix} M_o \\ N_o \end{bmatrix} = \left[\begin{array}{c|c} A + BF & B \\ \hline F & I \\ \mathcal{R}F - F_o & \mathcal{R} \end{array}\right]. \tag{4.8}$$

The state space realization for N is obtained by carrying out the cascade

operation of G_i and N_o

$$G_i N_o = \left[\begin{array}{cc|c} A + B\mathcal{R}^{-1}F_o & B\mathcal{R}^{-1}(RF - F_o) & B \\ 0 & A + BF & B \\ \hline C + \mathcal{Q}F_o & DF - \mathcal{Q}F_o & D \end{array}\right] \tag{4.9}$$

followed by a state similarity transformation using

$$\left[\begin{array}{cc} I & I \\ 0 & I \end{array}\right]$$

This is exactly the coprime factorization of [21]. □

The IMC anti-windup design then reduces to finding an appropriate right coprime factorization of the outer factor G_o of the plant G such that the closed-loop system of Fig. 4.1 is stable and the nonlinear performance is enhanced. This can be reduced to a convex search over linear matrix inequality constraints.

4.3 Stability and Performance Analysis

In this section, we demonstrate a sector bound condition for the stability of the proposed IMC anti-windup via the multivariable circle criterion [52]. The following definition is important for the derivation of the stability result.

Definition 21 (Strictly Positive Realness[52])**.** A square transfer function matrix G is strictly positive real if;

1. G is asymptotically stable.
2. $G(jw) + G^*(jw)$ is positive definite $\forall w$
3. $G(\infty) + G(\infty)^T > 0$.

Lemma 4 (Strictly Positive Realness[60])**.** For a given stable transfer function matrix G with state-space matrices $G = \left[\begin{array}{c|c} A & B \\ \hline C & D \end{array}\right]$, the following are equivalent

1. G is strictly positive real.
2. $\exists X = X^T > 0$ satisfying the quadratic matrix inequality

$$A^T X + XA + (XB - C^T)(D + D^T)^{-1}(XB - C^T)^T < 0.$$

3. $\exists X = X^T > 0$ such that the LMI

$$\begin{bmatrix} A^T X + XA & XB - C^T \\ B^T X - C & -(D + D^T) \end{bmatrix} < 0$$

is feasible.

4.3.1 Unconstrained Stability

For an unconstrained system (i.e $u = \text{Sat}(u)$), the closed-loop equation reduces to

$$\begin{bmatrix} y \\ u \end{bmatrix} = \begin{bmatrix} GQ & I - GQ \\ Q & -Q \end{bmatrix} \begin{bmatrix} r \\ d \end{bmatrix}. \tag{4.10}$$

Internal stability of the closed-loop is guaranteed if both the plant G and the controller Q are stable [19].

4.3.2 Constrained Stability

It is known that both Dz(.) and Sat(.) belong to the sector $[0, I]$ [52]. The nominal stability of the closed-loop system of Fig. 4.1 can be assessed through

the multivariable circle criterion [52].

From equation (4.2), the transfer function from the fictitious disturbance d_z to the unconstrained input u is given by

$$T_{ud_z} = I - M \tag{4.11}$$

where M is defined in (4.6). The state-space realization of T_{ud_z} is obtained as

$$T_{ud_z} = \left[\begin{array}{c|c} A+BF & B \\ \hline -F & 0 \end{array}\right]. \tag{4.12}$$

The anti-windup structure of Fig. 4.1 is asymptotically stable if $I - T_{ud_z}$ is strictly positive real (SPR). This stability condition can be reduced to an LMI feasibility problem via lemma 4. We now state the following stability result.

Theorem 1. Given a stable plant G with coprime factorization of (4.6) and a stable IMC controller Q, the closed-loop in Fig. 4.1 with closed-loop equations (4.2) is asymptotically stable if $\exists P = P^T > 0$ such that the following LMI with variables P and L is satisfied

$$\begin{bmatrix} AP + PA^T + BL + L^TB^T & B - L^T \\ B^T - L & -2I \end{bmatrix} < 0. \tag{4.13}$$

Proof. The closed-loop in Fig. 4.1 is asymptotically stable if $I - T_{ud_z}$ is strongly positive real or equivalently (using lemma 4)

$$\begin{bmatrix} XA + A^TX + XBF + F^TB^TX & XB - F^T \\ B^TX - F & -2I \end{bmatrix} < 0. \tag{4.14}$$

By a simple congruence transformation using $\mathrm{diag}(X^{-1}, I)$ and defining $P = X^{-1}$, $L = FP$ in equation (4.14), we obtain the LMI in (4.13). □

Remark 4. The stability result of (4.13) is slightly restrictive because we have not exploited the weighting matrix W associated with the sector bounded

condition (2.14). We will remove this restriction in section 4.4. A stronger stability condition may also be obtained by introducing multipliers such as the Popov and Zames-Falb [92] [see [93] for discussion involving static multipliers].

The anti-windup design objective is not only to guarantee the closed-loop stability but also to ensure graceful closed-loop performance degradation in the presence of control input nonlinearities. As earlier discussed, T_{yd_z} and $T_{\hat{u}d_z}$ must be small in some sense for good performance. Since d_z also depends on u through the nonlinearity, the performance objective may be realized by minimizing the $\mathcal{L}_2$ gain from u to the channels y_d and $\hat{u}_d$ representing the outputs of the filters T_{yd_z} and $T_{\hat{u}d_z}$ respectively. It follows from (4.2) that $y_d = y - y_{lin}$ and $\hat{u}_d = \hat{u} - u_{lin}$ where u_{lin} and y_{lin} denote the intended unconstrained control input and plant output respectively. The signals y_d and $\hat{u}_d$ thus represent the deviations between the constrained and the unconstrained control input and plant output respectively. Ideally, we will like to make $T_{\hat{u}d_z} = 0$ to achieve the best performance. However, this choice may create an ill-posed algebraic loop around the nonlinearity which may cause closed-loop instability. This is because the loop transfer function matrix around the nonlinearity can be expressed as $T_{ud_z} = I - T_{\hat{u}d_z}$. If we set $T_{\hat{u}d_z} = 0$, then $T_{ud_z} = I$ and the nonlinear loop reduces to the interconnection of a deadzone nonlinearity in feedback with the identity. Such a loop may not have any solution or have many solutions. On the other hand, the choice $T_{\hat{u}d_z} = I$ guarantees closed-loop stability but any slow poles of G will appear in T_{yd_z}, which may degrade closed-loop performance. In essence, $T_{\hat{u}d_z}$ is shaped as a sensitivity function whose magnitude approaches zero at high frequencies while T_{yd_z} is to be shaped as a complementary sensitivity function whose magnitude approaches unity at high frequencies. The trade-off arises because $T_{\hat{u}d_z}$ and T_{yd_z} are not independent of each other. Hence the trade-off between stability and performance must be accounted for during the anti-windup design to reach the best compromise. This can be achieved through an appropriate choice of performance objective.

In frequency-based anti-windup designs [36; 33], the trade-off between stability and performance is addressed through appropriate choice of frequency-dependent weightings for shaping the filters at closed-loop bandwidth of interest. In [36; 80], the anti-windup design problem is cast as a standard H_∞ optimization problem. In [2], the nonlinear performance is optimized in terms of the 1-norm of the instantaneous difference between the filtered version of the constrained and the unconstrained responses i.e $f[y - y_{lin}]$. A more common approach is to define the the performance objective in terms of optimization of the $\mathcal{L}_2$ gain from some exogenous input to the desired output [37; 5; 94; 15; 16]. This is the approach we adopt here. We will like to minimize a weighted combination of the two maps $u \to y_d$ and $u \to \hat{u}_d$. This can be represented as ensuring

$$\left\| \begin{array}{c} W_s^{\frac{1}{2}} y_d \\ W_p^{\frac{1}{2}} \hat{u}_d \end{array} \right\|_2 < \gamma \left\| u \right\|_2 \tag{4.15}$$

where W_p and W_s are weighting matrices which are chosen to capture the trade off between performance and stability robustness. The parameter γ is the $\mathcal{L}_2$ gain which will be used to indicate the performance level of the anti-windup design. The weights W_p and W_s can be used to determine the closed-loop bandwidth of interest as well as the low frequency gains of the anti-windup sensitivities as illustrated with the simulation example in section 4.5.

4.4 Anti-windup Synthesis Via Linear Matrix Inequalities

In this section, we incorporate the performance criterion (4.15) into the anti-windup design. From (4.2) and using the coprime factorization of (4.6), the

mapping from u to y_d and $\hat{u}_d$ admit the following state space realizations

$$\begin{bmatrix} \dot{x} \\ y_d \\ \hat{u}_d \end{bmatrix} = \left[\begin{array}{c|c} A+BF & B \\ \hline -(C+DF) & -D \\ -F & -I \end{array}\right] \begin{bmatrix} x \\ d_z \end{bmatrix} \tag{4.16}$$
$$d_z = \mathrm{Dz}(u).$$

Theorem 2 ($\mathcal{L}_2$ gain performance criterion)**.** Given a stable plant G with coprime factorization of (4.6), a stable IMC controller Q and diagonal weights $W_p > 0$ and $W_s > 0$ such that G and Q are interconnected as shown in Fig. 4.1 with closed-loop equations (4.2). Suppose there exists positive definite quadratic function $V(x)$, diagonal matrix $W > 0$ and $\gamma > 0$ such that for all t,

$$\dot{V(x)} + y_d^T W_s y_d + \hat{u}_d^T W_p \hat{u}_d - \gamma^2 u^T u + 2 d_z^T W (u - d_z) < 0 \tag{4.17}$$

for all x, d_z and u satisfying (4.16). Then the $\mathcal{L}_2$ gain of the map from u to y_d and $\hat{u}_d$ in Fig. 4.1 is less than γ. Moreover, condition (4.17) is equivalent to the existence of $P = P^T > 0$ such that the following LMI with variables P, L, diagonal matrix $W > 0$ and scalar $\alpha = \gamma^2 > 0$

$$\begin{bmatrix} PA^T + AP + L^T B^T + BL & B & 0 & PC^T + L^T D^T & L^T \\ B^T & -2W & W & D^T & I \\ 0 & W & -\alpha I & 0 & 0 \\ CP + DL & D & 0 & -W_s^{-1} & 0 \\ L & I & 0 & 0 & -W_p^{-1} \end{bmatrix} < 0 \tag{4.18}$$

is satisfied. A suitable choice of F is given as $F = LP^{-1}$ where L and P are feasible solutions of (4.18).

Proof. With a Lyapunov function choice of $V(x) = x^T R x$ with $R = R^T > 0$,

condition (4.17) reduces to

$$\begin{bmatrix} R\tilde{A} + \tilde{A}^T R + \tilde{C}^T W_s \tilde{C} + F^T W_p F & RB + \tilde{C}^T W_s D + F^T W_s & 0 \\ B^T R + D^T W_s \tilde{C} + W_p F & D^T W_s D + W_p - 2W & W \\ 0 & W & -\gamma^2 I \end{bmatrix} < 0 \tag{4.19}$$

for all $[x^T \ d_z^T \ u^T]^T \neq 0$ where $\tilde{A} = A + BF_o$ and $\tilde{C} = C + DF_o$. By applying Schur complements, a change of variable γ^2 *to* α and a congruence transformation using diag$(R^{-1},\ I,\ I,\ I)$, (4.19) reduces to

$$\begin{bmatrix} \tilde{A}R^{-1} + R^{-1}\tilde{A} & B & 0 & R^{-1}\tilde{C}^T & R^{-1}F^T \\ B^T & -2W & W & D^T & I \\ 0 & W & -\alpha I & 0 & 0 \\ \tilde{C}R^{-1} & D & 0 & -W_s^{-1} & 0 \\ FR^{-1} & I & 0 & 0 & -W_p^{-1} \end{bmatrix} < 0. \tag{4.20}$$

Defining $P = R^{-1}$, $L = FP$ in (4.20) as well as substituting for $\tilde{A}$ and $\tilde{C}$ gives the LMI result (4.18). □

Remark 5. The LMI (4.18) has a similar structure to LMI (23) in [21], although the details are different. The interpretation in terms of the internal model control allows for the explicit trade-off between stability and performance while providing a clear indication of the limitations imposed on the achievable closed-loop performance. The choice of performance criterion is such that fast poles are prevented from appearing in the anti-windup compensator. With appropriate choice of weightings, the designer has some control on the locations of the closed loop poles and hence the transient response. □

4.5 Simulation Example

To allow comparison of the design method to other dynamic anti-windup compensations as well as IMC-based schemes, we consider the case-study example of [2].

Example 2. We consider again the case-study example of [2]. In chapter 3, we illustrated for this problem the performance degradation associated with control windup when the control inputs are constrained as $|u_i| \leq 1$, $i = 1, 2$ using the standard IMC (uncompensated) and the conventional IMC anti-windup structures. The input and output responses are shown again in Fig. 4.2 for set-point change from $[0 \quad 0]^T$ to $[0.63 \quad 0.79]^T$ at time $t = 0$. The uncompensated system results in large oscillations in the plant outputs. For conventional IMC, the saturation effectively chops off the control input resulting in performance deterioration.

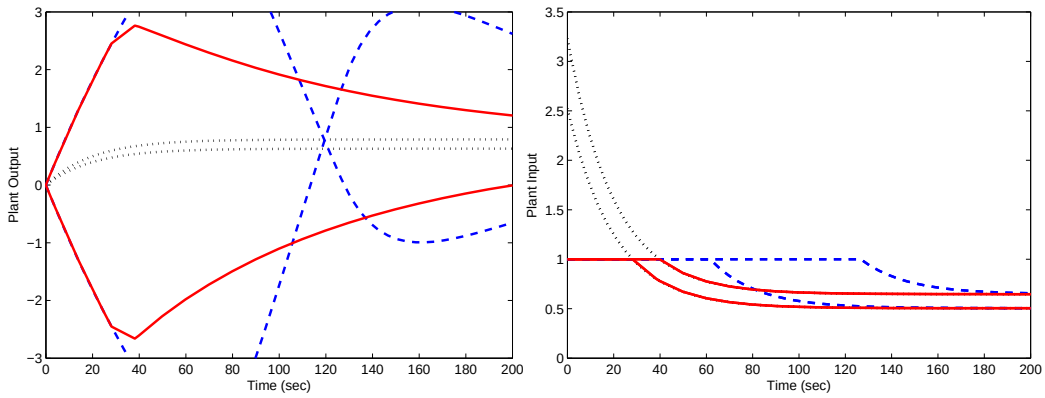

(a) Output Responses (b) Input Responses

Figure 4.2: Unconstrained (dotted), Uncompensated (dashed) and Conventional IMC (Solid)

To improve the behaviour of the system, a dynamic anti-windup compensation is designed based on the discussion in section 4.4. Solving the LMI (4.18) with the weights W_s and W_p set as the identity, we obtain an optimal gain

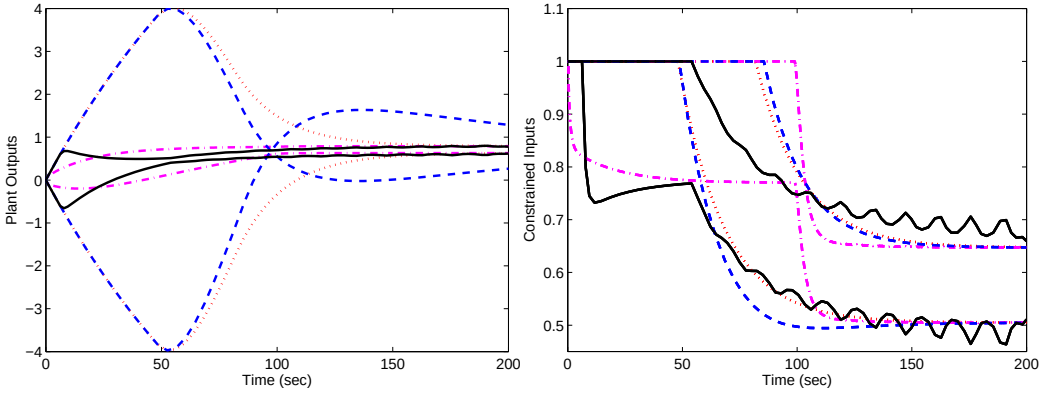

(a) Output Responses (b) Input Responses

Figure 4.3: IMC anti-windup of [1] (dotted), Modified IMC of [2] (dash-dotted), Dynamic compensation of [3] (dashed) and Proposed method (solid)

matrix F as

$$F = \begin{bmatrix} -0.4897 & 0.6153 \\ 0.6153 & -0.7974 \end{bmatrix} \tag{4.21}$$

and an $\mathcal{L}_2$ gain of $\gamma = 1$. Fig. 4.3 shows the responses of the proposed anti-windup design compared to other IMC-based and dynamic anti-windup compensation schemes [1; 2; 3; 5; 15]. The proposed scheme results in an enhanced performance with output responses which are close to the unconstrained responses and does not exhibit the significant overshoot associated with those of [1; 3]. In fact, the dynamic compensation in [3] results in no better performance than the conventional IMC anti-windup design. This can be explained from the control responses of Fig. 4.3b where both control inputs for the two schemes are kept saturated for some time resulting in directional change of the control input vector. The overshoot in the output responses in Fig. 4.3a can be attributed to this directionality change of control input vector [see chapter 5 for detailed discussions on directionality compensators design for multivariable plants]. On the other hand, the modified IMC scheme in [2] is such that the input directions are maintained. This is usually achieved through the choice of an appropriate non-causal linear filter. It is important to note that while the schemes [1; 2; 3] are such that the nonlinear performance is somewhat enhanced, they do not necessarily

provide any guarantee for internal stability of the overall closed-loop system.

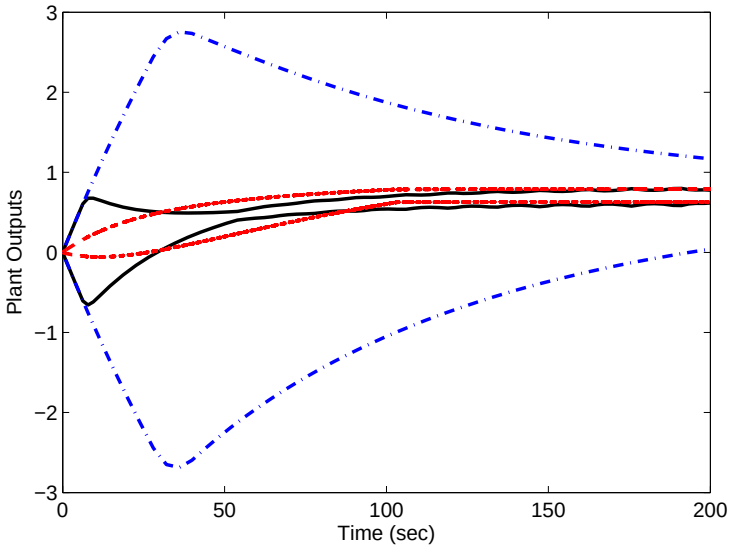

Figure 4.4: The proposed IMC anti-windup output response with weights $W_p = 0.00001,\ W_s = 1$ (dash-dotted), The proposed IMC anti-windup output response with weights $W_p = 1,\ W_s = 1$ (Solid) and The proposed IMC anti-windup output response with weights $W_p = 1,\ W_s = 0.00001$ (dashed)

We illustrate the trade-off between performance and stability robustness by adopting different weightings in the LMI constraints (4.18). For example, when performance is not a major concern, the weighting W_p can be chosen very small such that only stability is emphasized in the solution of (4.18). As shown in Fig. 4.4, when $W_p = 0.00001$, the conventional IMC response is recovered. In this instance, the feedback gain F is small (in the order of 10^{-3}) and the $\mathcal{L}_2$ gain obtained is $\gamma = 17.78$. On the other hand, when $W_s = 0.00001$, the modified IMC response of [2] is recovered. In this case, the performance is greatly improved with F of the order of 10^2 and an $\mathcal{L}_2$ gain of $\gamma = 1$. Figs. 4.5 through 4.7 depict the singular value plots for the sensitivities $T_{\hat{u}d_z}$ and T_{yd_z} for three cases of weight selections: Case 1 ($W_p = 0.00001,\ W_s = 1$), Case 2 ($W_p = 1\ W_s = 1$) and case 3 ($W_p = 1$,$W_s = 0.00001$).

Considering case 1, $T_{\hat{u}d_z}$ is almost all-pass with gain approximately unity over the frequency range. Here, the filter $T_{\hat{u}d_z}$ cannot reject the fictitious

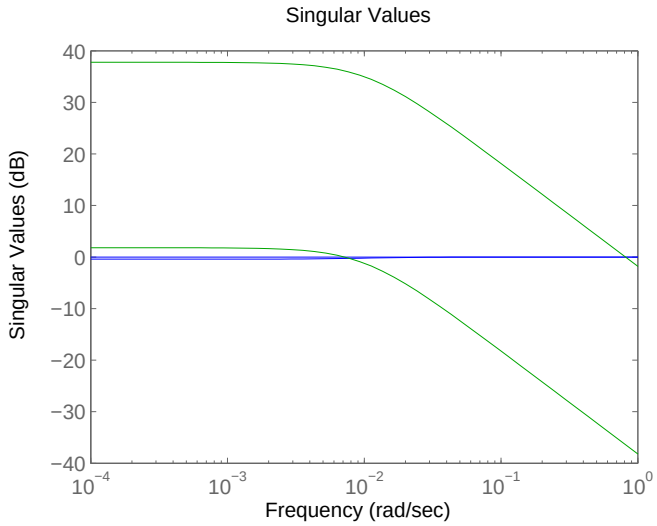

Figure 4.5: Singular value plots for the anti-windup filters $T_{\hat{u}d_z}$, T_{yd_z} with weights selection ($W_p = 0.00001,\ W_s = 1$)

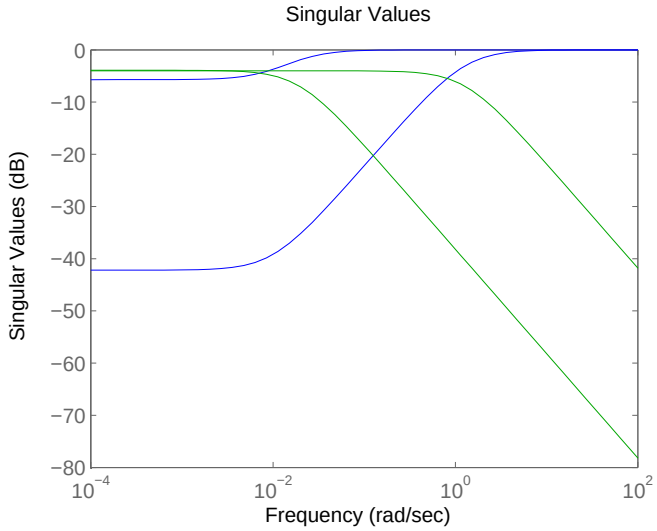

Figure 4.6: Singular value plots for the anti-windup filters $T_{\hat{u}d_z}$, T_{yd_z} with weights selection ($W_p = 1,\ W_s = 1$)

disturbance due to the control input nonlinearity and hence its associated performance is poor. In case 2, $T_{\hat{u}d_z}$ is shaped as a sensitivity function but the bandwidth of T_{yd_z} is limited to (between 0.01-1 rad/s) and hence the frequency range for which good performance is achievable is small. In the

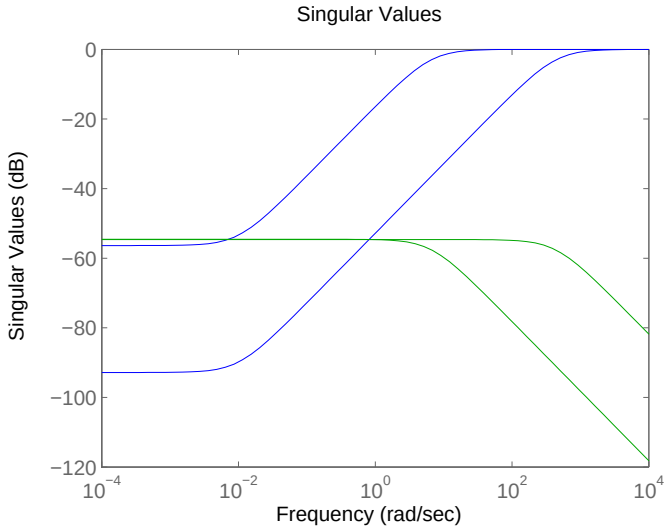

Figure 4.7: Singular value plots for the anti-windup filters $T_{\hat{u}d_z}$, T_{yd_z} with weights selection ($W_p = 1,\ W_s = 0.00001$)

last case, the bandwidth T_{yd_z} is improved to allow for larger frequency bandwidth (between 1-100 rad/s) for which good control is obtainable. The low frequency gain of $T_{\hat{u}d_z}$ is also reduced while its high frequency gain is unity. These characteristics explain the good performance obtained in this case. The trade-off however is that the low-frequency gain of the complementary sensitivity function T_{yd_z} is also reduced.

Finally, we compare the proposed IMC-based anti-windup method to other optimal schemes [5; 4]. Since performance improvement is the driving force in these methods, we will emphasize performance in the solution of (4.18) by choosing W_s very small (W_s=0.000001). As noted in [4], the static and dynamic anti-windup solutions for this example are the same and are both equivalent to the static anti-windup solution of [5]. Fig. 4.8 shows the output responses of the proposed IMC-based method and the optimal schemes [5; 4]. The responses of the other optimal schemes [5; 4] are more sluggish on both channels when compared to the unconstrained response. This is expected as the performance criteria used in these schemes are more general and do not relate directly to the swift recovery of linear performance after

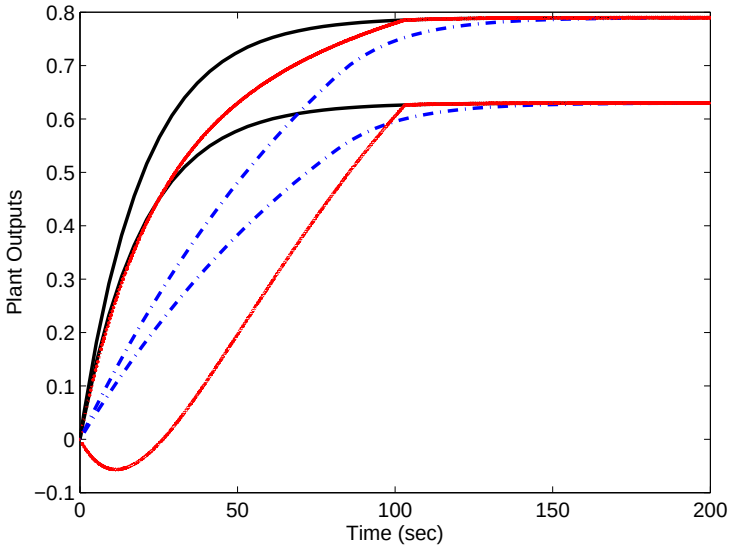

Figure 4.8: Unconstrained (Solid), Optimal anti-windup of [4; 5] (dash-dotted) and Proposed method (dotted, red)

a period of saturation. The first channel in the proposed method has a good behaviour at the expense of poor transient behaviour at the second channel. This is also what occurs when recovery of linear performance on one channel is emphasized over the other (e.g. [5]). As noted in [6], the initial inverse response is a symptom of another problem which is associated to the directional characteristics of the plant. The subject of directionality compensation design is exhaustively covered in subsequent chapters of this thesis.

4.6 Summary

We have developed a simple and systematic approach to anti-windup design based on the IMC structure. The proposed method combines the attractive features of classical IMC with enhanced nonlinear performance without introducing independent dynamics into the closed-loop. The trade-off between robust stability and performance is captured via static weights in the syn-

thesizing LMI. These weights are shown to have similar role to the frequency dependent weights in H_∞ control synthesis or loop shaping.

Chapter 5

Directionality Compensation for Multivariable Anti-windup Designs

5.1 Introduction

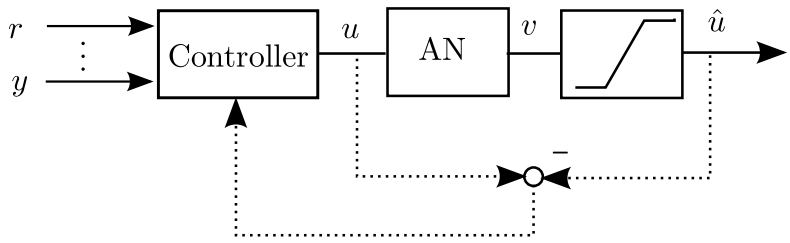

Figure 5.1: General anti-windup structure with directional compensation

For multivariable or multi-input multi-output (MIMO) systems, the presence of control input saturation introduces additional problems due to directional change in control action [39; 40; 42; 17] also known as process directionality [8] alongside the widely known controller windup phenomenon. These two problems, control windup and process directionality, can result in substantial

closed-loop performance degradation if not separately accounted for during the controller design [39; 42]. It has become, however, a common practice to incorporate an additional artificial nonlinearity (directionality compensator) in multivariable anti-windup designs to address the problem of directionality change in control action [39; 69; 6; 42; 41; 7; 44; 8; 95; 9; 96; 68; 97]. Such directionality compensators often take the form of dynamic optimization problems that are solved online either implicitly ([2; 43]) or explicitly ([7; 44; 95]) during control computation. When the control policy is obtained by an explicit solution of online optimization problem at each time step, the resulting scheme is termed optimizing anti-windup (for example [55; 54; 97]).

One class of strongly directional multivariable systems which has received extensive treatment in the literature (for example [98; 99; 6; 100; 77; 19]) is the class of ill-conditioned systems (those having large condition numbers or with gains that depend on both the input directions and magnitudes). Such systems are known to exhibit high sensitivities to model uncertainties and input nonlinearities/uncertainties [77; 19].

As shown in Fig. 5.1, the directionality compensator denoted as AN (artificial nonlinearity) is applicable to systems irrespective of the control or anti-windup structure and it is such that the input saturation nonlinearities are never violated. Generally, the saturating system is augmented with an additional compensation which modifies the system's behaviour during saturation to ensure graceful performance degradation and swift recovery of the desired linear performance.

In this chapter, a brief review of some of the existing directionality compensator designs is presented within the IMC framework of Fig. 5.2.

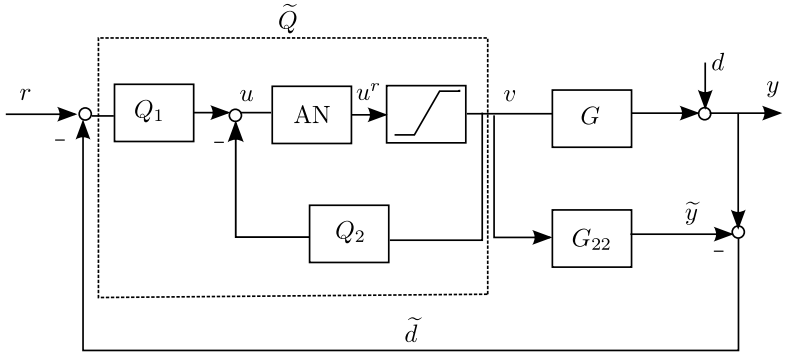

Figure 5.2: Modified IMC anti-windup with an artificial nonlinearity

5.2 The Modified Internal Model Control

The Modified IMC Anti-windup (MIA) structure [2] of Fig. 3.4 can be considered as a special case of the scheme in Fig. 5.1 where the directionality compensator AN is the identity. However, in order to preserve the output direction, the authors [2] recommend the choice $Q_1 = f_A GQ$ where the non-causal filter f_A must be designed to satisfy the following conditions:

Condition 1. The filter f_A must be diagonal in order not to introduce any change of output direction.

Condition 2. The filter f_A must be such that $f_A G$ is bi-proper and $f_A G|_{s=\infty} = I$ or $f_A G|_{z=1} = I$. This is to ensure that Q_2 is strictly proper which guarantees that there is no algebraic loop in the interconnection of Fig. 5.2.

Condition 3. For minimum phase Q, the filter f_A must be chosen such that $Q_1 = f_A GQ$ is both minimum phase and stable to guarantee internal stability of the closed loop system.

The requirements of conditions 1 and 2 may be sometimes restrictive. This is because the design choice f_A satisfying both conditions may require that the plant model G be diagonal or that the off-diagonal transfer function components of G have higher relative orders than the diagonal components. This is not always the case in multivariable systems where the dynamics are usually coupled across input channels and all the transfer function components

of G have the same relative orders. This is typical of chemical processes such as the distillation column model considered in the example. In order to get around this problem, f_A is usually designed for a slightly modified plant model such that both conditions 1 and 2 are satisfied. This may also raise robustness issues except for the case when the controller can be detuned to ensure that the closed-loop is robust.

5.3 Direction Preservation

In the Direction Preservation (DP) approach of [39; 6], the constrained control action is obtained by scaling down the controller outputs so that the u and v have same direction in the event of saturation. The nonlinearity block AN in Fig. 5.2 is defined as

$$\mathrm{AN}(u) = \min\left\{\frac{\mathrm{sat}(u_i)}{u_i}\right\} u, i = 1, \ldots, m. \tag{5.1}$$

The artificial nonlinearity is such that the component of u which most violates its corresponding constraints is fixed at the constraint while all other components are scaled so that they satisfy their respective constraints. In this case, subsequent saturation will have no effect since its input u^r always remains in the linear region i.e. $(\mathrm{Sat}(u^r) = u^r)$. This approach to directionality compensation is not necessarily the best choice as the scaled control input u^r may not be the closest possible to the unconstrained control input u. It does also not take into account the plant's directional characteristics[6]. Schemes that result in u_r which minimizes $u - u_r$ along the plant's high gain direction will generally perform better. These schemes are discussed subsequently. However, the concept of directional preservation has been shown to be beneficial for some class of constrained multivariable control problems such as the ill-conditioned systems [39; 6]. The directionality preservation heuristics can also be combined with the modified IMC scheme of [2] as shown in [41].

5.4 Optimization based Conditioning Techniques

A number of Optimization based Conditioning Techniques (OCT) have appeared in the literature [42; 44; 7]. All these are extensions of the conditioning techniques originally discussed in [69] which is based on the concept of realizable reference w^r. When a controller output is infeasible, a realizable control input u^r is obtained by solving an online optimization problem such that the realizable reference w^r is as close as possible to the actual process set-point r. The development of optimization based conditioning technique below follows that of [7] due to its ease of implementation.

Consider the modified IMC structure of Fig. 5.2. The realizable reference denoted as w^r is the reference input which would yield the realizable control signals u^r instead of the control signals u, achievable if there were no nonlinearities. Assuming no plant-model mismatch, the closed loop equation is given by

$$u = Q_1 [r - d] - Q_2 u^r. \tag{5.2}$$

The expression relating the realizable control input to the realizable reference is obtained as

$$u^r = Q_1 [w^r - d] - Q_2 u^r. \tag{5.3}$$

Subtracting (5.2) from (5.3) yields the following relationship between the control signals and the reference signals

$$u^r = u + Q_1 [w^r - r]. \tag{5.4}$$

We note here that the choice of Q_1 could follow any of the options earlier discussed in section 3.2. But for the purpose of keeping uniformity with the development in [7], we adopt the Hanus conditioning technique $Q_1 = K(\infty)$

[69]. Hence (5.4) can be rewritten as

$$\begin{aligned} u^r &= u + D_k\,[w^r - r] \quad \text{or equivalently as} \\ w^r &= r + D_k^{-1}\,[u^r - u] \end{aligned} \tag{5.5}$$

where D_k is the nonsingular feedthrough matrix of controller K i.e. $D_k = K(\infty)$. The intention is to make w^r as close as possible to r while not violating the constraints imposed by the actuators. This can be posed as a quadratic program (QP) involving the minimization of a quadratic objective function $J(w^r - r)$ subject to linear inequality constraints [42; 7]. A particular quadratic criterion is given as

$$J(w^r - r) = (w^r - r)^T \mathcal{Q} (w^r - r) \tag{5.6}$$

where $\mathcal{Q}$ is a diagonal positive definite weighting matrix. Its choice should take into account the relative importance of achieving the objectives represented by each component of r. The constraints on the control input can be expressed in compact matrix form as

$$Lu^r \leq b \tag{5.7}$$

where $L = [-I_m \quad I_m]^T$ and $b = [-u_1^{min}, \ldots, -u_m^{min}, u_1^{max}, \ldots, u_m^{max}]$. Using equation (5.5), the inequality constraints can be expressed as

$$LD_k(w^r - r) + Lu \leq b \tag{5.8}$$

Both the objective function and the constraint are convex and therefore the optimization problem always has a feasible solution which can be obtained via numerical means. Explicit or closed form solutions via the Karush-Kuhn-Tucker(KKT) conditions are discussed in [42; 69; 7].

Equations (5.6) and (5.8) can be expressed in the standard form as

$$\min_{w^r} \left\{ \frac{1}{2} (w^r)^T H w^r + f^T w^r \right\} \quad \text{subject to} : C_r w^r \leq g \tag{5.9}$$

where $H = 2D_k^T \mathcal{Q} D_k$, $f = -Hr$, $C_r = LD_k$ and $g = b + LD_k r - Lu$. Since the parameter g depends on a time varying signal u, the optimization must be carried out at every sample time instant.

The optimization criterion (5.6) can also be expressed in terms of the realizable control input u^r such that the optimization problem becomes

$$\min_{u^r} \left\{ \frac{1}{2} (u^r)^T \hat{H} u^r + \hat{f}^T u^r \right\} \quad \text{subject to : } Lu^r \leq b \tag{5.10}$$

where $\hat{H} = 2(D_k^{-1})^T \mathcal{Q} D_k^{-1}$ and $\hat{f} = -\hat{H}u$.

This scheme is applicable to systems with biproper nominal controller and will outperforms the Hanus conditioning technique [69] when the controller feedthrough D_k term is non-diagonal. If D_k is diagonal, then the Hessian matrix $\hat{H}$ in (5.10) is also diagonal. In this case, the scheme recovers the performance of the original Hanus conditioning technique [69] since the optimal solution of the QP (5.10) is identical to saturating or clipping the control.

5.5 Optimal Directional Compensator

In order to improve on the performances of both the modified IMC and direction preservation schemes, the optimal dynamic compensator (ODC) was proposed in [8]. This scheme is based on the solution of the following optimization problem.

$$\min_{u^r} |\mathcal{C}u^r - \mathcal{C}u|_{\mathcal{Q}}^2 \tag{5.11}$$

subject to the constraints

$$u_{min} \leq u_i^r \leq u_{max} \quad i = 1, \ldots, m$$

where $\mathcal{Q}$ is a diagonal positive definite matrix whose diagonal elements depend on the relative orders of each of the controlled output and $\mathcal{C}$ is the characteristic (or decoupling) matrix of the plant. The optimization problem in 5.11QP$_1$ is such that its optimal solution minimizes the Euclidean norm of the difference between the constrained and the unconstrained plant outputs subject to the input saturation constraints. The characteristic matrix $\mathcal{C}$ describes the transient behaviour of the system [101] and it is defined for a square system as

$$\mathcal{C} = \lim_{s\to\infty} [\text{diag}\{s^{r_m}\}G] \text{ or } \lim_{z\to\infty} [\text{diag}\{z^{r_m}\}G]$$

where $r_i = \min(r_{i1}, r_{i2}, \ldots, r_{im})$ and $r_{i,j}$ is the relative order of output y_i with respect to manipulated input u_j.

In this approach, the characteristic matrix $\mathcal{C}$ contains information about the directional nature of the plant [101]; thus the constrained optimization of (5.11) is such that the components of $u^r - u$ in the high gain plant direction are minimized. However, since the characteristic matrix only characterizes the initial response of the plant (i.e. the sensitivity of plant to input changes over a very short time), the optimality of the solution is only guaranteed over the transient period [8]. For system where the non-singular characteristic matrix $\mathcal{C}$ is diagonal or can be made diagonal by row or column rearrangements, the optimal directionality compensator is identical to clipping $\min_{\hat{u}} |\hat{u} - u|^2$ [8] as obtained from using the conventional IMC approach.

5.6 Optimal Steady State Scheme

The optimal steady state scheme was proposed in [9] within the context of cross-directional control. This scheme is based on the steady state structural property of the plant and guarantees optimal steady state performance by

solving the following optimization problem.

$$\min_{u^r} |\mathcal{K}_p u^r - \mathcal{K}_p u|^2_{\mathcal{Q}} \tag{5.12}$$

subject to the constraints

$$u_{min} \leq u_i^r \leq u_{max} \quad i = 1, \ldots, m \tag{5.13}$$

where $\mathcal{Q}$ is a diagonal positive definite matrix and $\mathcal{K}_p$ is the steady state gain $G(0)$ (or $G(1)$ for discrete systems). The steady state gain can be obtained from the plant's state space matrices as $G(0) = D - CA^{-1}B$ for $G(s)$ (or $G(1) = D + C(I - A)^{-1}B$ for $G(z)$) provided A (or $I - A$) is non-singular. This scheme may lead to a degraded transient performance especially when $\mathcal{K}_p$ is significantly different from $\mathcal{C}$. This is because steady state gain only characterizes the infinite-time response of the plant. For both the ODC and the OSS schemes, the underlying assumption is the non-singularity of the plant's structural matrices; the characteristic matrix $\mathcal{C}$ and the steady state gain $\mathcal{K}_p$ respectively.

5.7 Simulation Examples

In this section, the performances of the different directionality compensator schemes earlier discussed are compared using the modified IMC structure as a benchmark.

Example 3. Consider example 1 again. This example has become a benchmark for comparing anti-windup schemes [5; 4] and directionality compensators [6; 2; 8; 7; 41]. The plant's minimum relative order per channel are $r_1 = 1$ and $r_2 = 1$. The characteristic matrix $\mathcal{C}$, the steady state gain $\mathcal{K}_p$ and the $K(\infty)^{-1}$ are given as

$$\mathcal{C} = \begin{bmatrix} 0.4 & -0.5 \\ -0.3 & 0.4 \end{bmatrix}, \quad \mathcal{K}_p = \begin{bmatrix} 40 & -50 \\ -30 & 40 \end{bmatrix} \quad \text{and} \quad K(\infty)^{-1} = \begin{bmatrix} 8 & -10 \\ -6 & 8 \end{bmatrix}.$$

Observe that in this case

$$\mathcal{C} = \frac{1}{100}\mathcal{K}_p \quad \text{and} \quad K(\infty)^{-1} = \frac{1}{5}\mathcal{K}_p$$

so that the directionality compensators of (5.10) and (5.11) are equivalent and effectively meet the criterion for optimal nominal steady state performance of (5.12). This is depicted in Fig. 5.3 where the step responses for the optimization based conditioning technique (OCT) [7], the optimal directional compensator (ODC) [8] and the optimal steady state (OSS) [9] have exactly the same responses. As compared to the responses in Fig. 3.7 obtained from the conventional IMC anti-windups schemes, the directional compensators result in improved nonlinear performance. This is because the structural matrices are non-diagonal. Here, it happens that the modified IMC results in the best response on the second output channel (y_2). A tighter control of the second channel can be achieved with the optimization-based schemes by adjusting the weighting matrix $\mathcal{Q}$ which has been set to be the identity in the simulations.

Example 4. This example is taken from [8] where the state space model of the process is given as

$$\begin{aligned} \begin{bmatrix} \dot{x_1} \\ \dot{x_2} \end{bmatrix} &= \begin{bmatrix} -0.01 & -0.0002 \\ -0.5 & -0.03 \end{bmatrix} \begin{bmatrix} x_1 \\ x_2 \end{bmatrix} + \begin{bmatrix} 0.25 & 0 \\ 0 & 4 \end{bmatrix} \begin{bmatrix} u_1 \\ u_2 \end{bmatrix} \\ \begin{bmatrix} y_1 \\ y_2 \end{bmatrix} &= \begin{bmatrix} 1 & 0 \\ 0 & 1 \end{bmatrix} \begin{bmatrix} x_1 \\ x_2 \end{bmatrix} \end{aligned} \tag{5.14}$$

with $|u_1| \leq 0.12$ and $|u_2| \leq 0.12$ and a set point change of $[0.85 \quad 2.2]^T$.

The plant can be represented in continuous-time as

$$G(s) = \begin{bmatrix} \frac{0.25(s+0.03)}{s^2+0.04s+0.0002} & \frac{-0.0008}{s^2+0.04s+0.0002} \\ \\ \frac{-0.125}{s^2+0.04s+0.0002} & \frac{4(s+0.01)}{s^2+0.04s+0.0002} \end{bmatrix} \tag{5.15}$$

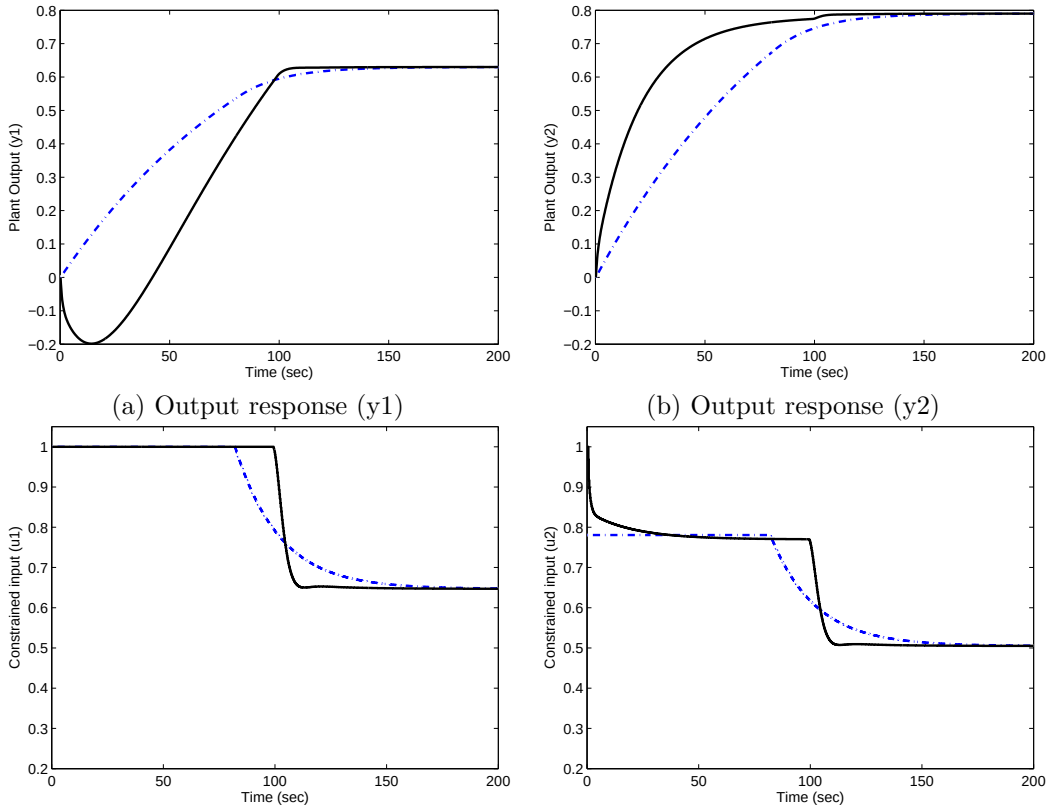

(a) Output response (y1)

(b) Output response (y2)

(c) Constrained input(u1)

(d) Constrained input(u2)

Figure 5.3: Example 3: solid- MIA [2], dashdot- DP [6], OCT [7], ODC [8] and OSS [9] produce same response

The classical IMC controller design for a step input is

$$Q(s) = \begin{bmatrix} \frac{4s+0.04}{5s+1} & \frac{0.0008}{2s+1} \\ \\ \frac{0.125}{5s+1} & \frac{0.25s+0.0075}{2s+1} \end{bmatrix} \tag{5.16}$$

and the corresponding error feedback controller is

$$K(s) = \begin{bmatrix} \frac{4s+0.04}{5s} & \frac{0.0008}{2s} \\ \\ \frac{0.125}{5s} & \frac{0.25s+0.0075}{2s} \end{bmatrix} \tag{5.17}$$

The controller $Q(s)$ is factorized based on the modified IMC approach as $Q_1 = f_A G Q$ and $Q_2 = f_A G - I$ with

$$f_A = \begin{bmatrix} 4(s+1) & 0 \\ 0 & 0.25(s+1) \end{bmatrix} \tag{5.18}$$

Here, f_A is chosen to satisfy the conditions 1, 2 and 3 in section 5.2. The minimum order per row is given by $r_1 = 1, r_2 = 1$ and the plant structural matrices are

$$\mathcal{K}_p = \begin{bmatrix} 37.5 & -4 \\ -625 & 200 \end{bmatrix}, \quad \mathcal{C} = \begin{bmatrix} 0.25 & 0 \\ 0 & 4 \end{bmatrix}, \quad \text{and} \quad K(\infty)^{-1} = \begin{bmatrix} 0.8 & 0 \\ 0 & 0.125 \end{bmatrix}$$

Since the characteristic matrix $\mathcal{C}$ and the matrix $K(\infty)^{-1}$ are both diagonal, the OCT and the ODC schemes will yield identical solutions to that of clipping the control inputs (as obtainable with the conventional IMC anti-windup). This is illustrated in Fig. 5.4 where the OCT and the ODC schemes result in similar responses to the modified IMC (MIA). As the steady state gain $\mathcal{K}_p$ is significantly different from the characteristic matrix $\mathcal{C}$, the OSS scheme resulted in a degraded transient response and with no better steady state performance than the DP and the MIA schemes. However, when the set-point change is set to $[0.85 \quad 2.2]^T$ such that some of the constraints are violated in steady states, the steady state performances of both the ODC

and the OCT schemes deteriorate significantly while the direction preserving (DP) scheme and the optimal steady state scheme (OSS) yield improved steady-state performances. This is illustrated in Fig. 5.5.

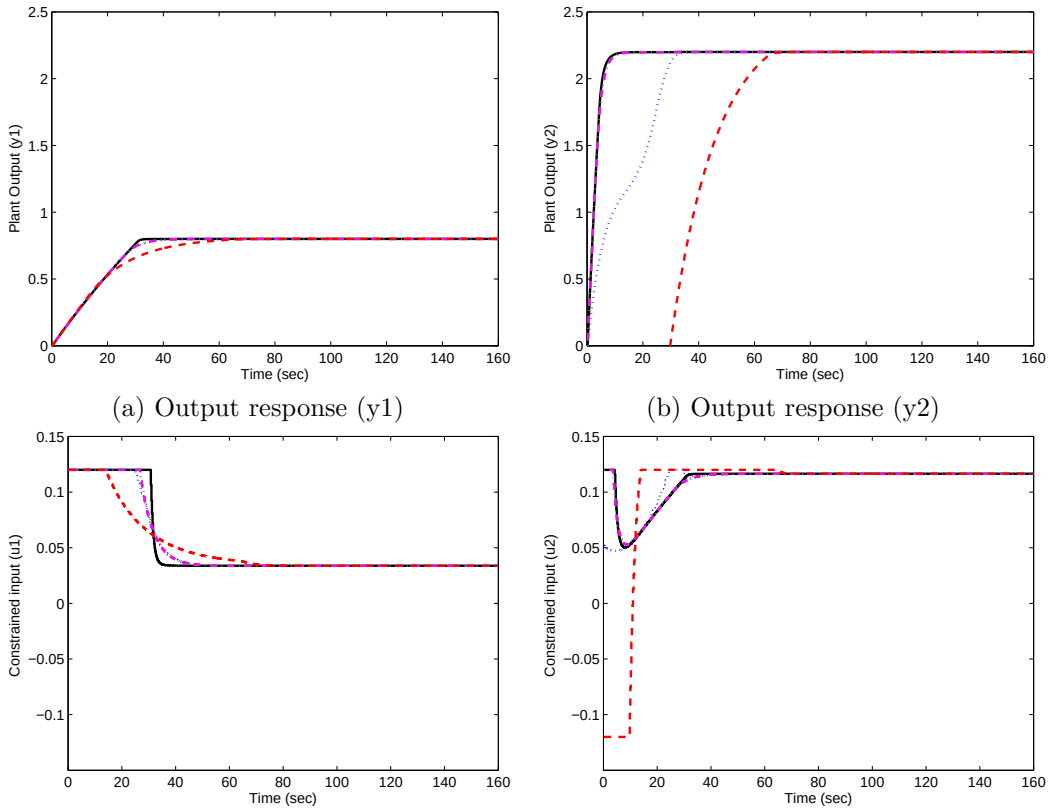

(a) Output response (y1)

(b) Output response (y2)

(c) Constrained input(u1)

(d) Constrained input(u2)

Figure 5.4: Example 4: solid- MIA [2], dotted- DP [6], dashdot- OCT [7] and ODC [8] produce same response and dashed- OSS [9]

In table 5.1, we categorize the directionality compensation schemes according to their performance characteristics during the transient and the steady state stages when one or more of the input constraints are active. It is apparent that none of the schemes guarantees optimal performance at both phases. The table suggests that the optimal directionality compensation over a wider range of operation may be obtained from the combination of two or more of the existing schemes. Details of this is covered in chapter 8.

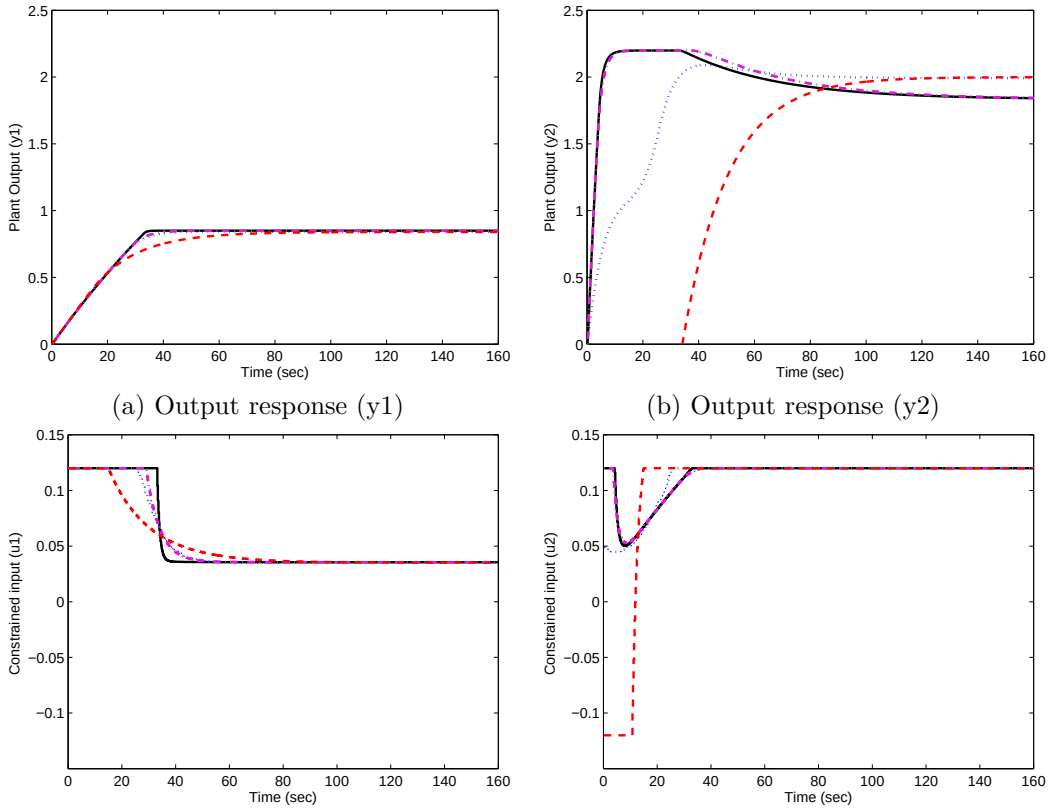

(a) Output response (y1)

(b) Output response (y2)

(c) Constrained input(u1)

(d) Constrained input(u2)

Figure 5.5: Example 4: solid- MIA [2], dotted- DP [6], dashdot- OCT [7] and ODC [8] produce same response and dashed- OSS [9]

5.8 Quadratic Program for Optimizing Anti-windup

As discussed in the preceding sections, the online optimization problem that is solved by optimizing anti-windup control can be expressed in the form of a positive definite quadratic program (QP)

$$\mathrm{QP}_1 : \quad \begin{aligned} v^* &= \arg\min_v \frac{1}{2} v^T H v - v^T H u \\ &\text{subject to } Lv \preceq b \end{aligned} \tag{5.19}$$

where $H = H^T > 0 \in \mathbb{R}^{m \times m}$. The fixed terms $L \in \mathbb{R}^{2m \times m}$ and $b \in \mathbb{R}^{2m}$ in the inequality constraints are respectively obtained as

$$L = \begin{bmatrix} -I_m \\ I_m \end{bmatrix} \text{ and } b = \begin{bmatrix} -u^{min} \\ u^{max} \end{bmatrix} \tag{5.20}$$

with $u^{min} = \begin{bmatrix} u_1^{min}, & \cdots, & u_m^{min} \end{bmatrix}^T$ and $u^{max} = \begin{bmatrix} u_1^{max}, & \cdots, & u_m^{max} \end{bmatrix}^T$.

In contrast to Model Predictive Control (MPC) algorithms, QP_1 does not require any horizon (prediction or control). In a sense, the optimizing anti-windup combines the efficiency of conventional anti-windup with the optimality properties of MPC while requiring considerably less computational effort. The quadratic program (QP_1) has the following attractive properties:

Table 5.1: Performance comparison of multivariable anti-windup schemes

	Modified IMC	Direction Preservation	Conditioning Technique	Optimal Dynamic Compensation	Optimal Steady State
Transient performance	Optimal	Poor	Optimal	Optimal	Poor
Steady State performance	Poor	Good	Poor	Poor	Optimal

1. It can be solved efficiently online [59; 7; 28].

2. Since the constraints are expressed as upper and lower bounds on the control inputs, the vector b in (5.19) can be obtained such that $b \geq 0$. This guarantees that the convex feasible region contains the origin. If we set the quadratic program (5.19) as $\psi(u)$, it then follows trivially that $\psi(0) = 0$ [54]. If further we have that $u^{min} = -u^{max}$, then ψ is also odd.

3. The positive definiteness of H guarantees the uniqueness of the optimal solution v^* [59]. If H is also diagonal, then the optimal solution is given by $v^* = \text{Sat}(u)$ [8; 43]. For optimizing anti-windup, the hessian matrix is such that $H = H_r^T H_r$ where H_r is usually defined in terms of the plant's non-singular structural properties (see [8; 68]).

4. For the unconstrained case, the optimal solution corresponds to the unconstrained control input i.e. $(v^* = u)$. Hence, for small signals, the QP does not interfere with the linear performance of the control structure.

5. Given properties 2 and 3 above, then QP_1 is sector-bounded (see lemma 1) satisfying
$$\psi(u)^T H \left(\psi(u) - u\right) \leq 0 \ \forall u \in \mathbb{R}^m. \tag{5.21}$$
Condition (5.21) is a generalized sector condition. A special case is when the nonlinearity is decoupled (i.e. $\psi_i(u) = \psi_i(u_i)$) with each component $\psi_i(u_i)$ inscribed in the sector $[0, 1]$. This corresponds to diagonal H.

6. Given properties 2 and 3, then the quadratic program QP_1 is bounded. It is also monotone nondecreasing and slope-restricted to the interval $[0, 1]$ as will be shown in lemma 6 below.

It is standard in saturating anti-windup synthesis literatures to express the saturated loop in terms of feedback interconnection involving a deadzone nonlinearity and a feedthrough term ([34; 5; 16; 102]). We note that the

quadratic program in optimizing anti-windup can be similarly expressed as a corresponding nonlinearity satisfying a sector-bound condition together with a feedthrough term. The information from the plant's structural characteristics and the quadratic program can then be incorporated into the optimizing anti-windup synthesis to guarantee closed-loop stability as well as improved nonlinear performance. We now show that the quadratic program $\psi(.)$ is equivalent to a feedthrough term in parallel to a related quadratic program as shown in Fig. 5.6.

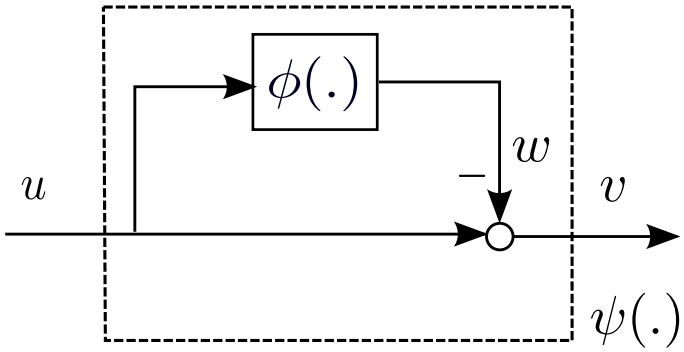

Figure 5.6: Directionality compensator expressed a deadzone-like QP

Lemma 5. Let the quadratic program (5.19) be set as $v = \psi(u)$ and let $w = \phi(u)$ be the quadratic program

$$\text{QP}_2: \quad \begin{aligned} \phi(u) = \arg\min_{w} \frac{1}{2} w^T H w \\ \text{subject to } Lu - Lw \preceq b. \end{aligned} \tag{5.22}$$

Then the interconnection of $w = \phi(u)$ with $v = u - w$ is equivalent to $v = \psi(u)$. Furthermore, $\phi(.)$ belongs to same sector as $\psi(.)$.

Proof. The Karoush-Kuhn-Tucker (KKT) conditions [59] for ϕ are given by

$$\begin{aligned} Hw - L^T\lambda = 0, \\ Lu - Lw - b + s = 0, \\ s \succeq 0, \quad \lambda \succeq 0, \quad \lambda^T s = 0. \end{aligned} \tag{5.23}$$

If we substitute $w = u - v$ into (5.23), we obtain

$$\begin{aligned} Hv - Hu + L^T\lambda &= 0, \\ Lv - b + s &= 0, \\ s \succeq 0, \quad \lambda \succeq 0, \quad \lambda^T s &= 0. \end{aligned} \tag{5.24}$$

The conditions in (5.24) are exactly the KKT conditions for ψ. Now, pre-multiplying the first KKT condition in (5.23) by w^T and substituting gives

$$w^T H w - u^T H w = -b^T \lambda \leq 0. \tag{5.25}$$

This can be expressed as $\phi(u)^T H(\phi(u) - u) \leq 0$. This is the generalized sector condition that is also satisfied by $\psi(u)$ [cf. (5.21)]. □

We now show in the spirit of [103] that $\phi(.)$ is bounded, monotone nondecreasing and slope restricted.

Lemma 6. Let ϕ be given by (5.22) with $H = H^T > 0 \in \mathbb{R}^{m\times m}$ and fixed terms $L \in \mathbb{R}^{2m\times m}$ and $b \succeq 0 \in \mathbb{R}^{2m}$. Then the nonlinearity ϕ is monotone nondecreasing (C1), slope restricted to the interval $[0, 1]$ (C2) and bounded by 1 (C3).

Proof. C1: Substituting for x and y in the first condition of the KKT conditions for ϕ gives

$$\begin{aligned} &[\phi(x) - \phi(y)]^T H (x - y) \\ &\quad = [\phi(x) - \phi(y)]^T \left[H\phi(x) + L^T\lambda(x) - H\phi(y) + L^T\lambda(y)\right] \\ &\quad = [\phi(x) - \phi(y)]^T H [\phi(x) - \phi(y)] + [\phi(x) - \phi(y)]^T \left[L^T\lambda(x) - L^T\lambda(y)\right] \\ &\quad = [\phi(x) - \phi(y)]^T H [\phi(x) - \phi(y)] + [s(y) - s(x)]^T [\lambda(x) - \lambda(y)] \\ &\quad = [\phi(x) - \phi(y)]^T H [\phi(x) - \phi(y)] + s(y)^T\lambda(x) + s(x)^T\lambda(y) \\ &\quad \geq 0. \end{aligned} \tag{5.26}$$

C2: Rearranging the second to the last equation of (5.26) gives

$$\begin{aligned}&[\phi(x)-\phi(y)]^T H\,[\phi(x)-\phi(y)] - [\phi(x)-\phi(y)]^T H\,(x-y)\\ &\quad = -\left[s(y)^T\lambda(x) + s(x)^T\lambda(y)\right] \qquad (5.27)\\ &\quad \le 0.\end{aligned}$$

C3: Setting $y = 0$ in (5.26) and (5.27), we have respectively

$$\phi(x)^T Hx \ge 0 \qquad (5.28)$$

$$\phi(x)^T H\phi(x) - \phi(x)^T Hx \le 0. \qquad (5.29)$$

Cauchy-Schwarz inequality gives

$$|\phi(x)^T Hx| \le \sqrt{\phi(x)^T H\phi(x)}\ \sqrt{x^T Hx}. \qquad (5.30)$$

Combining (5.28), (5.29) and (5.30), we have

$$\phi(x)^T H\phi(x) \le \phi(x)^T Hx \le \sqrt{\phi(x)^T H\phi(x)}\ \sqrt{x^T Hx} \qquad (5.31)$$

which implies that

$$\sqrt{\phi(x)^T H\phi(x)} \le \sqrt{x^T Hx} \qquad (5.32)$$

or alternatively

$$|H_r\phi(x)|_2 \le |H_r x|_2 \qquad (5.33)$$

since $H = H_r^T H_r$.

□

The following result shows that the available class of IQCs for the nonlinearity ϕ is no different from those of ψ. We first recall available IQCs satisfied by ψ.

Lemma 7. Let the quadratic program (5.19) be set as $v = \psi(u)$ with $b \succeq 0$ and $H = H^T \geq 0$.
(i) Then for all $u \in \mathcal{L}_2^m$ and $\Lambda = \lambda I$ with $\lambda > 0$,

$$\langle v, \Lambda H[u - v] \rangle \geq 0. \tag{5.34}$$

(ii) Further, let $z \in \mathcal{L}_1$ satisfy $||z||_1 < g$ for some $g \in \mathbb{R}$ and let ψ be odd or let $z(t) \geq 0 \ \forall t$. Then for all $\in \mathcal{L}_2^m$,

$$\langle v, g[Hu - Hv] \rangle \geq \langle v, z * [Hu - Hv] \rangle . \tag{5.35}$$

Proof. For (i) see [54]; for (ii) see [103]. □

The inequalities in lemma 7 may be expressed in the standard IQC form of section 2.6 (see also [64]) using Π with the following structure

$$\Pi = \begin{bmatrix} \Pi_{11} & \Pi_{12} \\ \Pi_{21} & \Pi_{22} \end{bmatrix}, \Pi_{11} = 0, \ \Pi_{21} = \Pi_{12}^* \text{ and } \Pi_{22} = -(\Pi_{12} + \Pi_{21}) \leq 0. \tag{5.36}$$

Specifically, we have $\Pi_{12} = \Lambda H$, $\Pi_{22} = -2\Lambda H$ for inequality (5.34) and $\Pi_{12} = (g - Z^*)H$, $\Pi_{22} = -(2g - Z - Z^*)H$ for inequality (5.35) with Z being the Fourier transform of z.

Theorem 3. Let $\Pi : \mathcal{L}_2^{2m} \to \mathcal{L}_2^{2m}$ be a self adjoint operator of the form of (5.36) and let $\psi : \mathbb{R}^m \to \mathbb{R}^m$ and $\phi : \mathbb{R}^m \to \mathbb{R}^m$ be the quadratic programs defined by (5.19) and (5.22) respectively. Suppose that ψ satisfies $\psi \in \text{IQC}(\Pi)$, then ϕ also satisfies $\phi \in \text{IQC}(\Pi)$.

Proof. Let us define $u_\psi = \begin{bmatrix} u \\ \psi(u) \end{bmatrix}$, $u_\phi = \begin{bmatrix} u \\ \phi(u) \end{bmatrix}$ and $T = \begin{bmatrix} I & 0 \\ I & -I \end{bmatrix}$ so that $T = T^{-1}$. We have that $u_\phi = T u_\psi$. If $\psi \in \text{IQC}(\Pi)$, then $\langle u_\psi, \Pi u_\psi \rangle \geq 0$ holds by the IQC definition. We also have the following equivalence

$$\langle u_\phi, \Pi u_\phi \rangle = \langle T u_\psi, \Pi T u_\psi \rangle = \left\langle u_\psi, T^T \Pi T u_\psi \right\rangle . \tag{5.37}$$

Given any Π of the form of (5.36), we have $T^T \Pi T = \Pi^*$. Since Π is self-adjoint, it follows that $\langle u_\psi, \Pi u_\psi \rangle \geq 0$ implies $\langle u_\phi, \Pi u_\phi \rangle \geq 0$. □

5.9 Summary

We have presented a review of some of the existing multivariable anti-windup schemes [2; 6; 7; 8; 54] for directionality compensation. While the MIA [2], the OCT [7] and the ODC [8] schemes offer superior dynamic performances compared with those of the DP [6] and the OSS [9], their performances deteriorate significantly in steady state especially when the constraints are active in steady state. From the discussions, the following two points become apparent;

i. No existing scheme offers an ideal solution for all scenarios. In particular, the synergy of the ODC and the OSS schemes may result in a compensation that can offer an equally optimal performances over a much wider operating range.

ii. It may be possible to develop a formal methodology for optimizing multivariable anti-windup performance while guaranteeing system stability. Using the properties 5 and 6, results from absolute stability theory can be extended to the optimizing framework to derive rigorous stability criterion as well as performance optimization.

These two issues are further investigated in subsequent chapters of this thesis. In particular, chapter 6 addresses item (ii) where we develop convex synthesis procedure for constrained multivariable systems with input nonlinearities expressed by a quadratic program. In chapter 8, we develop the two-stage IMC anti-windup algorithm which combines the optimality of both the ODC and the OSS schemes in one framework.

Chapter 6

Optimizing Anti-windup Synthesis

6.1 Introduction

The optimizing anti-windup control falls into a class of compensator commonly termed directionality compensation. The computation of the control involves the online solution of a low-order quadratic program in place of simple saturation. Simple optimizing anti-windup strategies exist in the literature but they are generally without stability and performance guarantees (e.g. [7; 8]). While the synthesis of non-optimizing anti-windup with both stability and performance guarantees has been studied extensively (see [5; 102; 15; 104; 16; 94; 18]), there have been few studies on the synthesis of optimizing anti-windup schemes with closed-loop stability guarantee. Most optimizing anti-windup schemes have focused on performance optimization in the presence of input constraints without consideration of closed-loop stability. The design of directionality compensators is usually carried out independently of the control design and with the assumption that the resulting optimizing structures inherit the stability of the unsaturated loop. An

exception is [54] where sector-bound result (multivariable circle criterion) is extended to demonstrate the stability of optimizing anti-windup. In [93; 68], we employed the theory of Integral Quadratic Constraints (IQCs) to develop a sufficient robust stability condition for optimizing anti-windup subject to any infinity-norm-bounded uncertainty.

In this chapter, we develop new synthesis procedures for optimizing anti-windup control applicable to open-loop stable multivariable plants where the input nonlinearities are expressed by a quadratic program. We exploit the equivalence of the quadratic program to a feedthrough term in parallel with a deadzone-like nonlinearity that satisfies a sector-bound condition. This allows for LMI-based synthesis using a decoupled structure similar to that proposed in the literature for anti-windup schemes with simple saturations. As compared to existing optimizing anti-windup schemes [42; 43; 44; 7; 8], the design approach is particularly attractive in that it allows the incorporation of the plant's structural and directional characteristics into the anti-windup synthesis to guarantee closed-loop stability as well as improved nonlinear performance. The design procedure exploits the extra degree of freedom in the anti-windup computation which have been hitherto considered difficult in saturating anti-windup synthesis [86]. This design freedom, usually termed the stability multiplier in saturating anti-windup design, is either not used, lost during computation [5; 16], chosen almost arbitrarily [15] or mainly used to eliminate algebraic loops [21] or to convexify the synthesizing matrix inequalities [46; 45]. Here, we exploit the extra design freedom through the directionality compensator. We demonstrate the effectiveness of the design compared to several schemes using both a highly ill-conditioned benchmark example and an example where the plant has lightly damped modes.

The rest of the chapter is structured as follows: In section 6.2, the optimizing anti-windup problem is formulated using the internal model control structure. In section 6.3, we show that the online quadratic program solved by the anti-windup can be decomposed into a related nonlinearity and a feedthrough link. We also note that both the original quadratic program

and the transformed quadratic program belong to the same sector after linear transformations. These observations allow the extension of existing results to the optimizing anti-windup. We construct a sufficient stability condition for the optimizing anti-windup based on results from passivity and IQC theory. We also specify appropriate performance criteria which relate directly to the optimizing anti-windup behaviour during and after saturation. In section 6.4, we present two results for optimizing anti-windup synthesis. The first guarantees closed-loop stability via a quadratic Lyapunov criterion. The second result guarantees both closed-loop stability and a level of performance. The performance criterion is such that the recovery of linear performance after a period of control input saturations is hastened. Finally, in section 6.5, we demonstrate the superiority of the design method over several existing schemes using a highly ill-conditioned distillation column benchmark example and a plant with lightly damped modes. Such plants are generally known to be difficult to control and the effects of control input saturations can result in serious performance degradation.

6.2 Problem Formulation

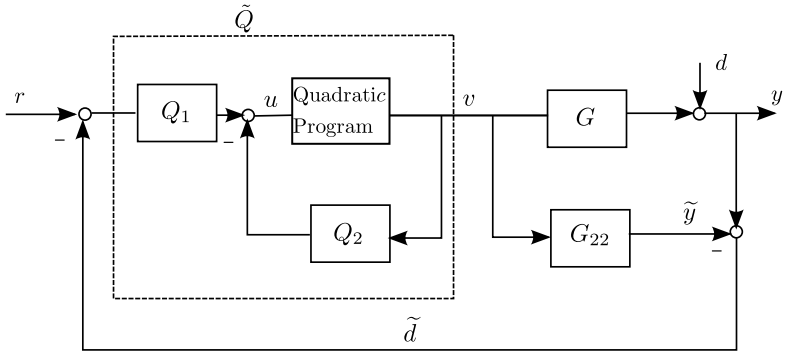

Figure 6.1: IMC anti-windup with a quadratic program as directionality compensator

We consider the modified internal model control anti-windup structure of Fig. 6.1 where G and G_{22} represent the plant and the nominal plant dynamics re-

spectively. The nominal IMC controller Q is assumed to have been designed to meet some nominal stability and performance specifications [19]. As previously discussed in section 3.4.1, the anti-windup compensators Q_1 and Q_2 to be synthesized are parameterized in terms of the coprime factorization of the nominal plant as

$$Q_1 = M^{-1}Q \tag{6.1}$$

$$Q_2 = M^{-1} - I \tag{6.2}$$

where M is part of the right coprime factorization of the plant $G = NM^{-1}$ with the state space realizations

$$\begin{bmatrix} M \\ N \end{bmatrix} = \left[\begin{array}{c|c} A + BF & B \\ \hline F & I \\ C + DF & D \end{array}\right]. \tag{6.3}$$

The anti-windup design problem reduces to finding an appropriate right coprime factorization of the nominal plant via the free design parameter F which must be chosen such that $A + BF$ is Hurwitz. When there are no saturations, we require that Q_1 and Q_2 are constrained to be $Q = (Q_2 + I)^{-1}Q_1$ such that the linear controller and performance are recovered. The quadratic program is as defined in (5.19). It serves the purpose of a directionality compensator. Its Hessian matrix is fully characterized by the plant's structural properties such as the characteristic matrix or the steady-state gain. As discussed in chapter 5, such structural matrices determine the directional nature of the plant output either during the transient condition or during steady states. The problem we seek to tackle is summarized as follows:

Problem: Given a stable plant G, a nominal internal model controller Q which meets certain linear performance specifications and a non-singular matrix H which contains the directional characteristics of the plant, synthesize the anti-windup compensator Q_1 and Q_2 such that the closed-loop system of Fig. 6.1 is stable, has a guaranteed level of nonlinear performance and recovers the linear performance when there are no

control saturations (i.e. $v = u$).

Using lemma 5, the optimizing anti-windup can be redrawn with the original quadratic program (5.19) replaced with a deadzone-like quadratic program (5.22). With further algebraic manipulations and the assumption of perfect model, the optimizing anti-windup can be represented in a decoupled architecture as shown in Fig. 6.2[cf. [34]]. This equivalent representation

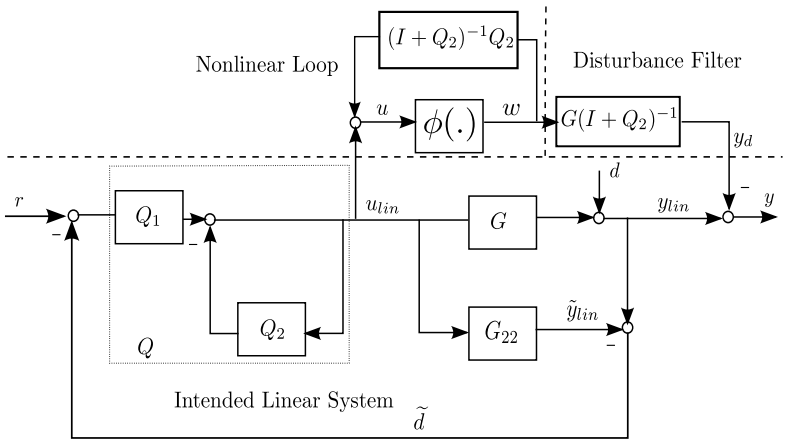

Figure 6.2: Decoupled Architecture for the Optimizing IMC anti-windup

is attractive as it decouples the optimizing anti-windup structure into the nominal linear system, the nonlinear loop involving a QP and the disturbance filter. The behaviour of the closed-loop system during saturation is then closely related to the nonlinear loop and disturbance filters. For stable systems, the equivalent nominal classical feedback controller K can be obtained from the relation $K = (I - QG)^{-1}Q$. Using this in Fig. 6.2 and setting $(I+Q_2)^{-1} = M$, we obtain a decoupled structure in M which may be interpreted as the single transfer function parameterization of anti-windup schemes with simple saturations [34]. The emphasis here is that the nonlinearity is allowed to take a more general structure as compared to existing saturating anti-windup schemes where the nonlinearity is implicitly assumed to be decentralized or decoupled.

6.3 Stability and Performance Analysis

From the decoupled architecture of Fig. 6.2, it is evident that the nominal stability of the optimizing anti-windup depends on the stability of the constituting sub-systems. The linear sub-system is internally stable if the plant G and the IMC controller Q are both stable [19]. With the assumption that Q has been designed to meet some specified nominal stability and performance requirements, the stability of the optimizing anti-windup is then determined by the stability of the nonlinear loop. The stability of such interconnections involving a class of nonlinearities has been widely studied using results from small gain, passivity, multiplier and IQC theories (See [36; 92] for saturating anti-windup). Properties 5 and 6 of the quadratic program in section 5.8 allow the extension of such results to the optimizing anti-windup. Here, we exploit the structure of the quadratic program (5.22) to construct sufficient stability conditions for the optimizing anti-windup. After carrying out two linear transformations ($\phi(u) = H_r^{-1}\varphi(x)$ and $u = H_r^{-1}x$ where $H = H_r^T H_r$) followed by loop transformations, the nonlinear loop can be redrawn as shown in Figs. 6.3 and 6.4 respectively.

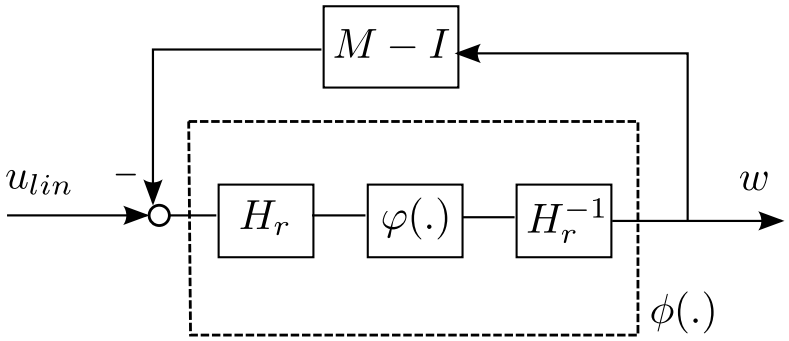

Figure 6.3: Nonlinear loop with quadratic program $\varphi \in$ sector $[0, I]$

It then follows from passivity result or the multivariable circle criterion [54] that a sufficient condition for asymptotic stability of the nonlinear-loop is

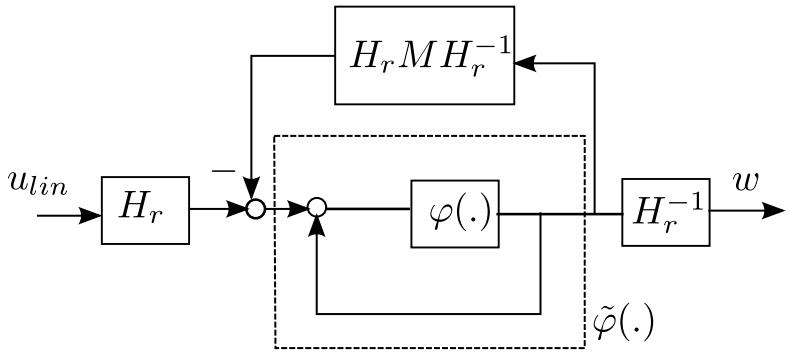

Figure 6.4: Nonlinear loop with quadratic program $\varphi \in$ sector$[0, I]$ transformed to $\tilde{\varphi} \in$ sector $[0, \infty]$ via loop transformation

that HM is strictly positive real (SPR). This condition is stated as

$$HM + M^*H > 0 \tag{6.4}$$

for all frequency. Stronger stability results may be obtained by introducing multipliers such as those discussed in [103; 105] into the nonlinear loop of Fig. 6.4. Typically, the stability multipliers are such that the positivity of the nonlinearity is preserved. The nonlinear loop is then stable if WHM is SPR. This can be stated as

$$WHM + M^*HW^* > 0. \tag{6.5}$$

where W is the stability multiplier. When W is restricted to be a constant positive definite diagonal matrix, the stability condition (6.5) reduces to a scaled version of the multivariable circle criterion (6.4) which corresponds to the sector condition of property 5 in section 5.8.

Note that the stability condition (6.4) or (6.5) is without reference to a particular factorization scheme for the nominal internal model control Q. Possible factorization options are discussed in [2; 1]. These options are known to lead to improved nonlinear performance at the expense of guaranteed closed loop stability. We will incorporate the above stability result into the choice of the compensators Q_1 and Q_2 for optimizing anti-windup of Fig. 6.1.

Another advantage of the decoupling structure of Fig. 6.2 is that it allows the specification of performance criterion which is directly related to the anti-windup behaviour during and after saturation [16]. The map from u_{lin} to y_d represents how the fictitious disturbance signal y_d due to the presence of control input nonlinearity affects the output of the intended linear system. Specifically, we would like to minimize the $\mathcal{L}_2$ gain of the map $u_{lin} \to y_d$ so that the adverse effects of the input nonlinearity is mitigated while the recovery of unconstrained performance is as fast as possible after saturation.

6.4 Anti-windup Compensator Synthesis

The results in this section extend the synthesis approach of [16; 106] to the optimizing anti-windup. Here, we consider a multi-objective synthesis approach which addresses *a*) closed-loop stability through a Lyapunov-based stability criterion; *b*) nonlinear performance by minimizing the $\mathcal{L}_2$-norm of the difference between the constrained output y and the unconstrained (nominal) output y_{lin} via the quadratic program (5.19) or (5.22); and *c*) recovery of linear performance through the minimization of the $\mathcal{L}_2$ gain of the map $u_{lin} \to y_d$ in Fig. 6.2.

Let the right coprime factors of the plant $G = NM^{-1}$ admit the state space realizations represented in (6.3). The mappings from $w \to (u - u_{lin})$ and $u_{lin} \to y_d$ in Fig. 6.2 are respectively obtained as

$$\begin{bmatrix} \dot{x} \\ u - u_{lin} \end{bmatrix} = \left[\begin{array}{c|c} A + BF & B \\ \hline -F & 0 \end{array}\right] \begin{bmatrix} x \\ w \end{bmatrix} \tag{6.6}$$

$$\begin{bmatrix} \dot{x} \\ u - u_{lin} \\ y_d \end{bmatrix} = \left[\begin{array}{c|c} A + BF & B \\ \hline -F & 0 \\ \hline C + DF & D \end{array}\right] \begin{bmatrix} x \\ w \end{bmatrix} \quad \text{with} \tag{6.7}$$

$$w = \phi(u). \tag{6.8}$$

Theorem 4 (Synthesis with Lyapunov stability criterion)**.** Given a stable plant G with coprime factorization (6.3), a stable Q and a given H such that the sector condition of lemma 5 is satisfied. Suppose there exist positive definite quadratic function $V(x)$ and $\tau > 0$ such that for all t,

$$\dot{V}(x) + 2\tau w^T H(u - w) < 0 \tag{6.9}$$

for all x, u, u_{lin} and w satisfying (6.6). Then the optimizing anti-windup in Fig. 6.2 is stable. Moreover, condition (6.9) is equivalent to the existence of $P = P^T > 0$ such that the following LMI in P, L and $\alpha > 0$

$$\begin{bmatrix} AP + PA^T + BL + L^T B^T & \alpha B - L^T H \\ \alpha B^T - HL & -2\alpha H \end{bmatrix} < 0. \tag{6.10}$$

is satisfied. A suitable choice of F is given as $F = LP^{-1}$ where L and P are feasible solutions of LMI (6.10).

Proof. Choosing $V(x)$ as $V(x) = x^T X x$ with $X = X^T > 0$, the expression in (6.9) is a direct application of S-procedure to $\dot{V}(x) < 0$ and the sector condition $w^T H(u - w) \geq 0 \; \forall \; \tau > 0$. Condition (6.9) is guaranteed $\forall \; [x^T \; w^T]^T \neq 0$ with $u_{lin} = 0$ if (6.11) is satisfied.

$$\begin{bmatrix} XA + A^T X + XBF + F^T B^T X & XB - \tau F^T H \\ B^T X - \tau FH & -2\tau H \end{bmatrix} < 0. \tag{6.11}$$

By a simple congruence transformation $\mathrm{diag}(X^{-1}, \tau^{-1} I)$ and defining $P = X^{-1}$, $\alpha = \tau^{-1}$, $L = FP$ in equation (6.11), we obtain the LMI in (6.10). □

Remark 6. The main result of theorem (6.2) is that existing optimizing anti-windup schemes such as those in [7; 8; 43] can now be equipped with stability guarantees for all nonlinearities of the form of (5.19) and satisfying the generalized sector condition 5.21. By construction, the Hessian matrix H is always positive definite and often assumes a non-diagonal structure (property 3 of section 5.8). The LMI result (6.10) can also be obtained by applying the positive real lemma (e.g. [60]) to the stability condition (6.5)

with W set as τI. We note that similar sufficient stability result based on the KKT conditions of the associated input nonlinearities have earlier been suggested in the literature [55; 54; 56] but only for posteriori stability checks. Here, the information from the QP (5.19) is incorporated into the synthesizing LMI such that closed loop stability is assured.

Theorem 5 (Synthesis with $\mathcal{L}_2$-gain performance)**.** Given a stable plant G with coprime factorization (6.3), a stable Q and a given H such that the sector condition of lemma 5 is satisfied. Suppose there exists positive definite quadratic function $V(x)$, $\tau > 0$ and $\gamma > 0$ such that for all t,

$$\dot{V}(x) + y_d^T y_d - \gamma^2 u_{lin}^T u_{lin} + 2\tau w^T H(u - w) < 0 \tag{6.12}$$

for all x, u, u_{lin} and w satisfying (6.8). Then the $\mathcal{L}_2$ gain of the map from u_{lin} to y_d in Fig. 6.2 is less than γ. Moreover, condition (6.12) is equivalent to the existence of $P = P^T > 0$ such that the following LMI in P, L, $\alpha > 0$ and $\gamma > 0$

$$\begin{bmatrix} AP + BL + PA^T + L^T B^T & \alpha B - L^T H & 0 & PC^T + L^T D^T \\ \alpha B^T - HL & -2\alpha H & H & \alpha D^T \\ 0 & H & -\gamma I & 0 \\ CP + DL & \alpha D & 0 & -\gamma I \end{bmatrix} < 0. \tag{6.13}$$

is satisfied. A suitable choice of F is given as $F = LP^{-1}$ where L and P are feasible solutions of LMI (6.13).

Proof. With a Lyapunov function choice of $V(x) = x^T Y x$ with $Y = Y^T > 0$, condition (6.12) reduces to

$$\begin{bmatrix} Y\tilde{A} + \tilde{A}^T Y + \tilde{C}^T \tilde{C} & YB + \tilde{C}^T D - \tau F^T H & 0 \\ B^T Y + D^T \tilde{C} - \tau HF & D^T D - 2\tau H & \tau H \\ 0 & \tau H & -\gamma^2 I \end{bmatrix} < 0 \tag{6.14}$$

for all $[x^T \; w^T \; u_{lin}^T]^T \neq 0$ where $\tilde{A} = A + BF$ and $\tilde{C} = C + DF$. By applying

Schur complement, change of variables $Y = \gamma X, \tau = \gamma\beta$ and congruence transformation using $\mathrm{diag}(X^{-1},\ \beta^{-1}I,\ I,\ I)$, (6.14) reduces to

$$\begin{bmatrix} \tilde{A}X^{-1} + X^{-1}\tilde{A}^T & \beta^{-1}B - X^{-1}F^TH & 0 & X^{-1}\tilde{C}^T \\ \beta^{-1}B^T - HFX^{-1} & -2\beta^{-1}H & H & \beta^{-1}D^T \\ 0 & H & -\gamma I & 0 \\ \tilde{C}X^{-1} & \beta^{-1}D & 0 & -\gamma I \end{bmatrix} < 0. \qquad (6.15)$$

Defining $P = X^{-1}$, $\alpha = \beta^{-1}$, $L = FP$ in (6.15) as well as substituting for $\tilde{A}$ and $\tilde{C}$ gives the LMI result (6.13). □

Remark 7. The key feature of this theorem is the freedom in choosing H which may now assume a more general non-diagonal structure as compared to existing anti-windup schemes. The appropriate choice of H is made based on the plant characteristics, giving the designer more control on the anti-windup design as well as offering insights into the anti-windup computation. When H is taken to be diagonal or the identity, the LMI (6.13) reduces to the synthesizing LMI result commonly found in saturating anti-windup designs. So, anti-windup design schemes of [5; 16; 86; 21; 46] may be considered as special cases of the result (6.13).

Remark 8. The feasibility of LMI (6.13) is sufficent for the feasibility of LMI (6.10) since the LMI (6.10) is a principal submatrix (upper left 2×2 block) of LMI (6.13). On the other hand, LMI (6.13) is feasible if and only if LMI (6.10) is feasible and γ is sufficiently large (as seen from the lower right 2×2 block of LMI(6.13)). Note that there is always a choice of F such that LMI (6.13) is feasible. Choosing $F = 0$ implies $M = I$ and hence $Q_2 = 0$. In this instance, LMI (6.13) reduces to a version of the bounded real lemma (e.g. [60]) and the $\mathcal{L}_2$ gain computed corresponds to the H_∞ norm of the stable plant G.

6.5 Simulation Example

In order to demonstrate the effectiveness of the proposed anti-windup synthesis method, we first consider an ill-conditioned example typical of distillation column control [19; 77]. This is a well-studied problem because of the strong directionality and interaction that exist in the plant dynamics as well as its high sensitivities to diagonal input nonlinearities and uncertainties. We compare four anti-windup approaches, namely the modified IMC anti-windup [2], the static anti-windup [5], the dynamic anti-windup design without directionality compensation [106] and the anti-windup scheme with directionality compensation of theorem 5. The second example demonstrates the superiority of the proposed method compared to existing optimization-based anti-windup when applied to plants with lightly damped modes. For this example, we compare the conventional IMC anti-windup [6], the dynamic anti-windup without directionality compensation [106], the optimal anti-windup with directionality compensation [7] and the proposed scheme based on theorem 5. Note that we did not include the static anti-windup of [5] for this example as the synthesizing LMI was infeasible. Table 6.1 shows the $\mathcal{L}_2$ gains attainable using three different anti-windup techniques. The proposed scheme combines the optimality of an online optimization with the efficiency of convex dynamic anti-windup synthesis leading to superior responses as shown in the simulations of Figs. 6.5 and 6.6.

Table 6.1: Performance levels γ_p for different anti-windup (AW) schemes

	Static AW [5]	Dynamic AW [21]	Proposed AW Scheme
Example 1	3.8200	1.9708	1.9708
Example 2	Infeasible	200.6473	200.6471

Example 5. The nominal plant model is given by the transfer function matrix

$$G(s) = \frac{1}{75s+1}\begin{bmatrix} 0.878 & -0.864 \\ 1.082 & -1.096 \end{bmatrix} \tag{6.16}$$

with both inputs constrained as $|u_i| \leq 100$, $i = 1, 2$. In the absence of control input saturations, the linear controller is designed to achieve a completely

decoupled closed-loop response represented as follows

$$G_F(s) = \frac{1}{1.43s+1} I.$$

The classical IMC controller design for a step input is

$$Q(s) = \frac{75s+1}{(1.43s+1)} \begin{bmatrix} 39.94 & -31.49 \\ 39.43 & -32.00 \end{bmatrix} \tag{6.17}$$

and the corresponding unity feedback controller is

$$K(s) = \frac{75s+1}{1.43s} \begin{bmatrix} 39.94 & -31.49 \\ 39.43 & -32.00 \end{bmatrix}. \tag{6.18}$$

We chose $H = H_r^T H_r$ with H_r as the characteristic matrix of the plant (in the notion of [8]). We have

$$H_r = \begin{bmatrix} 0.012 & -0.012 \\ 0.014 & -0.015 \end{bmatrix}.$$

For the modified IMC anti-windup design [2], the plant model is slightly modified as

$$\widetilde{G}(s) = \frac{1}{75s+1} \begin{bmatrix} 0.878 & \frac{-0.864}{0.1s+1} \\ \\ \frac{1.082}{0.1s+1} & -1.096 \end{bmatrix} \tag{6.19}$$

and the compensator Q_1 is designed as $Q_1 = f_A \widetilde{G} Q$ where

$$f_A = \begin{bmatrix} 85.42(s+1) & 0 \\ 0 & -68.43(s+1) \end{bmatrix}. \tag{6.20}$$

Figs 6.5 shows the input and output responses of the nominal plant to a set-point change from $[0 \quad 0]^T$ to $[0.99 \quad 0]^T$ at time $t = 10$ and from $[0.99 \quad 0]^T$ to $[0.99 \quad 0.01]^T$ at time $t = 50$ respectively for the different control configu-

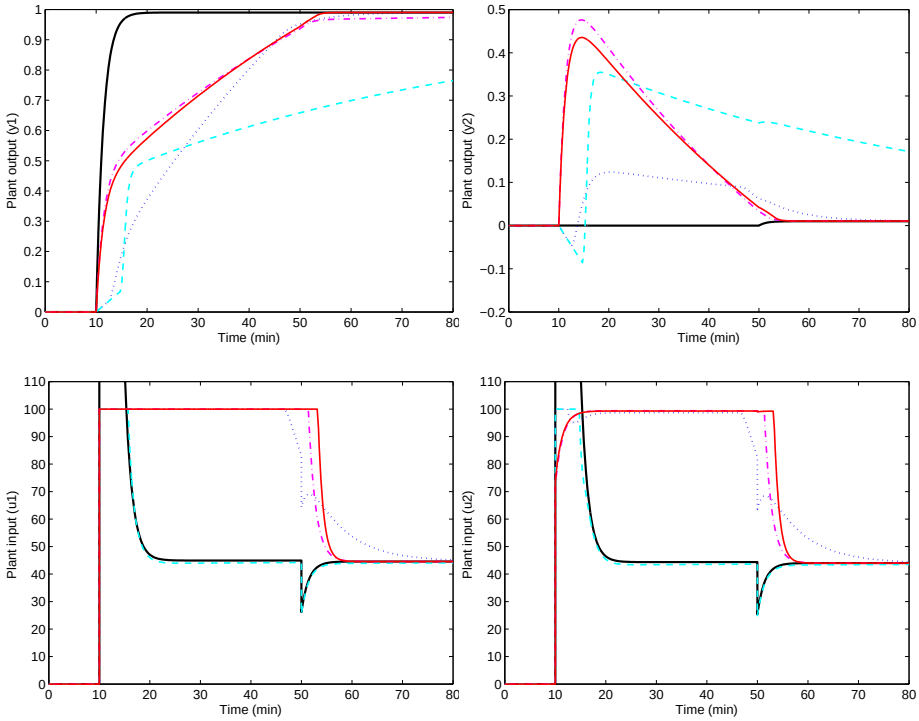

Figure 6.5: Example 5-Input and output Responses of the proposed anti-windup scheme as compared with existing schemes

Table 6.2: Legend for the responses in Figs. 6.5a through 6.5d

System	Line Type
Unconstrained	Bold
Modified IMC [2]	Dotted
Dynamic anti-windup [106]	Dashed
Static anti-windup [5]	Dashdotted
Proposed anti-windup [Theorem 5]	Solid

rations listed in Table 6.2. Note that the unconstrained case requires a very aggressive control action during transient condition to achieve the decoupled response. The modified IMC anti-windup [2] has an improved transient response on one channel at the expense of a more sluggish output response on the other. This is not unexpected as the anti-windup compensator is designed to instantaneously minimize the 1-norm of a filtered difference between the unconstrained and the constrained outputs which is based on a

related plant model. In addition, there are no design guidelines for the filter which is chosen purely based on intuition and has nothing to do with the plant's characteristics. The dynamic anti-windup of [106] results in a sluggish transient response. This is because the scheme does not compensate for the effects of plant's directionality. It only chops off the control inputs leading to degraded response. Since the LMI synthesis resulted in a compensator with a very fast pole (requiring a very high sampling frequency), we have constrained the poles to a region comparable to those of the unconstrained controller poles for ease of implementation. The proposed scheme not only results in an improved time domain response but also attains a lower $\mathcal{L}_2$ gain when compared with the static anti-windup scheme of [5]. The $\mathcal{L}_2$ gain of the scheme [21] is the same as that obtained with proposed scheme.

Example 6. We consider another example with a pair of lightly damped modes at $-0.01 \pm j0.01$. The plant has the following dynamics

$$G(s) = \frac{s + 0.001}{s^2 + 0.02s + 0.0002} \begin{bmatrix} 0.25 & -0.08 \\ -0.125 & 4 \end{bmatrix} \tag{6.21}$$

with $|u_i| \leq 0.2$, $i = 1, 2$ and set-point changes from $[0 \quad 0]^T$ to $[0.99 \quad 0.03]^T$ at time $t = 0$ corresponding to the plant low-gain direction. In the absence of control input saturation, the linear controller is designed to cancel the plant's lightly damped dynamics and to achieve a completely decoupled closed-loop response given by

$$G_F(s) = \begin{bmatrix} \frac{1}{5s+1} & 0 \\ 0 & \frac{1}{2s+1} \end{bmatrix}.$$

Since the plant is both stable and of minimum phase, we obtain the classical IMC controller using $Q = G^{-1}G_F$ and the corresponding unity feedback controller from the relation $K = (I - QG)^{-1}Q$. For this plant, H_r is computed as

$$H_r = \begin{bmatrix} 0.250 & -0.080 \\ -0.125 & 4.000 \end{bmatrix}$$

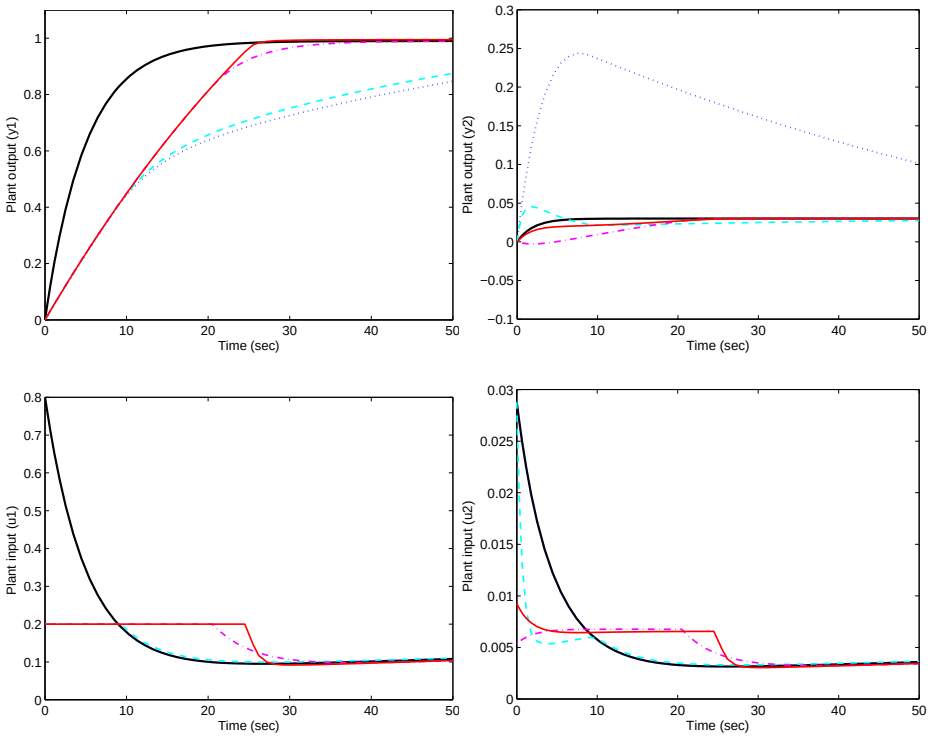

Figure 6.6: Example 6-Input and output Responses of the proposed anti-windup scheme as compared with existing schemes

Table 6.3: Legend for the responses in Fig. 6.6a through 6.6d

System	Line Type
Unconstrained	Bold
Conventional IMC anti-windup[6]	Dotted
Dynamic anti-windup [106]	Dashed
Optimal anti-windup (with QP)[7]	Dashdotted
Proposed anti-windup (with QP) [Theorem 5]	Solid

Fig. 6.6 shows the responses of the plant for different anti-windup schemes for a set-point is change from $[0 \quad 0]^T$ to $[0.99 \quad 0.03]^T$ at time $t = 0$ which corresponds to the plant's low-gain direction. Note that for this example, the static anti-windup scheme [5] is infeasible which implies that there is no static

anti-windup gain that can guarantee the quadratic stability of the closed-loop using the static anti-windup scheme. The poor transient responses associated with the conventional IMC can be attributed to the effects of directionality [6] since the scheme just chops off the control inputs. The dynamic anti-windup [21] results in an improved response as compared to the conventional IMC. While the problem of directionality is solved by incorporating directionality compensator in the optimal anti-windup scheme of [7], the proposed scheme recovers the linear performance faster and it is closest to the unconstrained response.

6.6 Summary

We have presented a multivariable optimizing anti-windup design which guarantees closed-loop stability while compensating for both windup and directionality change in the control input vector. The simulated examples demonstrate the benefits that ensue: both from introducing directionality compensation into an anti-windup structure and from applying our proposed design procedures. The results are especially beneficial when the plant is ill-conditioned or has lightly damped modes. The method allows an explicit trade-off between stability and performance. We are currently investigating how significantly the balance is shifted when we replace input saturations with a quadratic program. We have also restricted our discussions to the nominal case where there are no model uncertainties. We will remove this restriction in the subsequent chapters by incorporating robustness norm-bounded uncertainty into the anti-windup framework.

Chapter 7

Robust Optimizing Anti-windup Synthesis: An Integral Quadratic Constraint Approach

7.1 Introduction

In optimizing anti-windup schemes, an additional nonlinearity is incorporated to account for problems associated with plant or control directionality. Most optimizing anti-windup schemes derive from the optimization-based conditioning techniques [69; 42] which were developed to deal with the issues of control windup and directionality. In chapter 5, we noted that the quadratic program associated with the optimizing anti-windup is equivalent to an interconnection of a related quadratic program with a feedthrough link. This allows an LMI-based synthesis using a decoupled structure similar to those proposed for anti-windup schemes with simple saturations. In chapter 6, we developed a synthesis procedure for the optimizing anti-windup based

on the assumption that the plant is perfectly modeled. Here, we remove such assumptions and incorporate plant uncertainties into the anti-windup development.

The main contribution of this chapter is the robust synthesis of optimizing anti-windup subject to H_∞-norm bounded uncertainties such as those arising from unmodeled or neglected dynamics. In particular, we apply the synthesis approach of [21; 45] to the optimizing anti-windup design problem. Aside from allowing the incorporation of robustness in a less conservative manner, the design approach captures the directional characteristics of the plant into the anti-windup design giving the synthesizing LMIs an extra degree of freedom. An additional pay off is that the resulting scheme offers a systematic way of dealing with algebraic loops and well-posedness of the arising interconnection as compared to [46; 57].

The rest of the chapter is structured as follows. In section 7.2, we define the robust optimizing anti-windup design problem using the internal model control architecture. In section 7.3, the problem is reformulated in the IQC framework. We state a sufficient LMI-based condition which guarantees both closed-loop stability and a specified level of performance. In section 7.4, the synthesis problem is reduced to the feasibility of two LMI constraints. In section 7.5, we suggest a practical implementation method for the algebraic loop arising from the anti-windup interconnection. We note that optimality condition of the directionality compensator necessarily guarantees the well-posedness of the closed-loop interconnection.

7.2 Problem Statement and Formulation

7.2.1 Unconstrained System

We denote the state-space realizations associated with the nominal plant G_{22} as

$$G_{22} \sim \left[\begin{array}{c|c} A & B \\ \hline C & D \end{array}\right]. \tag{7.1}$$

The nominal unconstrained linear controller denoted as K (for feedback controller) or Q (for internal model controller) is assumed to have been designed to meet some acceptable nominal stability and performance criteria [19]. This implies that Q is such that the nominal closed-loop system

$$\begin{aligned} y_{lin} &= G_{22}Qr + (I - G_{22}Q)d \\ u_{lin} &= Q(r - d) \end{aligned} \tag{7.2}$$

is internally stable. The signals y_{lin} and u_{lin} are the nominal unconstrained (linear) plant output and control input respectively. The exogenous signals r and d represent the reference and the disturbance signals respectively. The IMC controller Q can be considered the special case of the Youla-parametrization of all stabilizing controllers K for stable plant G where K and Q are related by $K = Q(I - G_{22}Q)^{-1}$.

7.2.2 Uncertainty Description

The plant uncertainty is assumed to be described by additive-type uncertainties such that the actual plant G can be expressed as

$$G = G_{22} + W\Delta_r. \tag{7.3}$$

where Δ_r is a bounded operator satisfying $\|\Delta_r\|_\infty \leq 1/\gamma_r$ and W is a known frequency dependent stable transfer functions or weighting. We will represent the state space realization of QW as

$$QW \sim \left[\begin{array}{c|c} A_q & B_q \\ \hline C_q & D_q \end{array}\right]. \tag{7.4}$$

7.2.3 Coprime Factorization Representation

Let the coprime factorization of the nominal plant $G_{22} = NM^{-1}$ be given by the following state space realization

$$\begin{bmatrix} M \\ N \end{bmatrix} \sim \left[\begin{array}{c|c} A+BF & BE \\ \hline F & E \\ C+DF & DE \end{array}\right] \tag{7.5}$$

where F must be chosen such that $A+BF$ is Hurwitz and E is any arbitrary invertible matrix (e.g. [81]). In the subsequent sections, the anti-windup synthesis problem is reduced to a convex search (in terms of F and E) over the space of all right-coprime factors of the nominal plant satisfying the design objectives.

7.2.4 Nonlinearity Characterization and Directionality Compensation

For the optimizing anti-windup framework, the nonlinearity is assumed to take the form of the positive definite quadratic program (QP) as in (5.19). The nonlinearity termed the directionality compensator belongs to a general class of coupled multivariable nonlinearities satisfying the generalized sector condition (2.14). As earlier discussed in chapter 3, H can be chosen differently depending on the overall design objectives and it allows the

incorporation of the plant's directional characteristics into the anti-windup design. We consider the optimizing anti-windup structure of Fig. 6.1. The transfer function matrices Q_1 and Q_2 are the anti-windup compensations to be designed and are related to the nominal IMC controller through

$$Q = (Q_2 + I)^{-1} Q_1. \tag{7.6}$$

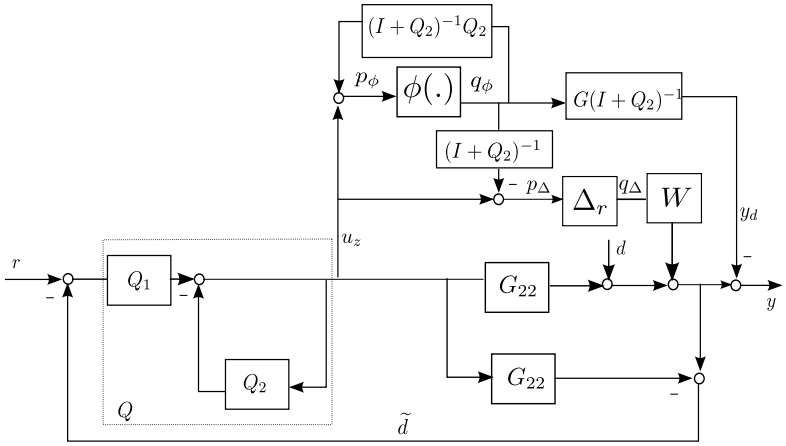

Figure 7.1: IMC anti-windup with a quadratic program as directionality compensator

As earlier discussed in section 5.8, the input nonlinearity is equivalent to feedthrough term in parallel to a related quadratic program denoted as $\phi(.)$ in (5.22). Using this equivalent representation, the optimizing anti-windup of Fig. 6.1 can be restructured into the decoupled architecture of Fig. 7.1 where the signals q_Δ and y_d can be considered as fictitious disturbance signals perturbing the nominal plant output due to the presence of plant uncertainty Δ_r and the nonlinearity ϕ. In the spirit of [21] for saturation nonlinearities, we choose Q_2 such that $(I+Q_2)^{-1} = M$ where M is part of the right coprime factorization of (7.5). Then, the loop transmission around the nonlinearity

$\phi(.)$ becomes $(I - M)$. The factorizations of Q can then be obtained as

$$\begin{aligned} Q_1 &= M^{-1}Q \\ Q_2 &= M^{-1} - I. \end{aligned} \tag{7.7}$$

We now state the optimizing anti-windup synthesis problem.

Problem Definition: Given a stable nominal plant G_{22} which admits a right coprime factorization (7.5), a stable nominal Q and an admissible plant perturbation level γ_r, synthesize optimizing anti-windup compensators Q_1 and Q_2 such that for all nonlinearities of the form (5.19) with fixed $H = H^T > 0$, L and $b > 0$, the interconnection of Fig. 7.1

(i) is well-posed,

(ii) is stable,

(iii) has an $\mathcal{L}_2$ gain performance level of less than γ_p, and

(iv) recovers the linear performance when there are no control saturations (i.e. when $u = \text{Sat}(u)$).

Remark 9. Well-posedness may not be an issue if we choose the constant matrix E in (7.5) as the identity. With this restriction, the algebraic loop in Fig. 7.1 disappears and well-posedness is guaranteed by the uniqueness of the solution of the quadratic program represented by ϕ. Similarly, the choice of $F = 0$ corresponds to the conventional IMC structure ($Q_1 = Q,\ Q_2 = 0$) which guarantees closed-loop stability provided G_{22} and Q are both stable. There is therefore always a choice of compensator that ensures items (i) and (ii) of the problem definition. However, we require E to convexify the matrix inequalities in the synthesis procedure of section 7.4. We will therefore explore the flexibilities in the choice of F and E via a convex search to synthesis the optimal compensators Q_1 and Q_2 which guarantees both closed-loop stability and a given level of performance. □

Remark 10. The satisfaction of items (iii) and (iv) of the problem definition depend on the properties of the nonlinearity, the choice of performance criterion and the channels to which the performance is associated. Since in the unconstrained case, the optimal solution corresponds to the unconstrained control input i.e. $(v^* = u)$, therefore the QP does not interfere with the linear performance of the control structure for small signals. The recovery of linear performance is thus expected when there are no input saturations. □

7.3 An Integral Quadratic Constraints Approach to Robust Stability and Performance Analysis

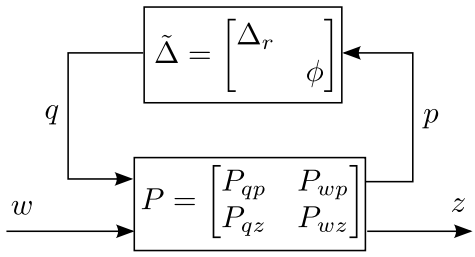

Figure 7.2: Standard feedback interconnection for robust stability and performance analysis

We consider the standard feedback interconnection of Fig. 7.2 with the input-output map

$$\begin{bmatrix} p \\ z \end{bmatrix} = \begin{bmatrix} P_{qp} & P_{wp} \\ P_{qz} & P_{wz} \end{bmatrix} \begin{bmatrix} q \\ w \end{bmatrix} \tag{7.8}$$

$$q = \tilde{\Delta}(p) \tag{7.9}$$

so that the linear time invariant generalized plant P admits the following

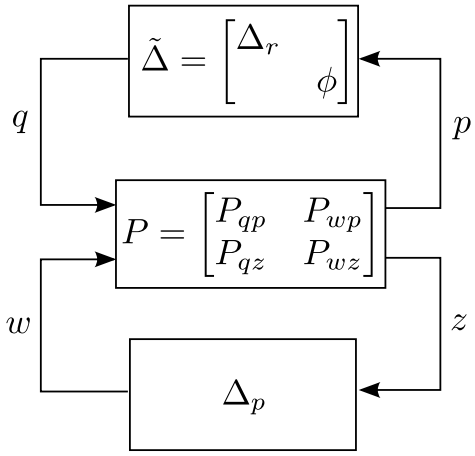

Figure 7.3: Equivalent feedback interconnection

state-space representation

$$P \sim \left[\begin{array}{c} \dot{x} \\ \hline p \\ z \end{array}\right] = \left[\begin{array}{c|cc} A_p & B_{qx} & B_{wx} \\ \hline C_{xp} & D_{qp} & D_{wp} \\ C_{xz} & D_{qz} & D_{wz} \end{array}\right] \left[\begin{array}{c} x \\ \hline q \\ w \end{array}\right]. \tag{7.10}$$

The map from w to z represents the channel with which we would like to associate some performance criterion. Among various possible choices of performance measures, we will consider the induced $\mathcal{L}_2$ gain. In particular, we want to make the effects of the nonlinearity ϕ on both the input and output of the plant G to be as small as possible. From the decoupled representation of Fig. 7.1, we have the following mappings

$$\begin{aligned} y_d &= -G(1+Q_2)^{-1} q_\phi \\ u_z &= u_{lin} - QW q_\Delta. \end{aligned}$$

The map from q_ϕ to y_d dictates how the nonlinearity ϕ affects the plant output while the map from q_Δ to u_z represents the combined effects of both the nonlinearity ϕ and the uncertainty Δ_r at the plant input. It is therefore, natural to specify the performance objective in terms of the $\mathcal{L}_2$ gain from u_{lin} to the output of the disturbance filter y_d. Such a specification has been observed to be central to the anti-windup design problem [36; 16] for the sat-

urated case. We note that the framework of Fig. 7.2 allows the specification of different performance objectives such as for disturbance rejection [46] or the more general criteria [5; 15]. The requirement that the induced $\mathcal{L}_2$ gain of the map from w to z be less than γ_p is equivalent to checking that the interconnection of Fig. 7.3 is stable for all unstructured Δ_p which is norm bounded by γ_p. Δ_p can therefore be absorbed into the block diagonal Δ for the purpose of performance analysis as is standard (e.g. [64]).

Let us define $p = [p_\Delta^T, p_\phi^T]^T$, $q = [q_\Delta^T, q_\phi^T]^T$ and $\Delta = \text{diag}(\Delta_r, \phi, \Delta_p)$. Then, we can write the input-output map of Fig. 7.3 as

$$\begin{bmatrix} p_\Delta \\ p_\phi \\ y_d \end{bmatrix} = \begin{bmatrix} -QW & -(1+Q_2)^{-1} & I \\ -QW & (1+Q_2)^{-1}Q_2 & I \\ 0 & -G_{22}(1+Q_2)^{-1} & 0 \end{bmatrix} \begin{bmatrix} q_\Delta \\ q_\phi \\ u_{lin} \end{bmatrix} \tag{7.11}$$

$$q = \Delta(p). \tag{7.12}$$

7.3.1 Available IQCs for the uncertainties (Δ_r, Δ_p) and the nonlinearity ψ.

The norm-bound condition $q_\Delta = \Delta_r p_\Delta$, $||\Delta_r||_\infty \leq 1/\gamma_r$ on the plant uncertainty Δ_r can be equivalently stated as requiring $\|p_\Delta\|^2 - \gamma_r^2 \|q_\Delta\|^2 \geq 0$. This can be expressed in the IQC notation as $\Delta_r \in \text{IQC}(\Pi_{\Delta_r})$ with

$$\Pi_{\Delta_r} = \begin{bmatrix} I & 0 \\ 0 & -\gamma_r^2 I \end{bmatrix}. \tag{7.13}$$

Similarly, the $\mathcal{L}_2$ gain performance condition in terms of the fictitious operator Δ_p satisfying $\|z\|^2 - \gamma_p^2 \|w\|^2 \geq 0$ can be expressed as $\Delta_p \in \text{IQC}(\Pi_{\Delta_p})$ with

$$\Pi_{\Delta_p} = \begin{bmatrix} I & 0 \\ 0 & -\gamma_p^2 I \end{bmatrix}. \tag{7.14}$$

As earlier discussed in sections 2.2 and 5.8, the input-output map of the nonlinearity $\phi(.)$ satisfies the generalized sector condition

$$\lambda q_\phi^T H(q_\phi - p_\phi) \leq 0 \tag{7.15}$$

for a positive scalar $\lambda > 0$. This can be stated as $\psi \in \text{IQC}(\Pi_\psi)$ with

$$\Pi_\phi = \begin{bmatrix} 0 & \lambda H \\ \lambda H & -2\lambda H \end{bmatrix}. \tag{7.16}$$

The block diagonal operator Δ formed by the combination of Δ_r, ϕ and Δ_p i.e. $\Delta = \text{diag}(\Delta_r, \phi, \Delta_p)$ satisfies the IQC defined by

$$\Pi_\Delta = \begin{bmatrix} \Pi_{\Delta_{11}} & \Pi_{\Delta_{12}} \\ \Pi^*_{\Delta_{12}} & \Pi_{\Delta_{22}} \end{bmatrix} \tag{7.17}$$

where

$$\Pi_{\Delta_{11}} = \begin{bmatrix} I & 0 & 0 \\ 0 & 0 & 0 \\ 0 & 0 & I \end{bmatrix}, \Pi_{\Delta_{12}} = \begin{bmatrix} 0 & 0 & 0 \\ 0 & \lambda H & 0 \\ 0 & 0 & 0 \end{bmatrix} \text{ and} \tag{7.18}$$

$$\Pi_{\Delta_{22}} = \begin{bmatrix} -\gamma_r^2 I & 0 & 0 \\ 0 & -2\lambda H & 0 \\ 0 & 0 & -\gamma_p^2 I \end{bmatrix}. \tag{7.19}$$

It is also possible to introduce weighting matrices W_r and W_p in the IQC definitions for Δ_r and Δ_p respectively to reflect the relative importance of robustness and performance [46]. With this, the top-left partition of (7.17) can be expressed as

$$\Pi_{\Delta_{11}} = \begin{bmatrix} W_r & 0 & 0 \\ 0 & 0 & 0 \\ 0 & 0 & W_p \end{bmatrix}. \tag{7.20}$$

The IQC approach of [64] can be extended to perform robust performance analysis for the standard feedback interconnection of Fig 7.3. We first state

the IQC theorem.

Theorem 6 (IQC Theorem [64])**.** Let P be a stable transfer function matrix and let Δ be a bounded causal operator, then the feedback interconnection of P and Δ is stable if the following conditions hold:

(i) the interconnection of P and $\tau\Delta$ is well-posed for all $\tau \in [0, 1]$;

(ii) $\tau\Delta$ satisfies the IQC defined by Π_Δ for all $\tau \in [0, 1]$;

(iii) there exists $\epsilon > 0$ such that

$$\begin{bmatrix} P(jw) \\ I \end{bmatrix}^* \Pi_\Delta(jw) \begin{bmatrix} P(jw) \\ I \end{bmatrix} \leq -\epsilon I \text{ for all } w \in \mathbb{R}. \tag{7.21}$$

□

Since $\Pi_{\Delta_{11}} \geq 0$ and $\Pi_{\Delta_{22}} \leq 0$, the IQC defined by Π_Δ is also satisfied by $\tau\Delta \ \forall \ \tau \in [0, 1]$ [64]. Hence, the dependence of item (ii) on τ in the IQC stability theorem 6 can be eliminated.

We state a time-domain equivalent result as follows:

Theorem 7. Let P be a stable linear time invariant system with the state-space realization of (7.10) and let $\Delta = \text{diag}(\Delta_r, \phi, \Delta_p)$ be a bounded operator satisfying the IQC condition defined by Π_Δ (7.17) where $\Pi_{\Delta_{11}} \geq 0$ and $\Pi_{\Delta_{22}} \leq 0$. Assume that:

(i) the interconnection of P and $\tau\Delta$ is well-posed for all $\tau \in [0, 1]$;

(ii) there exist a positive definite matrix $R = R^T$ and positive scalars $(\gamma_r, \ \gamma_p, \ \lambda)$ such that for all x, q, w satisfying (7.10), the following matrix inequality holds;

$$\begin{bmatrix} A_p^T R + R A_p & R B_{qx} & R B_{wx} \\ B_{qx}^T R & 0 & 0 \\ B_{wx}^T R & 0 & 0 \end{bmatrix} + \tilde{\Pi} < 0 \tag{7.22}$$

with

$$\tilde{\Pi} = \begin{bmatrix} C_{xp} & D_{qp} & D_{wp} \\ C_{xz} & D_{qz} & D_{wz} \\ 0 & I & 0 \\ 0 & 0 & I \end{bmatrix}^T \begin{bmatrix} \Pi_{\Delta_{11}} & \Pi_{\Delta_{12}} \\ \Pi_{\Delta_{12}}^T & \Pi_{\Delta_{22}} \end{bmatrix} \begin{bmatrix} C_{xp} & D_{qp} & D_{wp} \\ C_{xz} & D_{qz} & D_{wz} \\ 0 & I & 0 \\ 0 & 0 & I \end{bmatrix}$$

where $\Pi_{\Delta_{11}}$, $\Pi_{\Delta_{12}}$ and $\Pi_{\Delta_{22}}$ are as defined in (7.17).

Then, the feedback interconnection of P and Δ is stable for all $w \in \mathcal{L}_2$ and the $\mathcal{L}_2$-gain from w to z is less than γ_p.

Proof. Using the state-space realizations for P in (7.10) and the IQC frequency condition (7.21), the matrix inequality condition (7.22) follows directly from the application of KYP lemma [107]. □

Remark 11. The stability condition (7.22) can also be obtained via the existence of a quadratic function of the form $V(x) = x^T R x$ with $R > 0$ and $\gamma_p > 0, \lambda > 0$ such that for all t,

$$\dot{V}(x) + \lambda q_\phi^T H(p_\phi - q_\phi) + (p_\Delta^T p_\Delta - \gamma_r^2 q_\Delta^T q_\Delta) + (z^T z - \gamma_p^2 w^T w) < 0 \quad (7.23)$$

for all x and w satisfying (7.10). Since the second and third terms are always non-negative by the IQC definitions of (7.13) and (7.16). Using the fact that $V(x)$ is positive definite for all $x \neq 0$, the integration of (7.23) from 0 to t with initial conditions $x(0) = 0$ reduces to

$$\|z\|^2 - \gamma_p^2 \|w\|^2 \leq 0 \quad (7.24)$$

which implies that the $\mathcal{L}_2$-gain from w to z does not exceeds γ_p [60]. The matrix inequality constraint (7.22) follows from the substitutions of x, q and z from (7.10) into the condition (7.23) and after some algebraic manipulations.

We will use the analysis result of theorem 7 for the synthesis of suitable anti-windup compensation that guarantees both closed-loop stability and a

given level of performance. The discussions on well-posedness and real-time implementation of the resulting optimizing control are covered in section 7.5.

7.4 LMI-Based Synthesis

We now state the main result for robust optimizing anti-windup synthesis.

Theorem 8. Consider the system of Figure 7.1 where $G_{22} \in \mathcal{RH}_\infty^{n_y \times n_u}$, $Q \in \mathcal{RH}_\infty^{n_u \times n_y}$ and $W \in \mathcal{RH}_\infty^{n_y \times n_y}$ are the nominal plant, the IMC controller and the frequency dependent weighting respectively. Let G_{22} have the coprime factorization (7.5) and Let $H = H^T > 0$ be given such that for all nonlinearities of form (5.22), condition (7.15) holds. Suppose there exist a positive definite matrix R and positive scalars $(\gamma_r,\ \gamma_p,\ \lambda)$ such that for all x, q, w satisfying (7.10)

$$\Psi + \Gamma^T \Theta^T \Omega + \Omega^T \Theta \Gamma < 0 \tag{7.25}$$

where

$$\Psi = \begin{bmatrix} A_o^T R + R A_o & R B_o + \lambda \bar{C}_o^T \tilde{H} & 0 & \bar{C}_o^T & C_o^T \\ B_o^T R + \lambda \tilde{H} \bar{C}_o & \lambda(\tilde{H} \bar{D}_o + \bar{D}_o^T \tilde{H}) - \gamma_r^2 \tilde{I} & \lambda \hat{H} & \bar{D}_o^T & 0 \\ 0 & \lambda \hat{H}^T & -\gamma_p^2 I & \hat{I}^T & 0 \\ \bar{C}_o & \bar{D}_o & \hat{I} & -W_r^{-1} & 0 \\ C_o & 0 & 0 & 0 & -W_p^{-1} \end{bmatrix}$$

$$\Theta = [F \quad E] \tag{7.26}$$

$$\Omega = \begin{bmatrix} \Omega_1 R & \lambda \Omega_2 \tilde{H} & 0_{n_u} & \Omega_2 & \Omega_3 \end{bmatrix} \text{ and} \tag{7.27}$$

$$\Gamma = \begin{bmatrix} \Gamma_1 & \Gamma_2 & 0_{(n+n_u)\times n_u} & 0_{(n+n_u)\times(n_u+n_y)} & 0_{(n+n_u)\times n_y} \end{bmatrix} \tag{7.28}$$

with

$$
\begin{aligned}
A_o &= \begin{bmatrix} A_q & 0_{n_q \times n} \\ 0_{n \times n_q} & A \end{bmatrix}, B_o = \begin{bmatrix} B_q & 0_{n_q \times n_u} \\ 0_{n \times n_y} & 0_{n \times n_u} \end{bmatrix}, \bar{C}_o = \begin{bmatrix} 0_{n_y \times n_q} & 0_{n_y \times n} \\ -C_q & 0_{n_u \times n} \end{bmatrix}, \\
\bar{D}_o &= \begin{bmatrix} 0_{n_y \times n_y} & 0_{n_y \times n_u} \\ -D_q & 0_{n_u \times n_u} \end{bmatrix} C_o = \begin{bmatrix} 0_{n_y \times n_q} & -C \end{bmatrix}, \\
\Omega_1 &= \begin{bmatrix} 0_{n_u \times n_q} & B^T \end{bmatrix}, \Omega_2 = \begin{bmatrix} 0_{n_u \times n_y} & -I_{n_u} \end{bmatrix}, \Omega_3 = -D^T, \\
\Gamma_1 &= \begin{bmatrix} 0_{n \times n_q} & I_n \\ 0_{n_u \times n_q} & 0_{n_u \times n} \end{bmatrix}, \Gamma_2 = \begin{bmatrix} 0_{n \times n_y} & 0_{n \times n_u} \\ 0_{n_u \times n_y} & I_{n_u} \end{bmatrix}, \tilde{H} = \begin{bmatrix} I_{n_y} & 0_{n_y \times n_u} \\ 0_{n_u \times n_y} & H \end{bmatrix}, \\
\tilde{I} &= \begin{bmatrix} I_{n_y} & 0_{n_y \times n_u} \\ 0_{n_u \times n_y} & 0_{n_u \times n_u} \end{bmatrix}, \hat{I} = \begin{bmatrix} 0_{n_y \times n_u} \\ I_{n_u} \end{bmatrix}, \hat{H} = \begin{bmatrix} 0_{n_y \times n_u} \\ H \end{bmatrix}.
\end{aligned}
\tag{7.29}
$$

Then there exists a plant-order anti-windup compensator of the form (7.7) which

(i) guarantees the well-posedness of the interconnection,

(ii) renders the closed loop system stable with an $\mathcal{L}_2$ gain from w to z less than γ_p for all Δ satisfying the IQC defined by (7.17).

Furthermore, let R be partitioned as $R = \begin{bmatrix} R_{11} & R_{12} \\ R_{12}^T & R_{22} \end{bmatrix}$. Then (7.25) is solvable for Θ if and only if the following LMIs in variables α_r, α_p, R_{11} and R with $\alpha_r = \gamma_p^2$ and $\alpha_p = \gamma_p^2$ hold.

$$
\begin{bmatrix} A_q^T R_{11} + R_{11} A_q & R_{11} B_q & 0 & -C_q^T \\ B_q^T R_{11} & -\alpha_r I_{n_y} & 0 & -D_q^T \\ 0 & 0 & -\alpha_p I_{n_u} & I_{n_u} \\ -C_q & -D_q & I_{n_u} & -W_r^{-1} \end{bmatrix} < 0 \tag{7.30}
$$

and

$$\begin{bmatrix} A_{CL}^T R + R A_{CL} & R B_{CL} & R \hat{B}_{CL} & C_{cl}^T \\ B_{CL}^T R & -\alpha_r I_{n_y} & 0 & D_{cl}^T \\ \hat{B}_{CL}^T R & 0 & -\alpha_p I_{n_u} & -D^T \\ C_{cl} & D_{cl} & -D & -W_p^{-1} \end{bmatrix} < 0 \tag{7.31}$$

with

$$\begin{aligned} A_{CL} &= \begin{bmatrix} A_q & 0 \\ -BC_q & A \end{bmatrix}, B_{CL} = \begin{bmatrix} B_q \\ -BD_q \end{bmatrix}, \hat{B}_{CL} = \begin{bmatrix} 0 \\ B \end{bmatrix} \\ C_{CL} &= \begin{bmatrix} DC_q & -C_p \end{bmatrix}, D_{CL} = DD_q. \end{aligned} \tag{7.32}$$

Proof. Using (7.4) and the coprime-factor based realizations for Q_2, we obtain a particular state-space realizations for P as

$$P \sim \left[\begin{array}{c|cc} A_p & B_{qx} & B_{wx} \\ \hline C_{xp} & D_{qp} & D_{wp} \\ C_{xz} & D_{qz} & D_{wz} \end{array}\right] = \left[\begin{array}{cc|ccc} A_q & 0 & B_q & 0 & 0 \\ 0 & A+BF & 0 & BE & 0 \\ \hline -C_q & -F & -D_q & -E & I \\ -C_q & -F & -D_q & I-E & I \\ 0 & -(C+DF) & 0 & -DE & 0 \end{array}\right] \tag{7.33}$$

with $A_p \in \mathbb{R}^{(n_q+n)\times(n_q+n)}$, $B_{qx} \in \mathbb{R}^{(n_q+n)\times(n_y+n_u)}$, $B_{wx} \in \mathbb{R}^{(n_q+n)\times n_u}$, $C_{xp} \in \mathbb{R}^{(2n_u+n_y)\times(n_q+n)}$, $C_{xz} \in \mathbb{R}^{n_y\times(n_q+n)}$, $D_{qz} \in \mathbb{R}^{(2n_u+n_y)\times(2n_u+n_y)}$ and $D_{wz} \in \mathbb{R}^{n_y\times n_u}$. Substituting (7.33) into the condition (7.22), we obtain the

following inequality

$$\begin{bmatrix} A_p^T R + R A_p & R B_{qx} + \lambda \bar{C}_h^T \tilde{H} & 0 & \bar{C}_h^T & C_{xz}^T \\ B_{qx}^T R + \lambda \tilde{H} \bar{C}_h & \lambda(\tilde{H} \bar{D}_h + \bar{D}_h^T \tilde{H}) - \gamma_r^2 \tilde{I} & \lambda \hat{H} & \bar{D}_h^T & D_{qz}^T \\ 0 & \lambda \hat{H}^T & -\gamma_p^2 I & \hat{I}^T & 0 \\ \bar{C}_h & \bar{D}_h & \hat{I} & -W_r^{-1} & 0 \\ C_{xz} & D_{qz} & 0 & 0 & -W_p^{-1} \end{bmatrix} < 0 \tag{7.34}$$

with $\bar{C}_h = \begin{bmatrix} 0 & 0 \\ -C_q & -F \end{bmatrix}$ and $\bar{D}_h = \begin{bmatrix} 0 & 0 \\ -D_q & -E \end{bmatrix}$.

Making the following substitutions in (7.34)

$$\begin{aligned} &A_p = A_o + \Omega_1^T \Theta \Gamma_1,\ B_{qx} = B_o + \Omega_1^T \Theta \Gamma_2,\ \bar{C}_h = \bar{C}_o + \Omega_2^T \Theta \Gamma_1 \\ &\bar{D}_h = \bar{D}_o + \Omega_2^T \Theta \Gamma_2,\ C_{xz} = C_o + \Omega_3^T \Theta \Gamma_1,\ D_{qz} = \Omega_3^T \Theta \Gamma_2, \end{aligned} \tag{7.35}$$

we obtain the matrix inequality in (7.25). From the projection lemma [108], the matrix inequality (7.25) is solvable for Θ if and only if $W_\Gamma^T \Psi W_\Gamma < 0$ and $W_\Omega^T \Psi W_\Omega < 0$ hold. Here, W_Γ and W_Ω are orthogonal matrices that form the bases for the null spaces of Γ and Ω respectively. Let us define $\Omega = \Omega_0 T$ with $T = \text{diag}(R, \tilde{H}, I_{n_u}, I_{n_u}, I_{n_u})$ and $W_{\Omega o} = T W_\Omega$. Then, the second solvability condition $W_\Omega^T \Psi W_\Omega < 0$ can be equivalent expressed as $W_{\Omega o}^T T^{-1} \Psi T^{-1} W_{\Omega o} < 0$ where $W_{\Omega o}$ forms the basis for the null space of Ω_o. The null space bases W_Γ

and $W_{\Omega o}$ are respectively computed as

$$W_\Gamma = \left[\begin{array}{cc|cc|c|cc|c} I_{n_q} & 0_{n_q\times n} & 0 & 0 & 0 & 0 & 0 & 0 \\ 0 & 0 & I_{n_y} & 0 & 0 & 0 & 0 & 0 \\ 0 & 0 & 0 & 0_{n_u} & I_{n_u} & 0 & 0 & 0 \\ 0 & 0 & 0 & 0 & 0 & I_{n_u} & 0 & 0 \\ 0 & 0 & 0 & 0 & 0 & 0 & I_{n_y} & 0 \\ 0 & 0 & 0 & 0 & 0 & 0 & 0 & I_{n_y} \end{array}\right]^T \tag{7.36}$$

$$W_{\Omega o} = \left[\begin{array}{cc|cc|c|cc|c} I_{n_q} & 0 & 0 & 0 & 0 & 0 & 0 & 0 \\ 0 & I_n & 0 & B & 0 & 0 & 0 & 0 \\ 0 & 0 & I_{n_y} & 0 & 0 & 0 & 0 & 0 \\ 0 & 0 & 0 & 0 & I_{n_u} & 0 & 0 & 0 \\ 0 & 0 & 0 & 0 & 0 & I_{n_y} & 0 & 0 \\ 0 & 0 & 0 & -I_{n_u} & 0 & 0 & I_{n_u} & 0 \\ 0 & 0 & 0 & -D & 0 & 0 & 0 & I_{n_y} \end{array}\right]^T \tag{7.37}$$

Using these orthogonal matrices and after some algebraic manipulations, the conditions $W_\Gamma^T \Psi W_\Gamma < 0$ and $W_{\Omega o}^T T^{-1} \Psi T^{-1} W_{\Omega o} < 0$ reduces to the LMI constraints of (7.30) and (7.31) respectively. □

7.5 Algebraic-Loop: Well-posedness and practical Implementation

The anti-windup design problem involves dealing with the algebraic loop of Fig. 7.4. The presence of such an algebraic loop, if not well-posed, can result in serious problems during practical implementation of control. Even when the algebraic loop is well-posed, numerical implementation is not straight forward in real-time applications. We consider an approach for well-posedness which generalizes the results of [15; 16; 46] to cases where the nonlinearity is coupled (i.e. non-diagonal). From the perspective of numerical computation, algorithms based on fixed-point iterations have been suggested in [8; 57] for

such a multivariable algebraic loop. We note that an optimal solution can be obtained by solving directly the KKT equations associated with such an algebraic loop. This corresponds to a particular convex optimization for which efficient solutions are well established (e.g.[109; 110]).

The algebraic loop of Fig. 7.4 is well-posed or has a well-defined state model if the equations

$$\begin{aligned} \dot{x} &= (A + BF)x + BEw \\ u &= u_z - Fx + (I - E)w \\ w &= \phi(u) \end{aligned} \tag{7.38}$$

with

$$\begin{aligned} \phi(u) = \arg\min \frac{1}{2} w^T H w \\ \text{subject to } Lu - Lw \leq b, \end{aligned} \tag{7.39}$$

have a unique solution u_d for every (x, u_z). We consider here, sufficient conditions under which a solution exists and the uniqueness of such a solution. Let us define $u_d = \hat{u}_d + \tilde{u}_d$ and $\tilde{x} = \tilde{u}_d + u$, then (7.39) can be decomposed

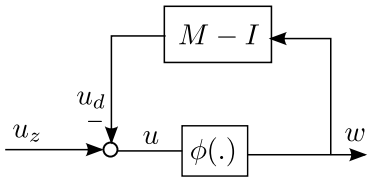

Figure 7.4: Algebraic loop involving a quadratic program and a dynamic feedback

into (7.41) and (7.40) denoted as the inner and the outer loop as follows

$$\text{Outer Loop}: \quad \begin{cases} x &= (A+BF)x + BEw \\ \hat{u}_d &= Fx \end{cases} \tag{7.40}$$

$$\text{Inner Loop}: \quad \begin{cases} w &= \phi(u) \\ u &= \tilde{x} - \tilde{u}_d \\ \tilde{u}_d &= (E-I)w. \end{cases} \tag{7.41}$$

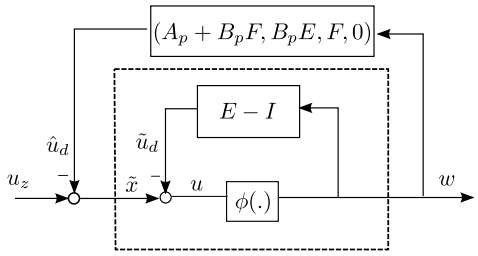

Figure 7.5: Algebraic loop decomposition into static and dynamic loops

Since the algebraic loop is now restricted to the static inner loop, checking the well-posedness of the algebraic loop of Fig. 7.4 is equivalent to checking the well-posedness of the inner-loop as depicted in Fig. 7.5. We further observe that the static feedback link of the inner loop can be subsumed into the feedforwad path containing the nonlinearity ϕ to obtain an equivalent optimization problem which may be interpreted in the framework of linear complementarity problems [110].

We briefly recall the linear complementarity problem definition and we define some matrix classes required for our main result.

Definition 22 (Linear Complementary Problem (LCP))**.** Given a vector $\tilde{q} \in \mathbb{R}^m$ and a matrix $\widetilde{M} \in \mathbb{R}^{m \times m}$, find a vector $\tilde{z} \in \mathbb{R}^m$ such that

$$\tilde{z} \geq 0, \tag{7.42}$$

$$\tilde{q} + \widetilde{M}\tilde{z} \geq 0, \tag{7.43}$$

$$\tilde{z}^T(\tilde{q} + \widetilde{M}\tilde{z}) = 0. \tag{7.44}$$

The LCP is said to be feasible if there exists a vector $\tilde{z}$ satisfying eqs. (7.42) and (7.43).

Definition 23 ($\mathbf{P_0}$ and Adequate matrices)**.**

i. A matrix $\widetilde{M} \in \mathbb{R}^{m\times m}$ is said be a $\mathbf{P_0}$-matrix if its all principal minors are nonnegative.

ii. A matrix $\widetilde{M} \in \mathbb{R}^{m\times m} \in \mathbf{P_0}$ is said to be

   (a) column adequate if for each $\alpha \subseteq \{1, \ldots, m\}$,

$$[\det \widetilde{M}_{\alpha\alpha} = 0] \;\Rightarrow\; [\widetilde{M}_{\bullet\alpha} \text{ has linearly dependent columns}].$$

   (b) row adequate if $\widetilde{M}^T$ is column adequate.

   (c) adequate if $\widetilde{M}$ is both cloumn and row adequate.

The following lemmas give the existence and uniqueness results for LCP using the above defined matrix classes.

Lemma 8. Let $\widetilde{M} \in \mathbb{R}^{m\times m}$ be given, the following statements hold;

i. If the LCP($\tilde{q}$,$\widetilde{M}$) is feasible and $\widetilde{M}$ is positive semi-definite, then it is solvable.

ii. Let $\widetilde{M} \in \mathbb{R}^{m\times m}$ be adequate and let $\tilde{q} \in \mathbb{R}^m$ be arbitrary. If LCP($\tilde{q}$,$\widetilde{M}$) is feasible, then there exist a unique vector $\tilde{w}$ and a vector $\tilde{z}$ satisfying $\tilde{w} = \tilde{q} + \widetilde{M}\tilde{z} \geq 0, \tilde{z} \geq 0, \tilde{w}^T\tilde{z} = 0$.

The proofs of items (i) and (ii) can be found in [110, Theorem 3.1.2 and Corollary 3.5.6 respectively].

Lemma 9. Given the LCP $(\tilde{q},\, \widetilde{M})$ in eqs. (7.42) to (7.44), define the following convex QP problem

$$z^* = \arg\min_{\tilde{z}} \tilde{z}^T(\tilde{q} + \widetilde{M}\tilde{z}) \quad \text{subject to} \tag{7.45}$$

$$\tilde{q} + \widetilde{M}\tilde{z} \geq 0 \quad \text{and} \tag{7.46}$$

$$\tilde{z} \geq 0. \tag{7.47}$$

Then z^* solves eqs. (7.45) to (7.47) if and only if $(z^*, \widetilde{M}z^* + \tilde{q})$ is a solution of LCP $(\tilde{q},\, \widetilde{M})$ in eqs. (7.42) to (7.44).

The proof can be found in [109, Theorem 8.4].
Note that there is no restriction on whether $\widetilde{M}$ is symmetric or not in both lemmas lemmas 8 and 9. In general, $\widetilde{M}$ can be any arbitrary real square matrix and need not be symmetric. We now state the main result.

Theorem 9. Consider the system on Fig 7.5. Let $\phi(.) : \mathbb{R}^m \to \mathbb{R}^m$ take the form of (7.39) with $H = H^T > 0$ and fixed terms L and $b > 0$. Let $E \in \mathbb{R}^{m\times m}$ be a (asymmetric) positive definite matrix. Then the algebraic loop formed by the feedback interconnection of $\phi(.)$ and the static gain $E - I$ is equivalent to the LCP($\tilde{q}$,$\widetilde{M}$) where $\widetilde{M} = LEH^{-1}L^T$ and $q = b - L\tilde{x}$. Furthermore, let $\widetilde{M}$ be adequate. If the LCP($\tilde{q}$,$\widetilde{M}$) is feasible for any arbitrary $\tilde{q}$, then the algebraic loop is well-posed for any $\tilde{x} \in \mathbb{R}^m$. The unique solution of the algebraic loop is given by $u = H^{-1}L^T\tilde{z}$ where $\tilde{z}$ is the unique solution of the LCP($\tilde{q}$,$\widetilde{M}$).

Remark 12. Before providing the proof of this result, we quickly note that the matrix product EH^{-1} is positive definite(asymmetric). Recall that H is symmetric and positive definite by construction while E is invertible and enters the system via the particular choice of right coprime factorization (7.5). The solvability condition (7.34) guarantees that $E^TH + HE > 0$ $\forall\lambda > 0$. This can be seen from the (2,2) element of (7.34) where

$$\tilde{H}\bar{D}_h + \bar{D}_h\tilde{H} - \gamma_r^2\tilde{I} = \begin{bmatrix} -\gamma_r^2\tilde{I} & -\lambda\bar{D}_q^TH \\ -\lambda H\bar{D}_q & -\lambda E^TH - \lambda HE \end{bmatrix}.$$

Since E is invertible, we can pre and post multiply $E^T H + HE$ by E^{-T} and E^{-1}. We have $HE^{-1}+E^{-T}H > 0$. The positive definiteness of $HE^{-1}+E^{-T}H$ implies that HE^{-1} is positive definite [111]. If $HE^{-1} > 0$, then $EH^{-1} > 0$.

Proof. Since $H = H^T > 0$, the necessary and sufficient Karoush-Kuhn-Tucker (KKT) conditions [59] for ϕ are given by

$$Hw - L^T\mu = 0, \tag{7.48}$$

$$Lu - Lw - b + s = 0, \tag{7.49}$$

$$s \geq 0, \quad \mu \geq 0, \quad \mu^T s = 0. \tag{7.50}$$

From (7.41), we have $u = \tilde{x} - (E - I)w$. Substituting for u in (7.49) gives

$$Hw - L^T\mu = 0, \tag{7.51}$$

$$L\tilde{x} - LEw - b + s = 0, \tag{7.52}$$

$$s \geq 0, \quad \mu \geq 0, \quad \mu^T s = 0. \tag{7.53}$$

Since H is nonsingular, we can eliminate (7.51) from the above set of conditions by rewriting it as $w = H^{-1}L^T\mu$ and then substituting for w in (7.52) to give

$$LEH^{-1}L^T\mu + b - L\tilde{x} - s = 0, \tag{7.54}$$

$$s \geq 0, \quad \mu \geq 0, \quad \mu^T s = 0. \tag{7.55}$$

Substituting for $\tilde{z} = \mu$, $\tilde{q} = b - L\tilde{x}$, $\widetilde{M} = LEH^{-1}L^T$ in eqs. (7.54) and (7.55) and re-arranging gives the LCP($\tilde{q}$,$\widetilde{M}$).

Now we show feasibility. From Def. 22, the LCP($\tilde{q}$,$\widetilde{M}$) is feasible if there exists a vector $\tilde{z}$ satisfying eqs. (7.42) and (7.43). For our case, it is easy to construct such a $\tilde{z}$. Choose $z_1 \in \mathbb{R}^m$ such that $z_1 \geq 0$ and $z_1 - HE^{-1}\tilde{x} \geq 0$. Then choose

$$\tilde{z} = \begin{bmatrix} z_1 \\ z_1 - HE^{-1}\tilde{x} \end{bmatrix}. \tag{7.56}$$

By construction $\tilde{z} \geq 0$. Furthermore, $L^T\tilde{z} = HE^{-1}\tilde{x}$ so that

$$\begin{aligned}\tilde{q} + \widetilde{M}\tilde{z} &= b - L\tilde{x} + LEH^{-1}L^T\tilde{z} \\ &= b \\ &\geq 0.\end{aligned}$$

Note that this is sufficient for the LCP($\tilde{q}$,$\widetilde{M}$) to be solvable since $\widetilde{M}$ is semi positive definite (def. 1).
To show there is a unique solution, we need to show that $\widetilde{M}$ is adequate. In our case, $\widetilde{M} \in \mathbb{R}^{2m\times 2m}$, so we must choose $\alpha \subseteq \{1, \ldots, 2m\}$. In addition, $\widetilde{M}$ has the structure

$$\widetilde{M} = LEH^{-1}L^T = \begin{bmatrix} EH^{-1} & -EH^{-1} \\ -EH^{-1} & EH^{-1} \end{bmatrix}. \tag{7.57}$$

Furthermore EH^{-1} itself is (asymmetric) positive definite and hence adequate. Suppose α includes both i and $i + m$ for some i. Then $\widetilde{M}_{\bullet\alpha}$ has linearly dependent columns. If α includes no such pairs, then $\widetilde{M}_{\alpha\alpha}$ may be obtained from a corresponding principal submatrix of EH^{-1} via permutation and row/column scaling (by -1) since $\widetilde{M}_{\alpha\alpha} = L_{\alpha\bullet}EH^{-1}(L_{\alpha\bullet})^T$. It follows that in this case that $\widetilde{M}_{\alpha\alpha}$ must be positive definite and the rows of $L_{\alpha\bullet}$ are linearly independent. Following similar argument, it follows that $\widetilde{M}^T$ is also column adequate due to symmetry. Hence, $\widetilde{M}$ is adequate.
Finally, if we set $\tilde{w} = \tilde{q} + \widetilde{M}$ and substitute for $\tilde{q}$ and $\widetilde{M}$, we have that

$$\tilde{w} = b - L\tilde{x} + LEH^{-1}L^T\mu \text{ and} \tag{7.58}$$

$$w = H^{-1}L^T\mu. \tag{7.59}$$

Hence $\tilde{w} = b - L\tilde{x} + LEw$. It follows that if $\tilde{w}$ is unique then w is unique. □

Using the result of theorem 9, the algebraic loop of Fig. 7.4 can be redrawn with the original quadratic program (7.39) replaced with a related convex optimization eqs. (7.45) to (7.47) as shown in Fig. 7.6. Note that w^*, the

unique solution of the algebraic loop, is recovered using $w^* = H^{-1}L^T z^*$. The well-posedness of the algebraic loop thus reduces to checking existence and the uniqueness of the solution to the optimization problem involving $\tilde{\phi}(.)$.

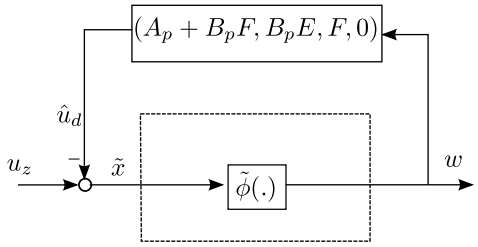

Figure 7.6: Practical implementation

The implication of above result is that if the system of eqs. (7.51) to (7.53) is solvable, any solution yields an optimal pair (w^*, μ^*) where w^* is the optimal solution of the algebraic loop. The solution is unique if $\widetilde{M}^T$ is adequate. If however, the system is not solvable, the algebraic loop does not have a solution and the associated optimization problem eqs. (7.42) to (7.44) is either infeasible or unbounded below.

Remark 13. When the nonlinearity $\phi(.)$ is decoupled such that $H > 0$ is diagonal, well-posedness of the algebraic loop then requires only that the constant matrix E be positive definite. In this case, the algebraic loop may admit an explicit solution [46]. □

Remark 14. When $H > 0$ and $E > 0$ are both diagonal, the well-posedness condition is trivially satisfied. In this case, E does not offer any extra degree of freedom in the anti-windup design [86] except for its role in the convexification of the synthesizing LMI. There is no algebraic loop in the interconnection of Fig. 7.4 when E is the identity matrix. □

Remark 15. When $H > 0$ and $E > 0$ are both non-diagonal, the well-posedness of the algebraic loop is guaranteed by theorem 9. In this case, the matrix H allows the incorporation of plant's directional characteristics into the anti-windup design. The anti-windup compensator search space is also enlarged to include all the right coprime factorization parameterized

by F and E in (7.5). Thus, E provides an extra degree of freedom in the anti-windup design and computation. □

Fig. 7.6 provides a convenient way of implementing the algebraic loop of Fig. 7.4. In general, there are efficient algorithms for solving the LCP problem eqs. (7.42) and (7.43). After that we have established that a unique solution exists, the algebraic loop can be implemented using an efficient quadratic program solver (for the QP formulation eqs. (7.45) to (7.47)). Several other algorithms are available for solving the LCP problem. Some of these may be found in [109; 110].

7.6 Summary

We have developed a robust synthesis procedure for optimizing anti-windup subject to infinity-norm bounded uncertainties. The arising algebraic loop in the anti-windup structure is expressed as a convex optimization problem. The condition for well-posedness of the anti-windup interconnection reduces to the condition for the existence and uniqueness of a solution to the optimization problem.

Chapter 8

Two-stage Internal Model Control anti-windup: Design and Stability Analysis

8.1 Introduction

Multivariable plants under input constraints such as actuator saturation are liable to performance deterioration due to control windup and directionality change. Anti-windup designs must therefore be augmented with dynamic compensators to account for process directionality in MIMO systems. One major drawback to some of the existing directionality compensation schemes[42; 7; 8] is that while they offer optimal dynamic behaviour, their performances deteriorate significantly in steady state especially when the constraints are active. Schemes that guarantee optimal steady state behaviour such as [9], may have poor transient characteristics.

In chapter 5, we provided a review of some of the existing directionality compensation scheme and their interpretations in terms of a standard quadratic

program. As observed, no single scheme offers an ideal solution for all scenarios in terms of transient and steady state performance in the presence of control input saturations. In chapter 6, a formal methodology for anti-windup design incorporating a quadratic program as input nonlinearity was developed. This framework allows equipping several existing directionality schemes with both closed loop stability and performance guarantees. In this chapter, we present a two-stage internal model control (IMC) anti-windup design for open loop stable plants. The design is based on the solution of two low-order quadratic programs (QP) at each time step which addresses both transient and steady state behaviours of the system.

We also develop tests for analyzing the robust stability of such systems against any infinity-norm bounded uncertainty. We note that the controller input-output mappings satisfy certain class of integral quadratic constraints (IQCs) and so sufficient conditions can be developed for analyzing robust stability of the closed-loop system. In particular, the unconstrained case reduces to the conventional IMC structure where the robust stability is guaranteed by the small gain theorem. Simulated examples show that the two-stage IMC has superior performance when compared to other existing optimization-based anti-windup methods. The stability test is illustrated for a plant with left matrix fraction uncertainty. We consider a scenario where the proposed two-stage IMC competes favourably with a long prediction horizon model predictive control (MPC).

The chapter is structured as follows. Section 8.2 contains the first contribution where we present the two-stage IMC anti-windup for not only dealing with the performance degradation associated with control windup and directionality but also for ensuring steady state performance in input constrained multivariable problem. In terms of nominal performance, the two-stage IMC compares favourably with a long prediction horizon MPC while its computational requirement is equivalent to that of a single-horizon MPC. The performance of the proposed approach is illustrated via two simulation examples involving ill-conditioned plants. Section 8.3 contains the second contribution

where sufficient robust stability tests are constructed for the two-stage IMC anti-windup based on IQC theory. We illustrate the stability test with a simulation example. The plant model has a left matrix fraction uncertainty as well as a control input nonlinearity.

8.2 Two-Stage Multivariable Internal Model Control anti-windup Structure

We consider the two-stage IMC anti-windup scheme of Fig. 8.1. The approach is based on the solution of two quadratic programs (QP) termed the dynamic QP and the steady-state QP. While the former addresses the transient behaviour of the plant and ensures that the constrained plant response is as close as possible to the unconstrained plant response, the latter ensures optimal steady state performance and it is based on steady state properties of the plant. The idea of using a separate QP to calculate steady state set-points has been previously introduced in MPC formulations [26; 10; 11; 112; 12]. Here, we introduce the concept of set-point optimization into the internal model control framework. When combined with the directionality compensation previously discussed, we obtain the two-stage IMC anti-windup structure of Fig. 8.1.

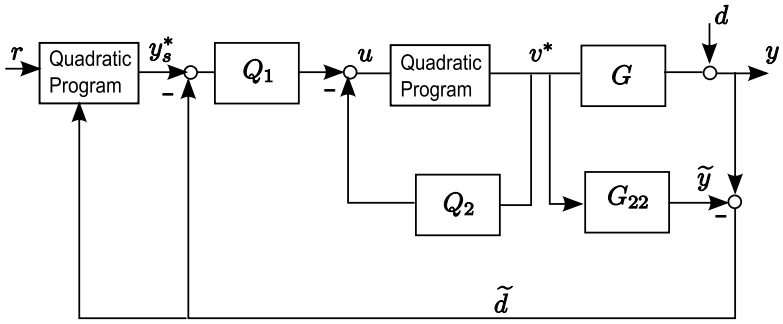

Figure 8.1: The two-stage IMC anti-windup

Because of the presence of saturation nonlinearities in the system, the output

of the constrained system y differs from y', the output of the unconstrained system. In general, the control objective is to keep every output y of the constrained system as close as possible to those of the unconstrained system y'. We define the mapping

$$y' = \mathcal{P}u \quad \text{and} \quad y = \mathcal{P}v \tag{8.1}$$

where $\mathcal{P}$ represents the plant operator. The signals v and u are the constrained and the unconstrained control inputs respectively. Mathematically, we seek a feasible control input v^* that is a solution to the following constrained optimization problem

$$v^* = \arg\min_v |\mathcal{P}v - \mathcal{P}u|^2_{\mathcal{Q}} \tag{8.2}$$

subject to the constraints

$$u_i^{min} \leq v_i \leq u_i^{max} \quad i = 1, \ldots, m. \tag{8.3}$$

$\mathcal{Q}$ is assumed to be diagonal positive definite matrix.

It should be noted that while the directionality compensation schemes discussed in chapter 5 attempted to solve the constrained optimization (8.2), they have either proffered approximate solutions or solve related problems by choosing the plant operator $\mathcal{P}$ either as the plant characteristic matrix $\mathcal{C}$ [8] or as the steady state gain [9] or differently (e.g [43; 7]).

For square systems, the initial response of the system output to step change in the input vector depends on the characteristics matrix $\mathcal{C}$ [101; 8]. Therefore, to address the transient behaviour of the closed system, the plant operator $\mathcal{P}$ can be chosen as the characteristic matrix $\mathcal{C}$ of the plant. Making this substitution in (8.2) results in the following optimization problem

$$v^* = \arg\min_v |\mathcal{C}v - \mathcal{C}u|^2_{\mathcal{Q}} \tag{8.4}$$

subject to the constraints

$$u_i^{min} \leq v_i \leq u_i^{max} \quad i = 1, \ldots, m.$$

The steady state aspect of the control problem is to determine appropriate values of (y_s and u_s) satisfying

$$y_s = \mathcal{K}_p u_s + \tilde{d} \tag{8.5}$$

where u_s is the steady state control input that makes the controlled variable achieve y_s in steady state. $\tilde{d}$ is the disturbance estimate obtained as the difference between the measured plant output y and the model output $\tilde{y}$. $\mathcal{K}_p$ is the non-singular steady state gain of the plant. Ideally, $y_s = r$. If, however, the input constraints are active in steady state, then y_s may not attain the target prescribed by the reference signal r. The objective is then to find feasible y_s (or u_s) such that y_s is as close as possible to r in some sense and within the limit imposed by the input constraints.

The solution of the following quadratic program can be used to determine a feasible steady state target y_s that should be applied as shown in Fig. 8.1 such that the closed loop response in steady state y_s is as close as possible to r.

$$y_s^* = \arg\min_{u_s, y_s} |r - y_s|^2_{\mathcal{Q}_{ss}} \tag{8.6}$$

subject to the constraints

$$u_i^{min} \leq u_{s_i} \leq u_i^{max} \quad i = 1, \ldots, m$$
$$\begin{bmatrix} -\mathcal{K}_p & I \end{bmatrix} \begin{bmatrix} u_s \\ y_s \end{bmatrix} = \tilde{d}$$

where $\mathcal{Q}_{ss}$ is a diagonal positive definite matrix for penalizing deviations in each of the controlled variables and their relative importance. The equality constraint guarantees the steady state requirement of (8.5). If the set-point target is achievable in steady state, the difference between the reference signal

r and the current disturbance estimate $\tilde{d}$ is passed to the dynamic optimization problem for computation of the control input v. If, on the other hand, the steady state target is not achievable due to the violation of one or more of the constraints in steady state, a feasible steady state target y_s is computed such that y_s is as close as possible to the reference signal r. The difference between the feasible steady state target and the current disturbance estimate is then passed to the dynamic optimization problem.

The equality constraint can be eliminated from (8.6) to obtain an equivalent optimization problem

$$u_s^* = \arg\min_{u_s} \left| r - \tilde{d} - \mathcal{K}_p u_s \right|_{\mathcal{Q}_s}^2 \tag{8.7}$$

subject to the constraints

$$u_i^{min} \leq u_{s_i} \leq u_i^{max} \quad i = 1, \ldots, m.$$

This transformed problem optimizes over variable u_s and takes as input the difference between the reference signal r and the disturbance estimate $\tilde{d}$. If u_s^* is an optimal solution of (8.7), then the optimal solution y_s^* of the original problem (8.6) is obtained via the steady-state model of (8.5).

The two artificial nonlinearities (8.4) and (8.7) may be re-written in the standard quadratic program form as

$$\begin{aligned} v^* = &\arg\min \frac{1}{2} v^T H_1 v - v^T H_1 u \\ &\text{subject to } Lv \preceq b \end{aligned} \tag{8.8}$$

$$\begin{aligned} u_s^* = &\arg\min \frac{1}{2} u_s^T H_2 u_s - u_s^T \tilde{H}_2^T (r - \tilde{d}) \\ &\text{subject to } Lu_s \preceq b \end{aligned} \tag{8.9}$$

where $H_1 = \tilde{H}_1^T \tilde{H}_1$ and $H_2 = \tilde{H}_2^T \tilde{H}_2$ are symmetric positive definite hessian matrices defined in terms of the plant structural properties i.e $\tilde{H}_1 = \mathcal{C}$ and $\tilde{H}_2 = \mathcal{K}_p$. The fixed terms L and b in the inequality constraints are

respectively obtained as

$$L = \begin{bmatrix} -I_m \\ I_m \end{bmatrix} \text{ and } b = \begin{bmatrix} -u^{min} \\ u^{max} \end{bmatrix} \tag{8.10}$$

with $u^{min} = \begin{bmatrix} u_1^{min}, & \cdots, & u_m^{min} \end{bmatrix}^T$ and $u^{min} = \begin{bmatrix} u_1^{max}, & \cdots, & u_m^{max} \end{bmatrix}^T$. The solutions v^* and u_s^* of (8.8) and (8.9) are unique if the characteristics matrix $\mathcal{C}$ and the steady gain $\mathcal{K}_p$ are respectively non-singular. We now summarize the first contribution of this chapter in the following control algorithm.

Two-stage IMC anti-windup Control algorithm: Given an open-loop stable plant G with a nominal model G_{22}, and feasible optimal values v^* and u^* satisfying (8.8) and (8.9) respectively. The control law that achieves combined optimal transient and steady-state performance for the two-stage IMC anti-windup structure of Fig. 8.1 is given by

$$\begin{aligned} \tilde{d} &= y - G_{22}v^* \\ u_s^* &= \psi_2(r, \tilde{d}) \\ y_s^* &= \tilde{H}_2 u_s^* + \tilde{d} \\ u &= Q_1(y_s^* - \tilde{d}) - Q_2 v^* \\ v^* &= \psi_1(u) \end{aligned} \tag{8.11}$$

where ψ_1 and ψ_2 are nonlinear functions representing the quadratic programs (8.8) and (8.9) respectively. □

Without the constraints, the control law reduces to the unconstrained standard IMC control equation

$$\begin{aligned} \tilde{d} &= y - G_{22}u \\ u &= (I + Q_2)^{-1}Q_1(r - \tilde{d}) \end{aligned} \tag{8.12}$$

Correct steady state behaviour is ensured by designing Q such that $Q(0) = G(0)^{-1}$ for $G(s)$ or $Q(1) = G(1)^{-1}$ for $G(z)$. If constraints are active in steady state, then optimal steady state behaviour is guaranteed by solving

(8.9) subject to the constraints.

Remark 16. For the class of systems whose characteristics matrix $\mathcal{C}$ and steady state gain $\mathcal{K}_p$ are similar, the optimization problem in (8.8) effectively meets the steady state requirement of (8.9). Hence only (8.8) need be solved to achieve both optimal transient and steady state responses in the presence of control input saturation. This is illustrated by the following example.

Example 7. We consider example 4 again where the set-point change from $[0\ 0]^T$ to $[0.85\ 2.2]^T$ is such that one of the constraints is violated in steady states. The plant's characteristics matrix and steady gain are respectively given as

$$\mathcal{C} = \begin{bmatrix} 0.25 & 0 \\ 0 & 4 \end{bmatrix}, \mathcal{K}_p = \begin{bmatrix} 37.5 & -4 \\ -625 & 200 \end{bmatrix}.$$

We first compare the two-stage IMC anti-windup (TIMA) with the directionality compensations schemes previously discussed in chapter 5. Fig. 8.2 shows that the two-stage IMC scheme results in the closest closed loop performance to the unconstrained case as compared to the other anti-windup schemes. This is not surprising, as the plant is statically coupled and has a steady state gain which is significantly different from the characteristic matrix. The steady state QP (8.9) ensures optimal steady state behaviour with the active constraint.

We also compare the performance of the two-stage IMC with a particular MPC formulation [13]. We consider two MPC cases; a single horizon MPC (prediction horizon $N_p = 1$ and control horizon $N_c = 1$) and a long horizon MPC (prediction horizon $N_p = 100$ and control horizon $N_c = 50$). The closed loop responses in Fig. 8.3 and Fig. 8.4 show that the two-stage IMC competes favourably with a long horizon MPC while only requiring the computation equivalent to that of a single horizon MPC [113]. It is however, envisaged that a long horizon MPC will outperform the two-stage IMC especially when there are high-order unmodeled dynamics in the system. The two-stage IMC does not require the receding horizon computation of MPC and may serve

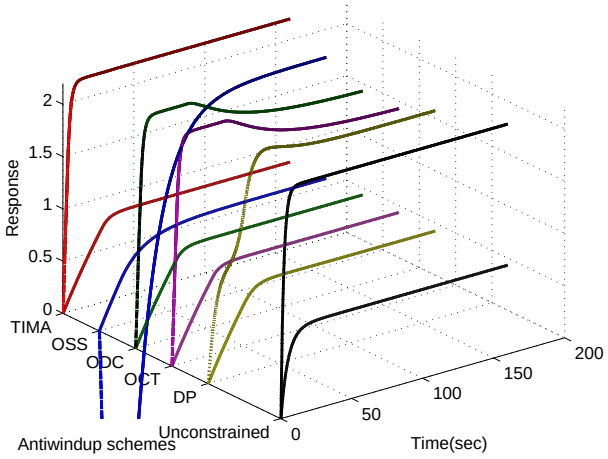

Figure 8.2: Example 7: Two-stage IMC (TIMA) yields the closest performance to the unconstrained case. DP [6] and OSS [9] schemes have improved steady state behaviours but poor transient characteristics as opposed to the OCT [7] and ODC [8] schemes both of which have optimal transient behaviours but degraded steady state performances.

as a less computationally intensive and more transparent (in terms of tuning for robustness) alternative to MPC.

8.3 Stability Analysis

We assume the plant is represented as in Fig. 8.5a where the generalized plant $\widetilde{G}$ maps $[q_\Delta^T, v^T]^T$ to $[p_\Delta^T, y^T]^T$ according to

$$\begin{bmatrix} p_\Delta \\ y \end{bmatrix} = \begin{bmatrix} G_{11} & G_{12} \\ G_{21} & G_{22} \end{bmatrix} \begin{bmatrix} q_\Delta \\ v \end{bmatrix} \tag{8.13}$$
$$q_\Delta = \Delta p_\Delta$$

and $\Delta \in \mathcal{RH}_\infty$ is an operator satisfying $||\Delta||_\infty < 1$.

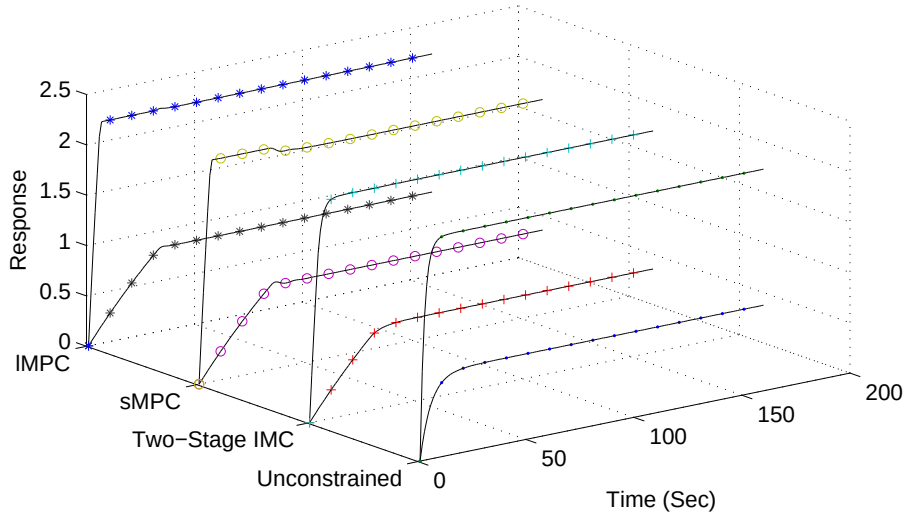

Figure 8.3: Example 7: Two-stage IMC ('+') outperforms the single horizon MPC (sMPC, 'o') and yields similar reponse to long horizon MPC (lMPC, '*')

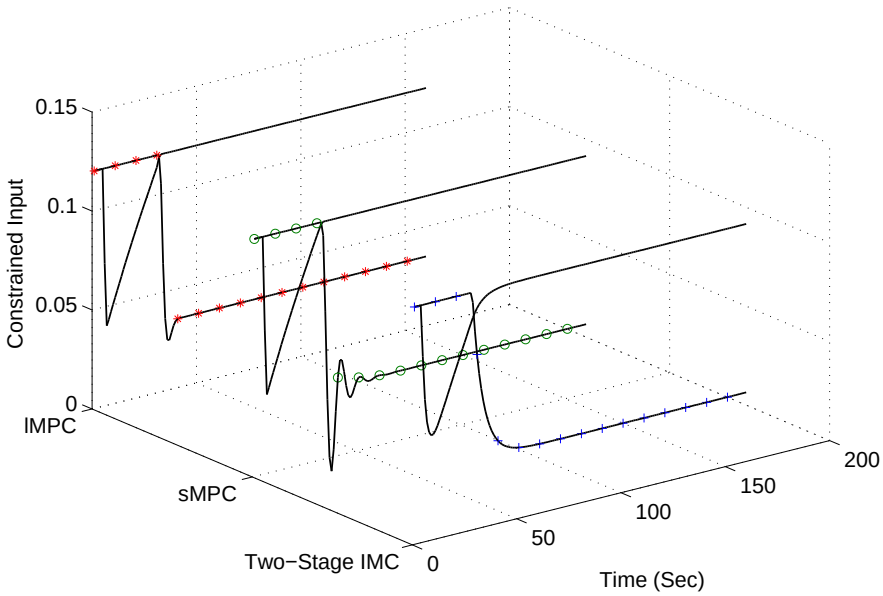

Figure 8.4: Constrained input: Two-stage IMC ('+'), single horizon MPC (sMPC, 'o') and long horizon MPC (lMPC, '*')

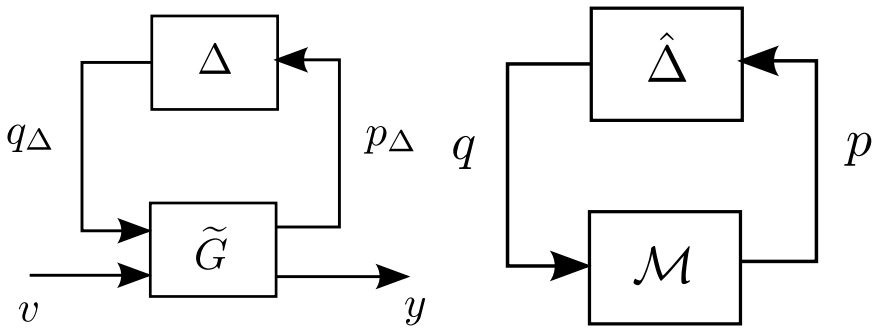

(a) Plant uncertainty (b) Feedback loop

Figure 8.5: General feedback interconnection for stability analysis

The transfer function from v to y is given by

$$y = [G_{22} + G_{21}\Delta(I - G_{11}\Delta)^{-1}G_{12}]v \tag{8.14}$$

where G_{22} is the nominal model and G_{11}, G_{12} and G_{21} are known transfer functions. As noted in section 2.5, a number of unstructured uncertainty descriptions (such as the additive, multiplicative and coprime factor type uncertainties) can be put into this general form.

For the purpose of stability analysis, we consider the standard feedback interconnection of Fig. 8.5b where all exogenous inputs and output signals have been ignored. $\mathcal{M}$ is a linear time invariant system operator and $\hat{\Delta}$ is a block diagonal operator defined by

$$\hat{\Delta} = \text{diag}(\psi_1, \psi_2, \Delta) \tag{8.15}$$

where $\psi_i : \mathbb{R}^m \to \mathbb{R}^m,\ i = 1, 2$ is a static operator and $\Delta \in \mathcal{RH}_\infty^n$ is some unknown operator satisfying $||\Delta||_\infty < 1$. The input-output map is defined by the equations

$$q = \hat{\Delta}(p), \quad p = \mathcal{M}q. \tag{8.16}$$

For the two-stage IMC anti-windup scheme, the nonlinearities defined by (8.8) and (8.9) satisfy respectively $\forall x$ the following generalized sector condi-

tions (see also section 2.2).

$$\psi_1(x)^T H_1 \psi(x)_1 - \psi_1(x)^T H_1 x \leq 0, \tag{8.17}$$

$$\psi_2(x)^T H_2 \psi(x)_2 - \psi_2(x)^T \tilde{H}_2 x \leq 0. \tag{8.18}$$

We then have that $\psi_1 \in \text{IQC}(\Pi_{\psi_1})$ and $\psi_2 \in \text{IQC}(\Pi_{\psi_2})$ with

$$\Pi_{\psi_1} = \begin{bmatrix} 0 & H_1 \\ H_1 & -2H_1 \end{bmatrix} \quad \Pi_{\psi_2} = \begin{bmatrix} 0 & \tilde{H}_2 \\ \tilde{H}_2 & -2H_2 \end{bmatrix}. \tag{8.19}$$

It follows immediately that $\psi_1 \in \text{IQC}(\beta_1 \Pi_{\psi_1})$ and $\psi_2 \in \text{IQC}(\beta_2 \Pi_{\psi_2})$ for $\beta_1, \beta_2 > 0$. We also have that $\Delta \in \text{IQC}(\alpha \Pi_\Delta)$ for $\alpha > 0$ with

$$\Pi_\Delta = \begin{bmatrix} \alpha I & \\ & -\alpha I \end{bmatrix}. \tag{8.20}$$

8.3.1 Robust Analysis of two-stage IMC anti-windup

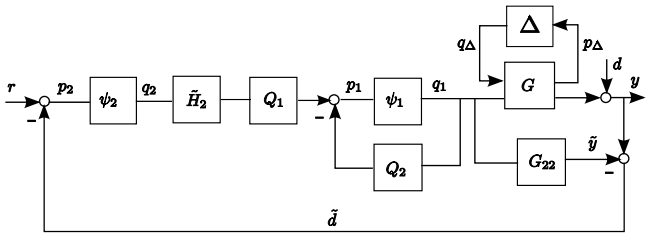

Figure 8.6: Two-stage IMC anti-windup for stability analysis

In this section, we consider the robust stability analysis of the two-stage IMC anti-windup scheme. Reorganising the two-stage structure of Fig. 8.1 in terms of the transformed steady-state quadratic program (8.9), we obtain an equivalent structure of Fig. 8.6. The IMC controller Q is designed *a priori* to meet some nominal performance specifications and then further augmentations are introduced to deal with performance deterioration in the face of control input saturations and model uncertainties. We analyze the stability of the two-stage IMC anti-windup for three cases; *a*) the robust

stability of the unconstrained structure, *b*) the constrained nominal stability and *c*) the complete stability involving the input nonlinearities and the model uncertainties.

8.3.1.1 Unconstrained Robust Stability Analysis

For the unconstrained case where $Q = (I + Q_2)^{-1}Q_1$, the two-stage IMC anti-windup scheme reduces to the standard IMC without an anti-windup compensation. In this case, the controller (8.11) reduces to

$$\begin{aligned} \tilde{d} &= y - G_{22}q_1 \\ q_1 &= (I + Q_2)^{-1}Q_1(r - \tilde{d}) = Q(r - \tilde{d}). \end{aligned} \tag{8.21}$$

The closed loop is completely described by

$$\begin{aligned} q_\Delta &= \Delta p_\Delta \\ p_\Delta &= (G_{11} - G_{12}QG_{21})q_\Delta + G_{12}Q(r - d). \end{aligned} \tag{8.22}$$

Robust stability result for this case is standard and can be obtained via the application of small gain theorem [19] or the IQC theorem [51].

Result 1: Given a stable plant G (8.13) in feedback interconnection with controller (8.21). Assuming that the interconnection of G and $\tau\hat{\Delta}$ is well-posed for all $\tau \in [0, 1]$. Then the closed loop system is stable for all $||\Delta||_\infty < 1$ provided

$$||G_{11} - G_{12}QG_{21}||_\infty < 1. \tag{8.23}$$

Proof. From the closed-loop equation (8.22), we have $\mathcal{M} = G_{11} - G_{12}QG_{21}$ and $\hat{\Delta} = \Delta$. The result follows from the application of IQC stability condition of theorem 6. □

8.3.1.2 Constrained Nominal Stability Analysis

When the plant is assumed to be perfectly known (i.e. $G_{22} = G$), the two-stage IMC anti-windup structure becomes a quasi-open loop system as the outer loop in Fig. 8.6 represents a feedforward of the influence of disturbance d and is not affected by the action of the manipulated variable. The only remaining closed loop is the feedback around the nonlinearity ψ_1. The overall system is stable if and only if both the plant and the algebraic loop are stable. The closed loop equations around the nonlinearity is given by

$$\begin{aligned} q_1 &= \psi_1(p_1) \\ p_1 &= -Q_2 q_1 + Q_1 \tilde{H}_2 q_2 \\ q_2 &= \psi_2(r - d) \end{aligned} \tag{8.24}$$

Result 2: Given a stable plant G with $G_{11} = 0$,$G_{12} = 0$ and $G_{21} = 0$ in feedback interconnection with controller of the form (8.11) with ψ_1 and ψ_2 satisfying the sector-bound conditions (8.17) and (8.18) respectively. Assuming that the interconnection of G and $\tau \hat{Delta}$ is well-posed for all $\tau \in [0, 1]$. Then the closed-loop anti-windup system is stable provided

$$\beta_1(H_1 Q_2 + Q_2^* H_1 + 2H_1) - \frac{\beta_1^2}{2\beta_2} H_1 Q_1 Q_1^* H_1 > 0 \tag{8.25}$$

for some $\beta_1,\ \beta_2 > 0$, for all ω.

Proof. From (8.24), we have

$$\mathcal{M} = \begin{bmatrix} -Q_2 & Q_1 \tilde{H}_2 \\ 0 & 0 \end{bmatrix} \text{ and } \hat{\Delta} = \begin{bmatrix} \psi_1 & \\ & \psi_2 \end{bmatrix}$$

with ψ_1 and ψ_2 satisfying the IQCs defined by (8.19). $\Pi_{\hat{\Delta}}$ then becomes

$$\Pi_{\hat{\Delta}} = \left[\begin{array}{cc|cc} 0 & & \beta_1 H_1 & \\ & 0 & & \beta_2 \tilde{H}_2 \\ \hline \beta_1 H_1 & & -2\beta_1 H_1 & \\ & \beta_2 \tilde{H}_2^T & & -2\beta_2 H_2 \end{array}\right]. \tag{8.26}$$

The result follows from the application of IQC stability condition of theorem 6 followed by the application of Schur complements. □

Remark 17. As noted in [51], the well-posedness requirement is generally weak . In particular, for this case, well-posedness is guaranteed by the existence and uniqueness condition on the solution of the optimization problem associated with the algebraic loop. (See also discussion on this in section 7.5).

8.3.1.3 Complete Stability Analysis of two-stage IMC anti-windup

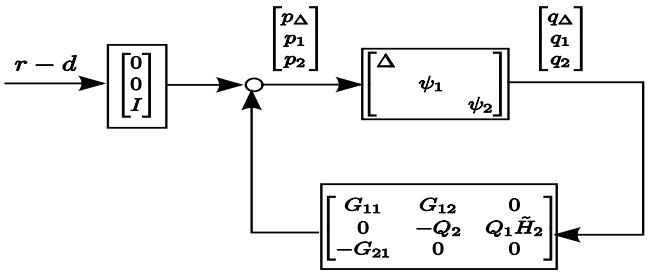

Figure 8.7: Feedback interconnection for two-stage IMC anti-windup

The anti-windup structure of Fig. 8.6 is transformed into the general feedback structure of Fig. 8.7 by defining

$$p = \begin{bmatrix} p_\Delta \\ p_1 \\ p_2 \end{bmatrix} \quad \text{and} \quad q = \begin{bmatrix} q_\Delta \\ q_1 \\ q_2 \end{bmatrix} \tag{8.27}$$

so that

$$\hat{\Delta} = \begin{bmatrix} \Delta & & \\ & \psi_1 & \\ & & \psi_2 \end{bmatrix} \tag{8.28}$$

$$\mathcal{M} = \begin{bmatrix} G_{11} & G_{12} & 0 \\ 0 & -Q_2 & Q_1\tilde{H}_2 \\ -G_{21} & 0 & 0 \end{bmatrix}. \tag{8.29}$$

We have $\Delta \in \text{IQC}(\Pi_\Delta)$, $\psi_1 \in \text{IQC}(\Pi_{\psi_1})$ and $\psi_2 \in \text{IQC}(\Pi_{\psi_2})$ where Π_Δ, Π_{ψ_1} and Π_{ψ_2} are as defined in (8.20) and (8.19).

The $\hat{\Delta}$ defined in (8.28) satisfies the IQC $\hat{\Delta} \in \text{IQC}(\Pi_{\hat{\Delta}})$ with

$$\Pi_{\hat{\Delta}} = \begin{bmatrix} \Pi_{11}^{\hat{\Delta}} & \Pi_{12}^{\hat{\Delta}} \\ \Pi_{21}^{\hat{\Delta}} & \Pi_{22}^{\hat{\Delta}} \end{bmatrix} = \text{daug}(\alpha\Pi_\Delta, \beta_1\Pi_{\psi_1}, \beta_2\Pi_{\psi_2}) \tag{8.30}$$

where

$$\Pi_{11}^{\hat{\Delta}} = \begin{bmatrix} \alpha I & & \\ & 0 & \\ & & 0 \end{bmatrix}, \; \Pi_{12}^{\hat{\Delta}} = \begin{bmatrix} 0 & & \\ & \beta_1 H_1 & \\ & & \beta_2\tilde{H}_2 \end{bmatrix}$$

$$\Pi_{21}^{\hat{\Delta}} = \begin{bmatrix} 0 & & \\ & \beta_1 H_1 & \\ & & \beta_2\tilde{H}_2^T \end{bmatrix} \text{ and}$$

$$\Pi_{22}^{\hat{\Delta}} = \begin{bmatrix} -\alpha I & & \\ & -2\beta_1 H_1 & \\ & & -2\beta_2 H_2 \end{bmatrix}$$

for any choice of multipliers $\alpha, \beta_1, \beta_2 > 0$. We note that the top left quadrant of $\Pi_{\hat{\Delta}}$ is positive semi-definite ($\Pi_{11}^{\hat{\Delta}} \geq 0$) while the bottom right quadrant of $\Pi_{\hat{\Delta}}$ is negative semi-definite ($\Pi_{22}^{\hat{\Delta}} \leq 0$) and so $\tau\hat{\Delta} \in \text{IQC}(\Pi_{\hat{\Delta}})$ for all $0 \leq \tau \leq 1$.

We now state the stability result for the complete two-stage IMC anti-windup

structure.

Result 3: Given a stable plant G (8.13) in feedback interconnection with controller of the form (8.11) with ψ_1, ψ_2 and Δ satisfying the IQC defined by (8.19) and (8.20) respectively. Assuming that the interconnection of G and $\tau\hat{\Delta}$ is well-posed for all $\tau \in [0, 1]$. Then the closed loop anti-windup system of Fig. 8.6 is stable provided

$$\left[\begin{array}{c|c} X_{11} & X_{12} \\ \hline X_{21} & X_{22} \end{array}\right] \geq \varepsilon I \tag{8.31}$$

for some $\varepsilon > 0$, for all ω with

$$\begin{aligned} X_{11} &= \alpha(I - G_{11}^* G_{11}) - \frac{\beta_2}{2} G_{21}^* G_{21} \\ X_{21} &= X_{12}^* = \frac{\beta_1}{2} H_1 Q_1 G_{21} - \alpha G_{12}^* G_{11} \\ X_{22} &= \beta_1(H_1 Q_2 + Q_2^* + 2H_1) - \alpha G_{12}^* G_{12} - \frac{\beta_1^2}{2\beta_2} H_1 Q_1 Q_1^* H_1. \end{aligned}$$

Proof. The two-stage IMC anti-windup structure of Fig. 8.6 can be transformed into the general feedback interconnection of Fig.8.5b with $\mathcal{M}$ and $\hat{\Delta}$ defined in (8.29) and (8.28) respectively. IQC stability condition of theorem 6 reduces to

$$\left[\begin{array}{cc|c} \alpha(I - G_{11}^* G_{11}) & -\alpha G_{11}^* G_{12} & \beta_2 G_{21}^* \tilde{H}_2 \\ -\alpha G_{12}^* G_{11} & \beta_1(H_1 Q_2 + Q_2^* H_1 + 2H_1) - \alpha G_{12}^* G_{12} & -\beta_1 H_1 Q_1 \tilde{H}_2 \\ \hline \beta_2 \tilde{H}_2^T G_{21} & -\beta_1 \tilde{H}_2^T Q_1^* H_1 & 2\beta_2 H_2 \end{array}\right] \geq \varepsilon I \tag{8.32}$$

The result follows after the application of Schur complements to (8.32) and using the fact that the bottom right block is positive definite and thus its inverse exists. □

Note that X on the left hand sides of (8.31) is a partitioned hermitian matrix.

The structure of X can be exploited to establish a relationship between the robustness of the two-stage IMC anti-windup and the standard IMC anti-windup with a QP. For the one-stage IMC anti-windup (i.e when we only have one nonlinearity ψ_1 in the system), the IQC stability condition is given by

$$\left[\begin{array}{c|c} S_{11} & S_{12} \\ \hline S_{21} & S_{22} \end{array}\right] \geq \varepsilon I \tag{8.33}$$

with

$$\begin{aligned} S_{11} &= \alpha(I - G_{11}^* G_{11}) \\ S_{21} &= S_{12}^* = \beta_1 H_1 Q_1 G_{21} - \alpha G_{12}^* G_{11} \\ S_{22} &= \beta_1(H_1 Q_2 + Q_2^* H_1 + 2H_1) - \alpha G_{12}^* G_{12}. \end{aligned}$$

Remark 18. Condition (8.33) is a necessary but not sufficient for (8.31) to hold. The condition (8.31) can be expressed as $X = S - Z > 0$ where Z is given as

$$\begin{bmatrix} \frac{\beta_2}{2} G_{21}^* G_{21} & \frac{\beta_1}{2} G_{21}^* Q_1^* H_1 \\ \frac{\beta_1}{2} H_1 Q_1 G_{21} & \frac{\beta_1^2}{2\beta_2} H_1 Q_1 Q_1^* H_1 \end{bmatrix} = \frac{1}{2\beta_2} \begin{bmatrix} \beta_2 G_{21}^* \\ \beta_1 H_1 Q_1 \end{bmatrix} \begin{bmatrix} \beta_2 G_{21} & \beta_1 Q_1^* H_1 \end{bmatrix} \geq 0. \tag{8.34}$$

The positive definiteness of X implies that S is also positive definite. On the other hand, X is positive definite if and only if $S > 0$ and $S > Z$.

Given a plant G, a nominal IMC controller Q and design parameters H_1 and H_2, checking for closed loop stability of the two-stage IMC anti-windup reduces to checking that the frequency dependent condition (8.31) holds for all frequency. This condition can be checked via frequency griding or by checking an equivalent time-domain condition obtained by applying KYP lemma to (8.31).

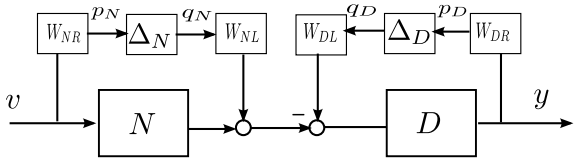

Figure 8.8: Plant with matrix fraction uncertainty for simulation

8.4 Simulation Example

We now illustrate the stability test for the two-stage IMC anti-windup where the plant nominal model has the following left matrix fraction factorization $D^{-1}N$ such that the perturbed plant (see Fig. 8.8) can be expressed as

$$G = (D + W_{DL}\Delta_D W_{DR})^{-1}(N + W_{NL}\Delta_N W_{NR}). \tag{8.35}$$

This can be put in the form of Fig.8.5a with

$$\widetilde{G} = \left[\begin{array}{cc|c} 0 & 0 & W_{NR} \\ W_{DR}D^{-1}W_{NL} & -W_{DR}D^{-1}W_{DL} & W_{DR}D^{-1}N \\ \hline D^{-1}W_{NL} & -D^{-1}W_{DL} & D^{-1}N \end{array}\right] \tag{8.36}$$

and

$$\Delta_u = \begin{bmatrix} \Delta_N & \\ & \Delta_D \end{bmatrix},\ p_1 = \begin{bmatrix} p_N \\ p_D \end{bmatrix},\ q_1 = \begin{bmatrix} q_N \\ q_D \end{bmatrix} \tag{8.37}$$

where W_{DL}, W_{DR}, W_{NL} and W_{NR} are weighting transfer function matrices. We will assume the uncertainties satisfy $||\Delta_N||_\infty < 1$ and $||\Delta_D||_\infty < 1$ so that $\Delta_u \in \text{IQC}(\Pi_u(\alpha_N, \alpha_D))$ with

$$\Pi_u(\alpha_N, \alpha_D) = \text{diag}(\alpha_N I, \alpha_D I, -\alpha_N I, -\alpha_D I) \tag{8.38}$$

for any $\alpha_N, \alpha_D > 0$.

Example 8. We consider example 4 again. The conventional IMC anti-windup designed for a step input based on option 1 discussed in chapter 3

is

$$Q_1 = \begin{bmatrix} 0.8 & 0 \\ 0 & 0.125 \end{bmatrix}$$

$$Q_2 = \frac{1}{\eta} \begin{bmatrix} 0.19s + 0.0058 & -0.0032s - 0.00064 \\ -0.03125s - 0.01563 & 0.47s + .0048) \end{bmatrix}$$

with $\eta = s^2 + 0.04s + 0.0002$. For the two-stage design, we chose $\tilde{H}_1$ and $\tilde{H}_2$ as the plant characteristic's matrix and steady state gain respectively (as discussed in section 8.2). We have

$$\tilde{H}_1 = \begin{bmatrix} 0.25 & 0 \\ 0 & 4 \end{bmatrix} \text{ and } \tilde{H}_2 = \begin{bmatrix} 37.5 & -4 \\ -625 & 200 \end{bmatrix}.$$

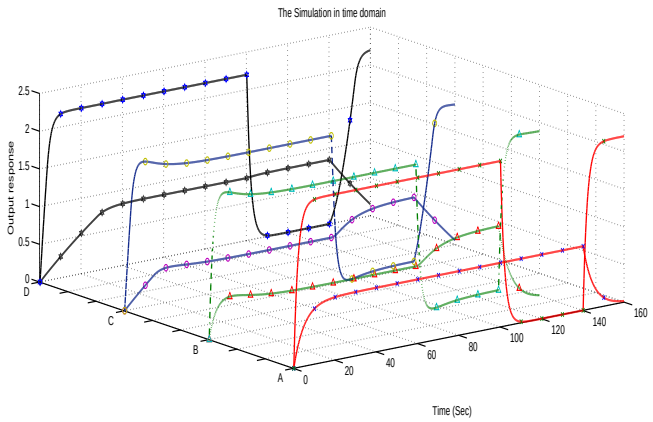

Figure 8.9: Simulations in time domain; A-Unconstrained nominal system, B-Perturbed unconstrained, C-Perturbed with a single stage IMC AW, D-Perturbed with two-stage IMC AW

A time-domain simulation of the plant was carried out for a particular value of model mismatch $\Delta_N = \Delta_D = (0.1s + 0.02)(s + 0.06)^{-1}$ with infinity norm of 0.33. The left fraction matrix nominal model for the plant was chosen as $G_{22} = D^{-1}N$ with $N = G_{22}$ and $D = I$. The uncertainty weights were set as $W_{NL} = W_{DL} = [1\ 1]^T$ and $W_{NR} = W_{DR} = [1\ 1]$. The simulation was carried out for a total of $160s$. Step changes were made to the reference inputs at time $t = 120s$ and $140s$ respectively. Fig. 8.9 shows the output

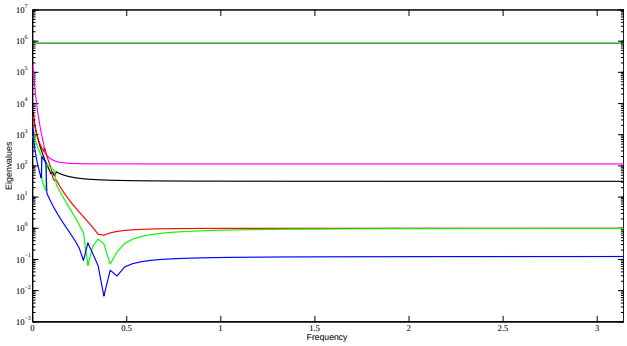

Figure 8.10: Eigenvalues of X evaluated $\forall w \in [0, \pi]$ and with $\alpha = \beta_1 = \beta_2 = 1$

responses of both the perturbed and the unperturbed systems. To show that the frequency dependent condition (8.31) is satisfied for all $\omega \in \mathbb{R}$, we check that $X(e^{j\omega T_s}) \geq \epsilon I$ for some ϵ and for all $\omega \in [-\pi, \pi]$ where T_s is the sampling time. Fig. 8.10 shows the eigenvalues plot of $X(e^{j\omega T_s})$ evaluated for $\omega \in [0, \pi]$ for a case where all the multipliers were set as unity. We have only shown the eigenvalues over the interval $[0, \pi]$ because of symmetry of the plot.

8.5 Summary

We have demonstrated the effectiveness of the two-stage internal model control anti-windup in dealing with the performance degradation associated with control windup and process directionality in input constrained multivariable systems. The two-stage IMC anti-windup involves two low-order quadratic programs that can be solved efficiently as compared to the intensive receding horizon control computation of MPC algorithms. We have also shown that sufficient robust stability conditions for the two-stage IMC anti-windup can be constructed via the theory of IQCs. While we have limited our discussions to a restricted class of static IQCs for describing the plant uncertainties and input nonlinearities, stronger results may be obtained by allowing a larger class of IQCs with dynamic multipliers such as those discussed in [103]. We note that the overall performance of optimizing anti-windups can be im-

proved without necessarily trading off on robustness as demonstrated via the simulation examples.

Chapter 9

Conclusion and Recommendations for Future Research

9.1 Conclusion

We have developed optimizing control strategies for open-loop stable multivarible systems with saturating actuators. The proposed control designs combine the efficiency of conventional anti-windup schemes with the optimality of model predictive control (MPC) algorithms. In particular, the classical internal model control law was enhanced for optimal performance by incorporating an online optimization. The resulting control scheme offers both stability and performance guarantees with moderate computational expense.

The optimizing anti-windup framework provides an attractive alternative to either the computationally expensive MPC algorithms or the conventional anti-windup schemes. The choice of control design will typically be informed

by some selection criteria such as the severity of constraints; the plant's structural characteristics; the presence of lightly damped modes or non-minimum phase zeros; process directionality and computational requirement. When directionality is an issue, especially for highly ill-conditioned plants, the optimizing anti-windup framework of chapter 6 and 7 offers a systematic way of incorporating such directional characteristics into the control synthesis. In situations where operating near or on the constraints at steady state is desirable or unavoidable, the novel two-stage architecture of chapter 8 offers a means for optimizing performance while operating close to the constraints. In terms of prospects for industrial applications, the optimizing anti-windup of chapter 6 has been successfully implemented on a low-end/low-cost programmable logic controller (PLC) as a Master's degree dissertation using a customized algorithm for a two-input two-output multivariable plant.

9.2 Recommendations for Future Research

Potential areas of future research are highlighted as follows.

Research Direction 1. Comparison of MPC and IMC structure

Some connections have been identified between single-horizon MPC and certain anti-windup schemes [9; 113]. Existing results in this area include [114; 115] where the authors have shown that there are cases where anti-windup control policies are equivalent to those of MPC for constrained single-input systems. A similar link has also been established between MPC and saturated LQR [116]. More recently, it has been reported that MPC control parametrization in terms of affine state or disturbance feedback is closely related to the well known Youla parametrization and thus MPC can be restructured into the IMC framework [117; 31]. Exploring the relationships between such classes of affine feedback policies and the IMC control law may pave a way for importing the attractive robust features of IMC into MPC. The two-stage IMC structure provides an opportunity to incorporate output

constraints into the anti-windup design and thus allows for performance comparison between anti-windup schemes and MPC algorithms which explicitly incorporates both input and output constraints.

Research Direction 2. Application

Implementation of MPC algorithms have been a major concern due to their huge computational power requirement. Despite the potential benefits of such advanced control algorithms (for example, allowing operation close to the plant limits and dealing with problems of multi-loop interactions) their deployment in the industry is often impeded by the limited computational power available in programmable logic controllers (PLCs). As a result, PLCs are restricted to low level control applications such as the on/off and Proportional-Integral-Derivative (PID) control implementations. Further exploration of the possibilities and limitations of these devices for the implementation of the two-stage IMC structure will be of great interest.

References

[1] G. C. Goodwin, S. E. Graebe, and W. S. Levine, "Internal model control of linear systems with saturating actuators," in *Proceedings of the European Control Conference*, Groningen, 1993, pp. 1072–1077.

[2] A. Zheng, M. V. Kothare, and M. Morari, "Anti-windup design for internal model control," *International Journal of Control*, vol. 60, no. 5, pp. 1015–1024, 1994.

[3] J. K. Park and C. H. Choi, "Dynamic compensation method for multivariable control systems with saturating actuators," *IEEE Trans. Automatic Control*, vol. 40, no. 9, pp. 1635–1640, 1995.

[4] G. Grimm, I. Postlethwaite, A. R. Teel, M. Turner, and L. Zaccarian, "Case studies using linear matrix inequalities for optimal anti-windup synthesis," *European Journal of Control*, vol. 9, pp. 463–473, 2003.

[5] E. F. Mulder, M. V. Kothare, and M. Morari, "Multivariable anti-windup controller synthesis using linear matrix inequalities," *Automatica*, vol. 37, pp. 1407–1416, 2001.

[6] P. J. Campo and M. Morari, "Robust control of processes subject to saturation nonlinearities," *Computers and Chemical Engineering*, vol. 14, no. 4/5, pp. 343–358, 1990.

[7] Y. Peng, D. Vrančić, R. Hanus, and S. R. Weller, "Anti-windup designs for multivariable controllers," *Automatica*, vol. 34, no. 12, pp. 1559–1565, 1998.

[8] M. Soroush and S. Valluri, "Optimal directionality compensation in processes with input saturation non-linearities," *International Journal of Control*, vol. 72, no. 17, pp. 1555–1564, 1999.

[9] W. P. Heath and A. G. Wills, "Design of cross-directional controllers with optimal steady state performance," *European Journal of Control*, vol. 10, pp. 15–27, 2004.

[10] K. R. Muske and J. B. Rawlings, "Model predictive control with linear models," *AIChE Journal*, vol. 39, no. 2, pp. 262–287, 1993.

[11] J. B. Rawlings and I. Chien, "Gage control of film and sheet-forming processes," *AIChE Journal*, vol. 42, no. 3, pp. 753–766, 1996.

[12] C. V. Rao and J. B. Rawlings, "Steady states and constraints in model predictive control," *AIChE Journal*, vol. 45, no. 6, pp. 1266–1278, 1999.

[13] J. M. Maciejowski, *Predictive Control with Constraints*. Harlow, Essex: Pearson Educational Limited, 2002.

[14] C. Edwards and I. Postlethwaite, "Anti-windup and bumpless transfer schemes," *Automatica*, vol. 34, no. 2, pp. 199–210, 1998.

[15] G. Grimm, J. Hatfiled, A. R. Teel, M. Turner, and L. Zaccarian, "Anti-windup for stable linear systems with input saturation: an LMI based synthesis," *IEEE Trans. Automatic Control*, vol. 48, no. 9, pp. 1509–1525, 2003.

[16] M. C. Turner and I. Postlethwaite, "A new perspective on static and low order anti-windup synthesis," *International Journal of Control*, vol. 77, no. 1, pp. 27–44, 2004.

[17] D. Horla, "On directional change and anti-windup compensation in multivariable control systems," *Int. J. Appl. Math. Comput. Sci.*, vol. 19, no. 2, pp. 281—-289, 2009.

[18] S. Tarbouriech and M. Turner, "Anti-windup design: an overview of some recent advances and open problems," *IET Control Theory Appl.*, vol. 3, no. 1, pp. 1—-19, 2009.

[19] M. Morari and E. Zafiriou, *Robust Process Control*. Englewood Cliffs: Prentice Hall, 1989.

[20] R. M. Morales, L. Guang, and W. P. Heath, "Anti-windup and the preservation of robustness against structured norm-bounded uncertainty," in *17th IFAC World Congress*, Seoul, July 6-11 2008.

[21] M. C. Turner, H. Guido, and I. Postlethwaite, "Incorporating robustness requirements into antiwindup design," *IEEE Transactions on Automatic Control*, vol. 52, no. 10, pp. 1842–1855, 2007.

[22] C. E. Garcia and M. Morari, "Internal model control-1. a unifying review and some new results," *Ind. Eng. Chem. Process Des. Dev.*, vol. 21, pp. 308–323, 1982.

[23] ——, "Internal model control-2. design procedure for multivariable systems," *Ind. Eng. Chem. Process Des. Dev.*, vol. 24, pp. 472–484, 1985.

[24] ——, "Internal model control-3. multivariable control law computation and tuning guidelines," *Ind. Eng. Chem. Process Des. Dev.*, vol. 24, pp. 484–494, 1985.

[25] N. L. Ricker, "Use of quadratic programming for constrained internal model control," *Ind. Eng. Chem. Process Des. Dev.*, vol. 24, pp. 925–936, 1985.

[26] C. Brosilow, G. Q. Zhao, and K. C. Rao, "A linear programming approach to constrained multivariable control," in *Proceedings of the American Control Conference*, San Diego, California, June 6-8 1984, pp. 667–674.

[27] L. Magni and R. Scattolini, "Robustness and robust design of MPC for nonlinear discrete-time systems," in *Assessment and Future Directions*

of Nonlinear Model Predictive Control, R. Findeisen, F. Allgöwer, and L. Biegler, Eds. Heidelberg: Springer, 2007, pp. 239–254.

[28] A. Wills, G. Knagge, and B. Ninness, "Fast linear model predictive control via custom integrated circuit architecture," *IEEE Transactions on Control Systems Technology (To appear)*, 2010.

[29] C. E. Garcia, D. M. Prett, and M. Morari, "Model predictive control: Theory and practice a survey," *Automatica*, vol. 25, no. 3, pp. 335–348, 1989.

[30] E. Coulibaly, S. Maiti, and C. Brosilow, "Internal model predictive control (IMPC)," *Automatica*, vol. 31, no. 10, pp. 1471–1482, 1995.

[31] S. A. Heise and J. M. Maciejowski, "Stability of constrained mbpc using an internal model control structure," in *Advances in Model-Based Predictive control*, D. Clarke, Ed. Oxford University Press, 1994, pp. 230–244, iSBN: 0-19-856292.

[32] K. S. Walgama and J. Sternby, "Inherent observer property in a class of anti-windup compensators," *International Journal of Control*, vol. 52, no. 3, pp. 705–724, 1990.

[33] W. Wu and S. Jayasuriya, "An internal model control anti-windup scheme with improved performance for input saturation via loop shaping," *J. Dynamic sys. Meas. and Contr.*, vol. 132, pp. 1–6, 2010.

[34] P. F. Weston and I. Postlethwaite, "Linear conditioning for systems containing saturating actuators," *Automatica*, vol. 36, pp. 1347–1354, 2000.

[35] M. V. Kothare, P. J. Campo, M. Morari, and C. N. Nett, "A unified framework for the study of anti-windup designs," *Automatica*, vol. 30, no. 12, pp. 1869–1883, 1994.

[36] S. Miyamoto and G. Vinnicombe, "Robust control of plants with saturation nonlinearity based on coprime factor representation," in *Pro-*

ceedings of the 35th IEEE conference on Decision and Control, Kobe, Japan, 1996, pp. 2838–2840.

[37] A. R. Teel and N. Kapoor, "The $\mathcal{L}_2$ anti-windup probelm: Its definition and solution," in *The Proceedings of the 4th European Control Conference*, Brussels, Belgium, July 1997.

[38] L. Zaccarian and A. R. Teel, "A common framework for antiwindup bumpless, transfer and relaible designs," *Automatica*, vol. 38, no. 10, pp. 1735–1744, 2002.

[39] J. C. Doyle, R. S. Smith, and D. F. Enns, "Control of plants with input saturation nonlinearities," in *Proceedings of the American Control Conference*, 1987, pp. 1034–1039.

[40] P. Kapasouris, M. Athans, and G. Stein, "Design of feedback control systems for stable plants with saturating actuators," in *Proceedings of the 27th IEEE Conference on Decision and Control*, Austin, Texas, December 7-9 1988, pp. 469–479.

[41] T. A. Kendi and F. J. Doyle, "An anti-windup scheme for multivariable nonlinear system," *Journal of Process Control*, vol. 7, no. 5, pp. 329–343, 1997.

[42] K. S. Walgama and J. Sternby, "Conditioning technique for multiinput multioutput processes with input saturation," in *Proceedings of the IEE Part D*, vol. 140(4), 1993, pp. 231–241.

[43] C. Chen and M. Perng, "Optimal anti-windup control of saturating discrete mimo systems," *International Journal of Control*, vol. 67, no. 6, pp. 933–959, 1998.

[44] ——, "An optimization-based anti-windup design for mimo control systems," *International Journal of Control*, vol. 69, no. 3, pp. 393–418, 1998.

[45] G. Li, W. P. Heath, and G. Herrmann, "Robust anti-windup compensator synthesis via integral quadratic constraints," in *18th IFAC World Congress*, Milano, Italy, August 28-September 2 2011.

[46] G. Li, G. Herrmann, D. P. Stoten, J. Tu, and M. C. Turner, "A novel robust disturbance rejection anti-windup framework," *International Journal of Control*, vol. 84, no. 1, pp. 123–137, 2011.

[47] Z. Kreyszig, *Introductory Functional Analysis with Applications*. Upper Saddle River, NJ: John Wiley & Sons, 2003.

[48] T. Kailath, *Linear systems*. Englewood Cliffs, NJ: Prentice-Hall, Inc., 1980.

[49] K. Zhou, J. C. Doyle, and K. Glover, *Robust and optimal control*. Upper Saddle River, NJ: Prentice-Hall, Inc., 1996.

[50] G. E. Dullerud and F. Paganimi, *A course in robust control theory: a convex approach*. New York: Springer-Verlag, 2000.

[51] U. Jönsson, "Lecture notes on integral quadratic constraints," Department of Mathematics, KTH, Stockholm, Tech. Rep., 2000.

[52] H. K. Khalil, *Nonlinear Systems*. Upper Saddle River, NJ: Prentice-Hall, Inc., 2000.

[53] W. M. Haddad and D. S. Bernstein, "Explicit construction of quadratic Lyapunov functions for the small gain, positivity, circle and Popov theorems and their application to robust stability. part 1: Continuous-time theory," *International Journal of Robust Nonlinear Control*, vol. 3, pp. 313–339, 1993.

[54] W. P. Heath, A. G. Wills, and J. A. G. Akkermans, "A sufficient condition for the stability of optimizing controllers with saturating actuators," *International Journal of Robust Nonlinear Control*, vol. 15, pp. 515–529, 2005.

[55] J. A. Primbs, "The analysis of optimization based controllers," *Automatica*, vol. 37, pp. 933–938, 2001.

[56] G. Li, W. P. Heath, and B. Lennox, "Concise stability conditions for systems with static nonlinear feedback expressed by quadratic program," *IET Control Theory Appl.*, vol. 2, no. 7, pp. 554–563, 2008.

[57] A. Syaichu-Rohman, R. H. Middleton, and M. M. Seron, "A multivariable nonlinear algebraic loop as a QP with application to MPC," in *The Proceedings of the European Control Conference*, Cambridge, September 1-4 2003, pp. 6193–6198.

[58] J. C. Willems, *The Analysis of Feedback Systems.* Cambridge, Massacchusetts: MIT Press, 1971.

[59] R. Fletcher, *Practical Methods of Optimization.* Chichester: John Willey & Sons, 1987.

[60] S. Boyd, L. E. Ghaoui, E. Feron, and V. Balakrishnan, *Linear Matrix Inequalities in System and Control Theory.* Society for Industrial and Applied Mathematics, Philadelphia, PA, USA, 1994.

[61] B. A. Francis, *A course in H_∞ control theory.* Berlin Heidelberg: Springer-Verlag, 1987.

[62] J. M. Maciejowski, *Multivariable Feedback Design.* Addison Wesley, Workingham England, 1989.

[63] G. Vinnicombe, *Uncertainty and Feedback: $\mathcal{H}_\infty$ loop-shaping and the v-gap metric.* London: Imperial College Press, 2001.

[64] A. Megretski and A. Rantzer, "System analysis via integral quadratic constraints," *IEEE Transactions on Automatic Control*, vol. 42, no. 6, pp. 819–830, 1997.

[65] U. Jönsson and A. Rantzer, "Optimization of integral quadratic constraints," in *Advances in linear matrix inequality methods in control:*

advances in design and control, L. E. Ghaoui and S. Niculescu, Eds. Philadelphia, USA: Society for Industrial and Applied Mathematics, 2000, pp. 109–127.

[66] M. C. Wellons and T. F. Edgar, "The generalized analytical predictor," *Ind. Eng. Chem. Res.*, vol. 26, pp. 1523–1536, 1982.

[67] A. A. Adegbege, "Formulation of model predictive control as a generalized form of internal model control," MSc.Dissertation, The University of Manchester, 2006.

[68] A. A. Adegbege and W. P. Heath, "Internal model control design for input constrained multivariable processes," *AIChE*, vol. 57, no. 12, pp. 3459–3472, 2011.

[69] R. Hanus and M. Kinnaert, "Control of constrained multivariable systems using conditioning technique," in *Proceedings of the American Control Conference*, Pittsburgh, 1989, pp. 1711–1718.

[70] K. Yamada and Y. Funami, "A design method of anti-windup control system with unknown external signal," in *Proceedings of the 6th Int. Workshop on Advanced Motion Control*, Nagoya, Japan, March 30-April 1 2000, pp. 205–210.

[71] J. K. Park, C. H. Choi, and H. Choo, "Dynamic anti-windup method for a class of time-delay control systems with input saturation," *Int. J. Robust Nonlinear Control*, vol. 10, pp. 457–488, 1995.

[72] B. R. Holt and M. Morari, "Design of resilient processing plants-vi. the effect of right-half-plane zeros on dynamic resilience," *Chemical Engineering Science*, vol. 40, no. 1, pp. 59–74, 1985.

[73] P. D. S. Reddy, M. Pandit, and M. Chidambaram, "Comparison of multivariable controllers for non-minimum phase systems," *International Journal of Modelling and Simulation*, vol. 26, no. 3, pp. 237–243, 2006.

[74] G. C. Goodwin, S. F. Graebe, and M. E. Salgado, *Control system design*. Upper Saddle River, NJ: Prentice-Hall, Inc., 2001.

[75] R. Hanus and Y. Peng, "Modified conditioning technique for controllers with nonminimum phase zeros and /or time-delays," in *Proceedings of the 13th IMACS world congress on computation and applied mathematics*, Dublin, 1991, pp. 1188–1189.

[76] Q. Wang, Y. Zhang, and M. Chiu, "Decoupling internal model control for multivariable systems with multiple time delays," *Chemical Engineering Science*, vol. 57, pp. 115–124, 2002.

[77] S. Skogestad and I. Postlethwaite, *Multivariable feedback control-analysis and design*. West Sussex: John Willey & Sons, Ltd., 2005.

[78] M. C. Tsai and L. W. Chen, "A numerical algorithm for inner-outer factorizations of real-rational matrices," *Systems & Control Letters*, vol. 20, pp. 209–217, 1993.

[79] R. Vadigepalli, E. P. Gatzke, and F. J. DoyleIII, "Robust control of a multivariable experimental four-tank system," *Ind. Eng. Chem. Res*, vol. 40, pp. 1916–1927, 2001.

[80] N. Wada and M. Saeki, "Design of a static anti-windup compensator which guarantees robust stability," *Trans. of Inst. syst. Conr. Inform. Eng.*, vol. 12, no. 11, pp. 664–670, 1996.

[81] G. Herrmann, M. C. Turner, and I. Postlethwaite, "Some new results on anti-windup-conditioning using the weston-postlethwaite approach," in *The Proceedings of the 43rd IEEE Conference on Decision and Control*, Atlantis, Bahamas, December 14-17 2004, pp. 5047–5052.

[82] G. Grimm, A. R. Teel, and L. Zaccarian, "Robust linear anti-windup synthesis for recovery of unconstrained performance," *Int. J. Robust Nonlinear Control*, vol. 14, pp. 1133–1168, 2004.

[83] G. Herrmann, M. C. Turner, I. Postlethwaite, and G. Guo, "Practical implementation of a novel anti-windup scheme in a hdd-dual-stage servo-system," *IEEE/ASME TRANSACTIONS ON MECHATRONICS,*, vol. 9, no. 3, pp. 580–592, 2004.

[84] J.-M. Biannic, C. Roos, and S. Tarbouriech, "A practical method for fixed-order anti-windup design," in *Proceedings of the 7th IFAC Symposium on Nonlinear Control Systems*, South Africa, August 22-24 2007.

[85] E. Villota, M. Kerr, and S. Jayasuriya, "A study of configurations for anti-windup control of uncertain systems," in *The Proceedings of the 45st IEEE Conference on Decision and Control*, San Diego, California, December 13-15 2006, pp. 6193–6198.

[86] M. C. Turner, I. Postlethwaite, and G. Herrmann, "Further results on full-order antiwindup synthesis: Exploiting the stability multiplier," in *6th IFAC Nonlinear Control System Design Symposium (NOLCOS)*, Stuttgart, 2004.

[87] K. Takaba, "Anti-windup control system design based on youla parametrization," in *The Proceedings of the American Control Conference*, San Diego, California, June 2-4 1999, pp. 2012–2017.

[88] ——, "Analysis and synthesis of anti-windup control system design based on youla parametrization," in *The Proceedings of the 41st IEEE Conference on Decision and Control*, Las Vegas, Nevada, December 10-13 2002, pp. 2692–2697.

[89] Y. Funami and K. Yamada, "An anti-windup control design method using modified internal model control structure," in *Proceedings of the IEEE Int.conference on Systems, Man and Cybernetics*, Tokyo , Japan, October 12-15 1999, pp. 74–79.

[90] C. S. Ling, M. D. Brown, P. F. Weston, and C. Roberts, "Gain tuned internal model control for handling saturation in actuators," in *The Proceedings of the American Control Conference*, Boston, Massachusetts, June 30-July 2 2004, pp. 4692–4697.

[91] J. M. Vandeursen and J. A. Peperstraete, "Internal model control with improved disturbance rejection," *International Journal of Control*, vol. 62, no. 4, pp. 983–999, 1995.

[92] M. V. Kothare and M. Morari, "Multiplier theory for stability analysis of anti-windup control systems," *Automatica*, vol. 35, pp. 917–928, 1999.

[93] A. A. Adegbege and W. P. Heath, "Stability conditions of a two-stage internal model control," in *The Proceedings of the 49th IEEE Conference on Decision and Control*, Atlanta, Georgia, December 15-17 2010, pp. 5251–5256.

[94] E. F. Mulder, P. Y. Tiwari, and M. V. Kothare, "Simultaneous linear and anti-windup controller synthesis using multiobjective convex optimization," *Automatica*, vol. 45, pp. 805–811, 2009.

[95] M. Soroush and N. Mehranbod, "Optimal compensation for directionality in processes with a saturating actuator," *Computers and Chemical Engineering*, vol. 26, pp. 1633–1641, 2002.

[96] A. A. Adegbege and W. P. Heath, "Two-stage multivariable antiwindup design for internal model control constraints," in *9th International Symposium on Dynamics and Control of Process Systems*, Leuven, Belgium, July 5-7 2010, pp. 276–281.

[97] ——, "Antiwindup synthesis for optimizing internal model control," To be presented at 50th IEEE Conference on Decision and Control, Orlando, Florida, December 2011.

[98] S. Skogestad and M. Morari, "Control of ill-conditioned plants: High-purity distillation," in *AIChE Annual Meeting*, Miami, Florida, November 1986, p. Paper 74a.

[99] ——, "Robust control of ill-conditioned plants: High-purity distillation," *IEEE Transactions on Automatic Control*, vol. 33, no. 12, pp. 1092—-1105, 1988.

[100] G. Pannocchia, "Robust disturbance modeling for model predictive control with application to multivariable ill-conditioned processes," *Journal of Process Control*, vol. 13, pp. 693—-701, 2003.

[101] P. Daoutidis and C. Kravaris, "Structural evaluation of control configurations for multivariable nonlinear processes," *Chemical Engineering Science*, vol. 47, no. 5, pp. 1091–1107, 1992.

[102] S. Crawshaw and G. Vinnicombe, "Anti-windup synthesis for guaranteed L_2 performance," in *Proceedings of the 39th IEEE conference on Decision and Control*, Sidney, Australia, 2000, pp. 1063–1068.

[103] W. P. Heath and A. G. Wills, "Zames-Falb multipliers for quadratic programming," *IEEE Transactions on Automatic Control*, vol. 52, no. 10, pp. 1948—-1951, 2007.

[104] M. Canale, "Robust control from data in presence of input saturation," *Int. J. Robust Nonlinear Control*, vol. 14, pp. 983—-997, 2004.

[105] W. P. Heath and G. Li, "Multipliers for model predictive control with structured input constraints," *Automatica*, vol. 46, no. 3, pp. 562—-568, 2010.

[106] M. C. Turner, G. Herrmann, and I. Postlethwaite, "Anti-windup compensation using a decoupling architecture," in *Advanced Strategies in Control Systems with Input and Output Constraints*, ser. Lecture Notes in Control and Information Sciences, S. Tarbourie, G. Garcia, and A. Glattfelder, Eds. Springer Berlin / Heidelberg, 2007, vol. 346, pp. 121–171.

[107] A. Rantzer, "On the kalman-yakubovich-popov lemma," *Systems & Control Letters*, vol. 28, pp. 7–10, 1996.

[108] P. Gahinet and P. Akparian, "A linear matrix inequality approach to h_∞ control," *International Journal of Robust Nonlinear Control*, vol. 4, no. 4, pp. 421–448, 1994.

[109] S. J. Wright, *Primal-Dual Interior-Point Methods*. Philadelphia, USA: Society for Industrial and Applied Mathematics, 1997.

[110] R. W. Cottle, J. Pang, and R. E. Stone, *The Linear Complementarity Problem*. Philadelphia, USA: Society for Industrial and Applied Mathematics, 2009.

[111] R. A. Horn and C. R. Johnson, *Matrix Analysis*. Cambridge: Cambridge University Press, 1985.

[112] K. R. Muske, "Steady-state target optimization in linear model predictive control," in *Proceedings of the American Control Conference*, Albuquerque, 1997, pp. 3597–3601.

[113] M. Soroush and K. R. Muske, "Analytical model predictive control," in *Nonlinear Model Predictive Control*, F. Allgöwer and A. Zheng, Eds. Switzerland: Birkhäuser Verlag Bassel, 2000, pp. 163–179.

[114] J. A. De Doná, G. C. Goodwin, and M. M. Seron, "Anti-windup and model predictive control: Reflections and connections," *European Journal of Control*, vol. 6, no. 5, pp. 467–477, 2000.

[115] E. N. Sakizlis, T. Pistikopoulos, M. Geyer, and M. Morari, "The equivalence of the anti-windup control design and the explicit model-based parametric controller," in *Proceedings of the European Control Conference*, Cambridge, September 1-4 2003.

[116] O. Marjanovic, B. Lennox, P. Goulding, and D. Sandoz, "Minimising conservatism in infinite-horizon LQR control," *Systems & Control Letters*, vol. 46, pp. 271–279, 2002.

[117] P. J. Goulart and E. C. Kerrigan, "Relationships between affine feedback policies for robust control with constraints," in *16th IFAC World Congress on Automatic Control*, Prague, 2005.